General Disclaimer

One or more of the Following Statements may affect this Document

- This document has been reproduced from the best copy furnished by the organizational source. It is being released in the interest of making available as much information as possible.

- This document may contain data, which exceeds the sheet parameters. It was furnished in this condition by the organizational source and is the best copy available.

- This document may contain tone-on-tone or color graphs, charts and/or pictures, which have been reproduced in black and white.

- This document is paginated as submitted by the original source.

- Portions of this document are not fully legible due to the historical nature of some of the material. However, it is the best reproduction available from the original submission.

Produced by the NASA Center for Aerospace Information (CASI)

TECHNICAL REPORT

CORNELL AERONAUTICAL LABORATORY

HYPERSONIC SHOCK TUNNEL

CAL No. AA-2977-Y-1

EXPERIMENTAL INVESTIGATION OF LEADING-EDGE SHOCK IMPINGEMENT AND INTERACTION HEATING ON A 1/80 SCALE MODEL OF A NASA STRAIGHT WING ORBITER CONFIGURATION AT MACH NUMBERS 8 AND 16

Prepared For:

Manned Spacecraft Center
National Aeronautics and Space Administration
Houston, Texas 77058

Contract No. NAS 9-11084

August 1971

N71-35196 (ACCESSION NUMBER)
29 (PAGES)
CR-115159 (NASA CR OR TMX OR AD NUMBER)
(THRU) G3
(CODE) 01
(CATEGORY)
FACILITY FORM 602

OCT 1971
RECEIVED
NASA STI FACILITY

CORNELL AERONAUTICAL LABORATORY, INC.

OF CORNELL UNIVERSITY, BUFFALO, N. Y. 14221

CR-115159

CORNELL AERONAUTICAL LABORATORY, INC.
BUFFALO, NEW YORK 14221

CAL REPORT NO. AA-2977-Y-1

EXPERIMENTAL INVESTIGATION OF LEADING-EDGE SHOCK IMPINGEMENT AND INTERACTION HEATING ON A 1/80 SCALE MODEL OF A NASA STRAIGHT WING ORBITER CONFIGURATION AT MACH NUMBERS 8 AND 16

AUGUST 1971

Prepared For:

MANNED SPACECRAFT CENTER
NATIONAL AERONAUTICS AND SPACE ADMINISTRATION
HOUSTON, TEXAS 77058

CONTRACT NO. NAS 9-11084

Prepared By: C.E. Rogers
Project Engineer

Approved By: Charles Treanor
C.E. Treanor, Head
Aerodynamic Research Department

Date: August 26, 1971

TABLE OF CONTENTS

Section		Page
I	SUMMARY	1
II	FOREWORD	2
III	TEST EQUIPMENT	3
IV	NOMENCLATURE AND SYMBOLS	7
V	TEST PROCEDURE	9
VI	TEST CONDITIONS	11
VII	DATA REDUCTION	13
VIII	PRESENTATION OF DATA	16
IX	PRECISION OF DATA	23
X	CONCLUSIONS AND RECOMMENDATIONS	24
XI	REFERENCES	25
XII	TABLE INDEX	27
XIII	FIGURE INDEX	28

SECTION I SUMMARY

The objective of this experimental program was the investigation of leading-edge shock impingement and interaction heating on a 1/80 scale model of a NASA straight-wing orbiter configuration. The tests were conducted in the Cornell Aeronautical Laboratory 96-inch Hypersonic Shock Tunnel at Mach number 8 (nominal) at Reynolds numbers of 2×10^6 through 10×10^6 per foot and at Mach number 16 at Reynolds numbers of 0.1×10^6 and 1×10^6 per foot. Model angle of attack was varied from 0 to 70 degrees and model side-slip angle was varied from 0 to 3 degrees.

Measurements of chordwise local heat-transfer rates were made at five locations on the wing from the leading edge to 20 percent of the chord length. Sensors were placed to measure the steep gradients occurring in regions where the fuselage bow shock intersected the wing, where interactions from the fuselage were expected and in non disturbed regions. In addition, measurements of spanwise local heat-transfer rates were made alcng the 17% chord line to help define the location and magnitude of the impingement and interaction heating. Schlieren photographs were also obtained to help define the flow field.

This report presents the details of the test program and a description of the model, instrumentation and shock tunnel. The results are presented in tabular and graphical form along with a brief discussion.

SECTION II FOREWORD

The experimental investigation reported herein was conducted by the Cornell Aeronautical Laboratory, Inc. for the Manned Spacecraft Center of the National Aeronautics and Space Administration under Contract No. NAS 9-11084. The test program was conducted during the periods January 22 to February 2 and February 22 to February 25, 1971 in the CAL 96-inch Hypersonic Shock Tunnel. The test model was provided by NASA/MSC and was instrumented by CAL. The program was administered under the direction of Mr. W. D. Goodrich of NASA/MSC who was in attendance at the start of the test.

The model and the results of this study are UNCLASSIFIED.

SECTION III TEST EQUIPMENT

Shock Tunnel

The 96-inch CAL Hypersonic Shock Tunnel in which these tests were conducted is shown in Fig. 1 and is described in Ref. 1. This tunnel employs a chambered reflected shock tube to process air to conditions suitable for supplying a convergent-divergent hypersonic nozzle. The shock-processed air is expanded through one of several interchangeable nozzles to the desired test conditions. The "tailored-interface" technique, wherein the acoustic impedances of the gases on either side of the driver-driven interface are matched, is used to supply test air of sufficient duration to allow accurate measurements of model forces, pressures or temperatures.

Contoured axisymmetric nozzles were employed for the expansion process to obtain Mach numbers of 8 and 16. The nozzles have a 24-inch and a 48-inch exit diameter, respectively, and employ removable throat inserts of various cross-section area to produce the test section Mach numbers required.

The test air passes downstream of the test section into a receiver tank of sufficient size to maintain the desired flow in the test section until after the period of uniform supply conditions. The speed of the incident shock and the pressure behind the reflected shock are measured and recorded for each run and are used to determine the nozzle supply conditions.

The test section is equipped with two 16-inch diameter schlieren windows mounted a short distance aft of the nozzle exit.

Model

An existing 1/80 scale model of the 12.5K straight-wing space shuttle orbiter was provided by NASA/MSC for this investigation. A sketch of the model is shown in Fig. 2. Two wings modified for special CAL heat-transfer gages were also provided by NASA/MSC. Photographs of the model are shown in Figures 3(a) and 3(b). The model and wings were fabricated from stainless steel.

The model was sting-mounted to the angle-of-attack sector through a 20 degree bent sting extension provided by NASA/MSC as shown schematically in Fig. 4. The bent sting was provided to set angles of attack greater than the 50 degree angle available on the sector. Angles less than 20 degrees were set by rolling the sting 180 degrees before pitching the model. A photograph of the model installed in the shock tunnel is shown as Fig. 5.

Instrumentation

Heat Transfer - Heat transfer rates were determined by a technique that relies on sensing the transient surface temperature of the model (Ref. 2). The sensing element is a thin platinum strip painted on a pyrex substrate which conforms to the local model contour. After the painting, the gage is fired at controlled conditions, and the result is a thin film of metal, typically 0.1 micron thick by 5 mm by 0.5 mm, fused to the pyrex insert. Since the heat capacity of the gage is negligible, the film temperature is equal to the instantaneous surface temperature and is related to the heat transfer rate to the model by the theory outlined in Section VII of this report and discussed in detail in Ref. 2.

Nominal locations of the heat-transfer gages are shown and tabulated in Figure 6. Five pyrex inserts, match ground to the contour of the leading edge, were fitted to the left wing. Station 1 insert was located near the wing root to measure fuselage/wing interference heating, and station 3 insert was located on the span at the predicted point of bow-shock impingement based on thermal paint results. The other leading edge inserts were spaced at non-perturbed positions. Each insert was instrumented with miniature thin-film gages measuring approximately 0.1 mm wide by 2.5 mm long. Gages were located on the stagnation line of each insert and back to the 20% chord line on the windward side and to the 8% chord line of the leeward side of the insert. These miniature gages were spaced as close as 0.5 mm on centers in order to obtain an accurate determination of the high heating gradients existing in the flow field. A photograph of the five inserts with the thin films applied is shown in Figure 7. Figure 8 is a close-up photograph of one of the inserts with the lead wires attached.

A spanwise pyrex strip contoured to the wing mold line was fitted to the right wing and instrumented with the standard size thin film gages to measure the spanwise heating distributions and determine the location of shock impingement. Three standard circular heat-transfer gages were also located on the wing centerline to provide reference values.

A photograph of the wing prior to assembly is shown in Figure 9.

Because of the high density of heat-transfer gages on the leading-edge inserts, it was projected that the power density might be undesirably high if the standard electrical circuit was used.* Therefore, the standard heat transfer gage circuit was modified to reduce the power to each element from approximately .05 watts to .005 watts. The results of this modification are discussed in Section V, Test Procedure.

Flow Visualization - The photographic system for viewing the model flow field at Mach number 8 was a single-pass collimated light "Z" system while a double-pass collimated system was used for Mach number 16 to obtain increased sensitivity. A horizontal knife edge was used in both systems to obtain schlieren photographs. A spark-type light source, with a pulse duration of 0.6 microseconds, was used.

Data Acquisition

The electrical outputs of heat transfer and pressure were recorded on two systems because of the volume of data. Forty-eight channels of heat transfer data were recorded in the form of temperature-time records on the magnetic storage drum of a Navigational Computer Corporation MCC-100 data acquisition system (NAVCOR) at 50 microsecond intervals during each run. The data stored on the magnetic drum were reproduced on a strip chart and were also transferred to a magnetic tape for processing on an IBM 360-65 computer. The output from each heat-transfer gage, as recorded on

*It is shown in Ref. 3 that the value of the lumped thermal properties of the substrate material $(\rho ck)^{1/2}$ necessary in data reduction is a function of the substrate ambient temperature. It is desirable to keep the ambient temperature near 70°F to simplify data reduction.

the NAVCOR drum, was additionally processed by a "q̇-meter", which is a passive electrical analog network that converts the analog voltage representation of the gage element temperature into an analog voltage representation of heat-transfer rate. These results were also reproduced on the strip chart.

The balance of the data was recorded photographically from Tektronix 502 dual beam oscilloscopes operated at a sweep rate of 1 msec/cm. The temperature output from each gage was recorded on the lower beam of the oscilloscopes. This output was additionally processed through a "q̇-meter" and displayed on the upper beam of the oscilloscopes.

SECTION IV NOMENCLATURE AND SYMBOLS

Symbols

C	Local wing chord, inches
C_h	Stanton number, $\dot{q}/\rho_\infty U_\infty (H_\infty - H_w)$
h	Heat-transfer coefficient, 778 (32.17) $\dot{q}/(H_o - H_w)$, lbm/ft^2-sec
H	Enthalpy, ft. lbs/slug
L	Fuselage length, inches
M	Mach number
p	Pressure, psia
P_r	Prandtl number
q	Dynamic pressure, psia
$\dot{q}$	Heat transfer rate, BTU/ft^2-sec
Re/ft	Reynolds number per unit length, $\frac{\rho_\infty U_\infty}{\mu_\infty}$
S	Wing span, inches
T	Temperature, °R
t	Time, seconds
U	Velocity, ft/sec
X	Chordwise distance, inches
y	Spanwise distance, inches
α	Angle of attack, degrees
β	Angle of sideslip, degrees
γ	Specific heat ratio
μ	Absolute viscosity, slugs/ft-sec
ρ	Density, slugs/ft^3

Subscripts

o	Nozzle supply conditions
o'	Stagnation conditions behind a normal shock
1	Initial driven gas condition
4	Gas conditions behind reflected shock
i	Incident shock in driven gas
ts	Test section initial conditions
w	Initial conditions at model surface
∞	Free stream or test section conditions

SECTION V TEST PROCEDURE

Calibration

The heat-transfer gages were calibrated prior to the tests to determine the changes in resistance of the elements with temperature. At the temperatures encountered in these tests, these changes are linear; therefore, the resistance values at only two temperatures were determined. This calibration was then used to set the gain of the recording equipment for the expected temperature increase.

The necessity for making corrections to the substrate properties as a result of an elevated ambient temperature on the leading edge inserts was determined by evaluating the temperature rise on the smallest insert caused by applying power to the gages. One of the 15 gages on the insert was used as a resistance thermometer, and the temperature rise of the substrate was determined between the poweroff condition and the condition where power was applied to the other 14 gages. The temperature rise was determined at the stagnation point (gage 501) and at the location of the most rearward gages on the lower and upper surfaces (gages 511 and 515) at ambient pressure and at about 80 μHg. The results and required correction to the lumped thermal parameter, $(\rho ck)^{1/2}$, are shown below:

GAGE	$\Delta T = (T_{\text{Power on}} - T_{\text{Power off}})^{(°F)}$		$\frac{(\rho ck)^{1/2}_T}{(\rho ck)^{1/2}_{70°F}}$
	1 Atm.	80 μHg	
501	37.7	41.3	1.03
511	22.4	24.3	1.02
515	17.3	19.4	1.02

The resultant error in thermal properties caused by applying power to the gage is considered sufficiently small to ignore.

These calibrations, in conjunction with estimated values of model flow field properties provided the basis for adjusting amplifier gains to achieve suitable "readability" of the data recording system.

The detailed calibration data are kept on file at CAL.

Test Program

The complete test program and test conditions are presented in Tables 1 and 2. The test program was specified by NASA/MSC. The selected test conditions of Reynolds number and Mach number were based on reentry trajectories at various angles of attack. Variations in sideslip angle were made in order to move the shock impingement region relative to leading edge insert number three.

Mr. W. D. Goodrich was present at CAL during the initial phases of testing as a representative of NASA.

SECTION VI TEST CONDITIONS

The values of free stream Mach number in the test section were determined from previous calibrations of the airflow in the tunnel; the calibration results are on file at CAL.

The test conditions of pressure, temperature and Reynolds number are computed by assuming isentropic expansion of the test gas from the conditions behind the reflected shock in the tube to the test section Mach number. The flow is expanded sufficiently so that the air in the test section is cool enough to obey the perfect gas laws.

The stagnation enthalpy and temperature of the air behind the reflected shock is determined from

$$H_o = H_1 \ (H_4/H_1) \tag{1}$$

$$\text{and } T_o = T_1 \ (T_4/T_1), \text{ respectively} \tag{2}$$

where H_4/H_1 and T_4/T_1 are functions of U_i, the incident shock velocity, (Refs. 4-6). U_i is obtained by measuring the time taken by the shock wave to pass between two stations in the shock tube. H_1 is taken from Ref. 7. Free stream static temperature is obtained from

$$T_\infty = \frac{H_o}{C_p} \left(1 + \frac{\gamma - 1}{2} M_\infty^2\right)^{\gamma - 1} \tag{3}$$

Free stream pressure is calculated using

$$p_\infty = \frac{P}{P_p} \ p_o \left(1 + \frac{\gamma - 1}{2} M_\infty^2\right)^{-\frac{\gamma}{\gamma - 1}} \tag{4}$$

where

$$\frac{P}{P_p} = \frac{(p/p_o)_{\text{real}}}{(p/p_o)_{\text{perf.}}}$$

is the real gas correlation to the ideal static-to-total pressure ratio as described in Ref. 8. The source data used in this technique are Refs. 7 and 9.

Free stream dynamic pressure is calculated from

$$q_\infty = \frac{\gamma}{2} p_\infty M_\infty^2 \qquad (5)$$

Values for absolute viscosity (μ) used to compute Reynolds numbers were obtained from Ref. 10 for temperatures below 500°R and from Ref. 11 for temperatures above 500°R.

Stagnation conditions behind a normal shock in the test section are based on the data of Ref. 9. The balance of the primary test section properties are based on perfect gas theory.

SECTION VII DATA REDUCTION

Heat Transfer

The "thin film" heat-transfer gage is a resistance thermometer which reacts to the local surface temperature of the model. The theory of heat conduction in a nonhomogeneous body is used to relate the surface temperature to the rate of heat transfer. Since the resistance element has negligible effect on the pyrex substrate surface temperature, the substrate can be characterized as being semi-infinite, homogeneous and isentropic. The general heat conduction equation is

$$\rho c(T) \frac{\partial T}{\partial t} = \frac{\partial}{\partial x} \left[k(T) \frac{\partial T}{\partial x} \right] \tag{6}$$

where ρ, c and k are substrate density, specific heat and thermal conductivity, respectively, and x is the substrate depth.

If the substrate properties are independent of temperature; i.e., if the temperature change is less than 100°R, a closed-form solution is obtained for the heat transfer rate,

$$\dot{q}(t) = \frac{1}{2} \left(\frac{\pi \rho c k}{t} \right)^{1/2} \left[T(t) + \frac{1}{\pi} \int_0^t \frac{\lambda^{1/2} T(t) - t^{1/2} T(\lambda)}{(t-\lambda)^{3/2}} \, d\lambda \right] \tag{7}$$

Two approaches are used at CAL for obtaining heat-transfer rates from the temperature-time records; i.e., a numerical procedure and an analog electrical network. The analog network approach was used in this case, but both approaches will be described for completeness.

Numerical Procedure - For evaluating the integral numerically, the equation is recast in the following form

$$\dot{q}(n) = \frac{1}{2\sqrt{\pi \Delta t}} (\rho c k)_n^{1/2} T_n \left(\frac{\pi + \sum_{p=0}^{p=n-1} \frac{p^{1/2}}{(n-p)^{1/2}}}{n^{1/2}} \right) - \sum_{p=0}^{p=n-1} \frac{T_p (\rho c k)_p^{1/2}}{(n-p)^{3/2}} \tag{8}$$

where	Δt	=	time interval between tabulated data points (50 microseconds)
	n	=	time index of the point
	p	=	running time index
subscript	n	=	value of parameters at nth time increment
subscript	p	=	value of parameters at pth time increment

The temperature dependence of $(\rho ck)^{1/2}$ and the variation of the electrical properties of the resistance element with temperature are accounted for in the computer program.

Analog $\dot{q}$-Meter - In cases where the surface temperature change is nominally less than 100°F, as is in these tests, Eq. (7) may be solved directly by use of $\dot{q}$-meters, which are passive electrical analog networks, in conjunction with the heat-transfer gage. The analog is based on the fact that the equation for heat conduction in a semi-infinite solid is identical to that for a semi-infinite electrical transmission line with distributed series resistance and shunt capacitance. In practice, it has been found feasible to construct the analog of a finite number of circuit elements consisting of parallel resistor-capacitor elements in a series arrangement. For temperatures greater than 100°F the variation of substrate properties and electrical properties of the resistance element with temperature causes a significant droop if the $\dot{q}$-meter output which is corrected by a time and heat transfer rate dependent factor.

Additionally, since the heat-transfer rate is a function of the instantaneous gage temperature, the following correction for the instantaneous wall temperature is applied to obtain the equivalent cold wall heat-transfer rate based on the initial wall temperature.

$$\dot{q}_w = \left[\frac{\dot{q}_{(n)}}{H_o - H_{w(n)}}\right]\left(H_o - H_{w(n=0)}\right) \tag{9}$$

Heat-Transfer Coefficients - The heat-transfer data were normalized in terms of a Stanton number and heat-transfer coefficient based on free stream conditions. The relations used for the calculations are given by

$$C_h = \frac{778\ \dot{q}_w}{\rho_\infty U_\infty (H_o - H_w)} \tag{10}$$

$$h = 778\,(32.17)\,\frac{\dot{q}_w}{(H_o - H_w)} \qquad (11)$$

where the wall conditions are based on the initial model surface temperature of 535° R.

In addition, a theoretical stagnation heating rate for a one-foot radius sphere is calculated by the method of Fay and Riddell (Ref. 12). The measured heat transfer rate is scaled to a full size model by multiplying the rate by $\sqrt{1/80}$ and then ratioed to (a) the theoretical stagnation heating rate above and (b) the measured stagnation heating rate scaled to a one-foot radius sphere.

SECTION VIII PRESENTATION OF DATA

The data are presented in the form of tables, plots and schlieren photographs. Table 3 is a listing of heat-transfer rate, Stanton number, heat transfer coefficient, theoretical stagnation heat-transfer rate and ratio of heat-transfer rate to theoretical stagnation heat-transfer rate for each run. Gage identification is shown in Fig. 6.

Plots of the tabulated data are presented in Figs. 10-24 as the ratio of scaled local to theoretical stagnation heat-transfer rate as a function of a) percent chord for the leading edge inserts and b) percent half-span for the spanwise set of gages. These plots are based on actual gage locations as determined by inspection of each gage element as opposed to the nominal location.

In general, the leading edge gages were within 0.5% chord of their nominal location, however, several were as much as 1% chord off their nominal location. The spanwise gages were all within 1.2% semispan of their nominal location. The chordwise center of the spanwise distribution gages was intended to be along a constant 15% chord line. The slot in the wing was skewed slightly causing the chordwise center of these gages to run from the 16% chord at the inboard gage (601) to the 18.2% chord at the outboard gage (613).

For reference purposes a curve of the estimated heat-transfer ratio for the shock-impingement region is shown on the chordwise distribution plots; the estimated impingement-region heat-transfer ratio at the 17% chord is shown on the spanwise plots. These estimates are based on thermal mapping and thin skin model data obtained by NASA/MSC (Ref. 13). In addition, an average of the experimental data from the three centerline gages is shown on Figs. 10-24 as a reference.

Schlieren photographs of the flow field over the forward 60% of the model are presented in Fig. 25.

Discussion

There are several prominent features of the data which are at once apparent from Figs. 10-24:

1. The location of inserts 1 and 3 were well selected based on previous thermal mapping data to measure heat-transfer rates in the wing root/fuselage interaction region and in the bow shock/wing impingement region.

2. The wing root/fuselage interaction heat-transfer rates on the windward side aft of the leading edge tend to be as severe as or more severe than those in the shock impingement region at angles of attack greater than zero. At angles of attack of 30° or greater, the heating in this region is between 40% and 80% of the theoretical three dimensional stagnation value.

3. The heat-transfer rates in the nonperturbed regions tend to be as high as the estimates for the shock impingement region while the heat-transfer rates in the nominal shock impingement region (insert 3) tend to run higher than the estimates.

4. The spanwise data generally exhibits the double peaked heating values in the impingement region seen in thermal mapping data.

5. At angles of attack characteristic of reentry ($\alpha \geq 45$ deg.) for this configuration the leeside heating is at least an order of magnitude less than that on the windward side in the first 8% of the chord.

Wing Root/Fuselage Interference - At zero angle of attack the wing root/fuselage interference heating demonstrates a strong Mach number dependence at the leading edge as can be seen in Fig. 26 which presents $\dot{q}/\dot{q}_o$ as a function of angle of attack. Here the heating ratio varies from about 0.2 at Mach 16 to 0.8 at Mach 8 which is on the order of 1/10 to 1/3 the shock impingement values. The leading edge values in this region remain on the order of 1/2 those in the shock impingement region with no significant Mach number dependence as angle of attack increases.

Further back on the windward side (e.g., X/C = .17) $\dot{q}/\dot{q}_o$ increases with angle of attack without a strong Mach number dependence and finally reaches a value of 0.7 to 0.8 at α = 60 deg. as shown in Fig. 27. At α = 15 deg. $\dot{q}/\dot{q}_o$ is equal (±30%) to that in the shock impingement region and at $\alpha \geq$ 45 deg. it is twice the shock impingement value.

No significant yaw sensitivity can be detected in the wing root/fuselage interference region.

Two anomalies or discontinuities appear at the wing root as a function of angle of attack and Mach number. In Fig. 26 it can be seen that for α = 0 deg. the heat-transfer rate at the stagnation point for Mach number 8 is about 4 times that at Mach number 16. In Fig. 27 opposite sense cusp-like discontinuities appear in the heat-transfer rate plots at x/c = 0.17 for the two Mach numbers at α = 30 deg. with the Mach 8 data tending to drop and the Mach 16 data tending to increase. It should be noted that the chordwise heat transfer distributions at α = 0 and 30 deg. is reasonable for both Mach numbers; a review of the original data records show that it would be impossible to force readings from either run sufficiently to delete the discontinuities. It is, therefore, concluded that they are real effects. These discontinuities are most likely caused by the location and movement of separated flow and attachment regions in this area as a function of Mach number and angle of attack similar to that discussed in the following subsection on bow shock/wing impingement.

From the spanwise data it can be seen that the interaction region increases in size or moves outward as a function of angle of attack. At 60 or 70 deg. angle of attack (Figs. 14b, 16b, 22b and 24b) the first few inboard gages of the spanwise insert show an increase in heating toward the fuselage while at lower angles the trend is either absent or reversed.

Bow Shock/Wing Impingement - At the leading edge the heat-transfer rate in the bow shock/wing impingement region agrees with the estimate within about ±50% for all angles of attack but the data does tend to lie above the estimate as can be seen in Fig. 28. There is an effect of Mach number on the heat transfer ratio, but the most prominent feature of the data is the cusp like shape with a minimum value of $\dot{q}/\dot{q}_o$ occurring at 15 and 30 deg. angle of attack for Mach numbers 8 and 16, respectively. This effect will be

discussed subsequently.

The heat-transfer rates back at the 17% chord (Fig. 29) generally lie above the estimates by a factor of about two to three at the low angles of attack and approach the estimates at the higher angles of attack. These data also exhibit a Mach number dependence and have a cusp-like feature of which more will be said later. The heat-transfer rates at this location are generally higher than the nonperturbed inserts by a factor of about 1.5 to 3 at low angles of attack and are about equal to the nonperturbed values at α = 70 deg.

Since this is the first known data on this configuration having sufficient detail to define accurately the heat-transfer rates in the high gradient regions near the leading edge, it is instructive to compare it with data available from previous techniques. The windward chordwise results of this investigation at α = 60 deg. in the unperturbed region (60% and 80% exposed span) are compared on Fig. 30 with those at 70% exposed span* reported by Seegmiller in Ref. 14 wherein thermal mapping techniques were used for test conditions similar to those of this investigation. While the present results at the leading edge are a factor of two lower than those of Ref. 14, the results at X/C = .01 are a factor of two higher than the faired data of Ref. 14. At X/C $\geq$ .10 where the gradients are less, the current results are 20 to 60% higher at M = 8 and 20% higher at M = 16. Also shown on Fig. 30 is a theoretical heating distribution of Ref. 15 which Seegmiller cites. Seegmiller notes that the peak in the theoretical distribution is a result of the method used in obtaining velocity gradients but that the verification of such a peak was unconfirmed at the time Ref. 14 was written. The present data verify the trend of the theory but indicate that the gradients are more severe over the first 1% chord aft of the leading edge and less severe beyond. These differences could arise as a consequence of basic differences in instrumentation techniques or in a knowledge of $\dot{q}_o$.

*Although Ref. 14 is not explicit at this point, it is assumed that "exposed" span is intended since the rest of the reference uses that presentation.

Cusp-Like Feature of Data - The cusp-like feature of the heat-transfer rate data on insert 3 as presented in Figs. 28 and 29 is apparently a result of the movement of the interaction point of the bow shock and the wing leading edge shock as a function of angle of attack coupled with the impingement of the actual bifurcated shock which finally strikes the boundary layer on the model wing as described in Ref. 14. The bifurcated shock causes two separation and reattachment regions on the wing which results in a double peaked spanwise heating distribution as detected on most runs, e.g., run 13 (Fig. 12b). (When the separated region is over a gage, the heating rate tends to be low, but as the reattachment region moves over the gage the heating rate peaks). As the angle of attack increases, the leading edge heat-transfer rate (Fig. 28) tends to decrease while further back on the wing, e.g., $X/c = 0.17$ (Fig. 29), the rate tends to rise. This is consistent with the change of surface inclination with respect to the freestream flow at these locations. The sudden change in these trends, e.g., the increase on the leading edge and decrease at $X/c = 0.17$ between $\alpha = 30$ and 60 deg. at $M = 16$, is explainable by the movement of the reattachment area over the leading edge and the separated region over the rear of the insert. This explanation indicates that the reattachment line is skewed with respect to the chordwise direction which is consistent with previous observations (e.g., Ref. 14). As the angle of attack is increased the reattachment region passes outboard of the insert and the heating rate drops. The fact that the reattachment point is outboard of insert 3 at high angles of attack is corroborated by the general agreement of the heat-transfer rate on insert 3 with the nonperturbed inserts.

Nonperturbed Regions - The heat-transfer rate in the nonperturbed region generally tends to agree with the estimate for the shock impingement region with the following exceptions:

1. At $\alpha = 0$ and 15 deg. the windward data aft of the leading edge are about twice the estimates.
2. At $\alpha = 70$ deg. the windward data near the leading edge are only about 1/10 the estimate.

Oscillating Leeside Flow - An unusual and heretofore unreported (to the author's knowledge) oscillation was observed in the records for leeside gages under certain conditions. An example of this phenomena is shown in Fig. 31. Presented in Fig. 31a are the temperature and heat-transfer rate records for the leading edge and top side gages of insert number 3 taken on run 15 ($\alpha = 0°$, $\beta = 0°$, $M \approx 8$, $Re/ft = .37 \times 10^6$). At this test condition the usable (driver gas free) test time is about 5 milliseconds measured from data rise. The traces all reach a steady level in the expected 2 milliseconds which is representative of the nozzle starting time. Presented in Fig. 31b are records for the same gages taken on run 10 ($\alpha = 45°$, $\beta = 0°$, $M \approx 8$, $Re = 2.1 \times 10^6$). At this test condition the usable test time is about 6 milliseconds. The response of the leading edge gage, and the gages at the one and two percent chord are characteristic of steady heat transfer rates but at the four percent chord a definite oscillation has appeared and at the eight percent chord it has become even more prominent.

This oscillating characteristic on the leeside is observed at both Mach numbers. At Mach 8 it is first evident on the outboard inserts 4 and 5, as early as $\alpha = 15$ at the four and eight percent chord; at $\alpha = 30$ it becomes evident on all leeside gages to some degree, always increasing in amplitude with distance aft of the leading edge. At Mach 16 it again appears first on the outboard inserts but is not detectable until $\alpha = 45$ where it starts at the one percent chord on insert 4 and at the four percent chord on insert 5; at $\alpha = 60°$ the oscillation has also appeared at the eight percent chord on inserts 1, 2 & 3.

At Mach 16 a yaw effect is also noticed. At $\alpha = 30°$, $\beta = 1°$ the oscillation appears as far forward as the one percent chord on the inboard insert where as at $\alpha = 30$, $\beta = 0$ the oscillation was not detected on this insert. At $\alpha = 60°$, $\beta = 0°$ the disturbance has moved forward to the one percent chord on insert 4 and to the two percent chord on insert 5 but is weak in both instances. However, at $\alpha = 60°$, $\beta = +1°$ the disturbance appears at the one percent chord on both inserts and has increased in magnitude.

Consideration has been given to the possibility that the flow was not fully established on the leeside. However, these oscillations are not characteristic of those in an establishing separated region. A typical heat-transfer record in an establishing separated flow shows two distinct levels: usually a high steady initial level of several milliseconds followed by a steady lower level (typically 1/2 the initial level). Electrical noise, amplifier gain, absolute heating level and boundary-layer transition have also been considered and ruled out as potential causes.

Another postulation is that the heat-transfer rate oscillation is caused by a periodic change in wing attitude with respect to the flow due to torsional vibration of the wing set up by the rapid start of the tunnel. However, an analysis of the data indicates that the wing at insert 3 would have to twist $\pm$ 2 deg. while the wing at the root would have to twist $\pm$8 deg. to impart the observed oscillations in heating rate. This is clearly not possible. The above observation along with the yaw sensitivity of the oscillation strongly imply that the phenomena is aerodynamic in nature, but the effort required to explain the phenomena is beyond the scope of the current study.

SECTION IX PRECISION OF DATA

Test Conditions

The stagnation enthalpy and the test section free stream conditions were calculated, using the thermodynamic properties of real air, the incident shock wave velocity and the nozzle supply pressure. The speed of the incident shock wave was measured to within ± 1 percent. Based on the agreement of pressure transducers, the nozzle supply pressure is considered accurate to within ± 2.6 percent. The test section Mach number was determined from airflow calibrations made prior to the test program. The computed values of free stream Mach number from a large number of airflow calibrations for each nozzle-throat combination were used to calculate variation coefficients in Mach number and these variations are ±1.0% for the Mach 8, and 16 test conditions. Accordingly, the determination of free stream static pressure is considered to be accurate to within ±7 percent of the true values.

The model angle-of-attack was set to within 0.1 degree of the desired angle.

Model Data

Calibrations to determine the heat-transfer gage's temperature resistance characteristics are conducted with an error potential of 1 percent. Far more significant than this is the repeatability of the heat transfer gage during testing. A series of shock tunnel tests designed to determine repeatability of the heat transfer data has shown that the RMS deviation of the repeatability is ±3 percent. A combination of these errors indicates that the relative RMS deviation of the heat transfer data is about ±3.2 percent.

SECTION X CONCLUSIONS AND RECOMMENDATIONS

Measurements of heat transfer rates have been made on a NASA straight wing orbiter configuration with particular emphasis being given to regions of wing root/body interference, bow shock/wing impingement, and interference free sections of the wing. Moreover, the use of thin-film heat-transfer gages permitted accurate measurements to be made with unusually high spatial resolution over the areas of interest.

The data clearly show that under typical reentry conditions, the wing root/body interference heating near the wing root can be as high as, and in some cases twice as high as, heating in the bow shock/wing impingement region.

The expected steep gradients near the leading edge were observed as were the double-peaked spanwise heating distributions due to the bifurcated shock that arises from the interaction of the bow shock and wing shock. In general, the heat-transfer rates measured in this set of experiments were higher than those predicted or measured by thermal mapping and thin-skin model techniques.

The uniqueness and basic nature of this data warrants a much more careful and detailed study than time and funds have allowed. First, an investigation should be made to isolate and understand the differences between the data of this program and other investigators. This would consist of a comparison of the instrumentation techniques including resolution and errors due to conduction. Methods of evaluating $\dot{q}_o$ should also be considered. However, a more detailed description of the movement and extent of the interference and interaction regions would be of greater interest to the user of this type of information. This could be deduced from further study of the present data, and further information could be obtained by additional experiments.

SECTION XI REFERENCES

1. Description and Capabilities, Cornell Aeronautical Laboratory, Inc., Hypersonic Shock Tunnel, April 1969.

2. Vidal, R.J., "Transient Surface Temperature Measurements," CAL Report No. 114, March 1962.

3. Bogdan, L., "Heat Transfer Instrumentation," CAL Report No. WTH-021, March 1963.

4. Reece, J.W., "Shock Tube Theory for Real Air with Application to Wind Tunnel Testing and to Flight Simulation," CAL Experimental Facilities Division, WTH-003, October 1958 (Revised August 1965).

5. Wittliff, C., "Unpublished Normal Shock Calculations Using Duff's Computing Procedure," Aerodynamic Research Department, CAL, about 1963.

6. Lewis, Clark H. and Burgess, E.G., "Charts of Normal Shock Wave Properties in Imperfect Air," AEDC-TDR-64-43, March 1964.

7. Hilsenrath, J., Beckett, C.W., et al., "Tables of Thermal Properties of Gases," National Bureau of Standards Circular 564, November 1955.

8. Reece, J.W., "Test Section Conditions Generated in the Supersonic Expansion of Real Air," Reader's Forum, Journal of Aerospace Science, Vol. 29, No. 5, May 1962, pp. 617-618.

9. Neel, C.A. and Lewis, Clark H., "Interpolations of Imperfect Air Thermodynamic Data, II at Constant Pressure," AEDC-TDR-64-184, September 1964.

10. Hirschfelder, J.O., Curtis, C.F., and Bird, R.G., Molecular Theory of Gases and Liquids, J. Wiley & Sons, 1954.

11. Hansen, F.C., "Approximations for Thermodynamic and Transport Properties of High-Temperature Air," NACA TN-4150, March 1958 (Revised NASA TR-50, 1959).

12. Fay, J.A. and Riddell, F.R., "Theory of Stagnation Point Heat Transfer in Dissociated Air," Journal of Aeronautical Sciences, February 1958.

13. Goodrich, W.D., "Private Communication," October 8, 1970.

14. Seegmiller, H. Lee., "Shock Interference Heating and Density-Ratio Effects Part I - Flow Field Visualization, Thermocouple Measurements, and Analysis," NASA TM X-2272, April 1971.

15. Katzen, E. D.; Marvin, J. G.; Seegmiller, H. L.; Axelson, J. A.; Brownson, J. J.; Cleary, J. W.; Lockman, W. K.; and Kaattari, G. E.: "Static Aerodynamics, Flow Fields and Aerodynamic Heating of Space Shuttle Orbiters," NASA TM X-52876, Vol. I, pp. 142-193, July 15-17, 1970.

SECTION XII TABLE INDEX

Table No.	Title
1	Run Schedule
2	Test Conditions
3	Heat Transfer Data

Table I

RUN SCHEDULE

RUN NO.	M_∞ NOMINAL	R_E/ft x 10^{-6} NOMINAL	α	β	REMARKS
1	16.5	0.097	0	0	
2	16.2	0.97	15	0	
3	16.2	0.96	30	0	
4	16.3	1.1	45	0	
5	16.3	1.1	60	0	
6	16.2	0.95	70	0	
7	16.2	0.98	30	+1	
8	16.2	0.95	60	+1	
9	$\approx$7.6	$\approx$ 0.37	0	0	NO H.T. OR P DATA
10	7.7	2.1	45	0	
11	7.8	2.6	60	0	
12	7.7	2.2	70	0	NO SCHLIEREN
13	7.8	4.5	30	0	
14	7.8	2.6	60	+3	NO SCHLIEREN
15	7.6	0.37	0	0	
16	8.0	10.8	15	0	

Table 2 TEST CONDITIONS

RUN NO.	1	2	3	4	5	6	7	8
α	0.0	1.500E 01	3.000E 01	4.500E 01	6.000E 01	7.000E 01	3.000E 01	6.000E 01
ψ	0.0	0.0	0.0	0.0	0.0	0.0	-1.000E 00	-1.000E 00
ϕ	1.800E 02	1.800E 02	0.0	0.0	0.0	0.0	5.700E 00	1.600E 00
M_i	4.450E 00	4.726E 00	4.727E 00	4.621E 00	4.660E 00	4.738E 00	4.741E 00	4.713E 00
P_0	1.822E 03	1.879E 04	1.947E 04	1.858E 04	1.828E 04	1.780E 04	1.787E 04	1.762E 04
H_0	2.991E 07	3.342E 07	3.410E 07	3.097E 07	3.145E 07	3.302E 07	3.257E 07	3.283E 07
T_0	4.277E 03	4.711E 03	4.799E 03	4.410E 03	4.467E 03	4.658E 03	4.600E 03	4.637E 03
M_∞	1.654E 01	1.622E 01	1.625E 01	1.631E 01	1.626E 01	1.615E 01	1.615E 01	1.617E 01
U_∞	7.668E 03	8.103E 03	8.186E 03	7.801E 03	7.861E 03	8.054E 03	7.999E 03	8.031E 03
T_∞	8.937E 01	1.038E 02	1.054E 02	9.511E 01	9.724E 01	1.034E 02	1.020E 02	1.026E 02
P_∞	1.015E-03	1.296E-02	1.308E-02	1.304E-02	1.294E-02	1.263E-02	1.282E-02	1.246E-02
q_∞	1.947E-01	2.388E 00	2.421E 00	2.432E 00	2.397E 00	2.310E 00	2.344E 00	2.283E 00
ρ_∞	9.535E-07	1.048E-05	1.041E-05	1.151E-05	1.117E-05	1.025E-05	1.055E-05	1.019E-05
μ_∞	7.519E-08	8.731E-08	8.871E-08	8.002E-08	8.181E-08	8.696E-08	8.578E-08	8.629E-08
Re/FT	9.725E 04	9.721E 05	9.602E 05	1.122E 06	1.073E 06	9.498E 05	9.840E 05	9.488E 05
P^*	3.642E-01	4.477E 00	4.541E 00	4.552E 00	4.489E 00	4.330E 00	4.393E 00	4.279E 00
T^*	1.226E 03	1.335E 03	1.356E 03	1.260E 03	1.275E 03	1.323E 03	1.309E 03	1.317E 03
μ^*	6.840E-07	7.220E-07	7.290E-07	6.959E-07	7.012E-07	7.179E-07	7.132E-07	7.159E-07
$\sqrt{C^*}$	8.144E-01	8.018E-01	7.995E-01	8.104E-01	8.086E-01	8.031E-01	8.047E-01	8.038E-01
H_w	3.213E 06	3.213E 06	3.213E 06	3.213E 06	3.213E 06	3.213E 06	3.213E 06	3.213E 06
T_w	5.350E 02	5.350E 02	5.350E 02	5.350E 02	5.350E 02	5.350E 02	5.350E 02	5.350E 02
P_{ts}	5.802E-05	5.802E-05	3.868E-05	5.802E-05	5.802E-05	3.868E-05	3.868E-05	3.868E-05
R_{es}	5.175E 03	5.644E 04	5.609E 04	6.160E 04	5.994E 04	5.529E 04	5.689E 04	5.488E 04

Table 2 (CONCLUDED)

RUN NO.	10	11	12	13	14	15	16
α	4.500E 01	6.000E 01	7.000E 01	3.000E 01	6.000E 01	0.0	1.500E 01
ψ	0.0	0.0	0.0	0.0	-3.000E 00	0.0	0.0
ϕ	0.0	0.0	0.0	0.0	4.700E 00	1.800E 02	1.800E 02
M_j	2.342E 00	2.389E 00	2.379E 00	2.495E 00	2.298E 00	4.204E 00	2.462E 00
P_o	6.430E 02	8.220E 02	6.982E 02	1.644E 03	7.730E 02	6.116E 02	3.763E 03
H_o	1.010E 07	1.044E 07	1.038E 07	1.117E 07	9.880E 06	2.728E 07	1.096E 07
T_o	1.587E 03	1.643E 03	1.632E 03	1.765E 03	1.551E 03	3.952E 03	1.737E 03
M_∞	7.729E 00	7.754E 00	7.734E 00	7.845E 00	7.762E 00	7.582E 00	7.968E 00
U_∞	4.319E 03	4.392E 03	4.378E 03	4.547E 03	4.274E 03	7.088E 03	4.510E 03
T_∞	1.299E 02	1.334E 02	1.333E 02	1.397E 02	1.261E 02	3.634E 02	1.332E 02
P_∞	8.333E-02	1.044E-01	8.988E-02	1.952E-01	9.832E-02	6.502E-02	4.263E-01
q_∞	3.488E 00	4.397E 00	3.767E 00	8.420E 00	4.151E 00	2.619E 00	1.897E 01
ρ_∞	5.385E-05	6.564E-05	5.659E-05	1.173E-04	6.546E-05	1.502E-05	2.686E-04
μ_∞	1.091E-07	1.121E-07	1.119E-07	1.172E-07	1.059E-07	2.842E-07	1.119E-07
Re/FT	2.132E 06	2.573E 06	2.214E 06	4.549E 06	2.641E 06	3.745E 05	1.083E 07
P'_∞	6.416E 00	8.090E 00	6.931E 00	1.550E 01	7.634E 00	4.891E 00	3.492E 01
T'_∞	6.183E 02	6.299E 02	6.279E 02	6.541E 02	6.104E 02	1.227E 03	6.458E 02
M'_∞	4.272E-07	4.331E-07	4.321E-07	4.454E-07	4.232E-07	6.845E-07	4.412E-07
$\sqrt{C'}$	9.069E-01	9.049E-01	9.052E-01	9.006E-01	9.082E-01	8.445E-01	9.019E-01
H_w	3.213E 06	3.213E 06	3.213E 06	3.213E 06	3.213E 06	3.213E 06	3.213E 06
T_w	5.350E 02	5.350E 02	5.350E 02	5.350E 02	5.350E 02	5.350E 02	5.350E 02
P_{ts}	3.868E-05	5.802E-05	7.736E-05	5.802E-05	7.736E-05	5.802E-05	3.868E-05
R_{es}	2.894E 05	3.512E 05	3.031E 05	6.222E 05	3.531E 05	7.833E 04	1.427E 06

Table 3 HEAT TRANSFER DATA

RUN	GAGE	$\dot{q}_w$	C_h	$\dot{q}_o$	$\dot{q}_w / \dot{q}_o$	h
1	101	1.138E 01	4.536E-02	7.324E 00	1.737E-01	1.067E-02
1	102	6.114E 00	2.437E-02	7.324E 00	9.333E-02	5.732E-03
1	103	3.521E 00	1.404E-02	7.324E 00	5.375E-02	3.301E-03
1	104	2.451E 00	9.771E-03	7.324E 00	3.742E-02	2.298E-03
1	105	2.178E 00	8.682E-03	7.324E 00	3.325E-02	2.042E-03
1	106	2.115E 00	8.430E-03	7.324E 00	3.228E-02	1.983E-03
1	107	1.850E 00	7.376E-03	7.324E 00	2.825E-02	1.735E-03
1	108	1.842E 00	7.344E-03	7.324E 00	2.812E-02	1.727E-03
1	109	1.329E 00	5.295E-03	7.324E 00	2.028E-02	1.246E-03
1	110	1.880E 00	7.492E-03	7.324E 00	2.869E-02	1.762E-03
1	111	1.325E 00	5.281E-03	7.324E 00	2.022E-02	1.242E-03
1	112	3.460E 00	1.379E-02	7.324E 00	5.282E-02	3.244E-03
1	113	2.302E 00	9.175E-03	7.324E 00	3.514E-02	2.158E-03
1	114	2.561E 00	1.021E-02	7.324E 00	3.909E-02	2.401E-03
1	115	1.665E 00	6.638E-03	7.324E 00	2.542E-02	1.561E-03
1	202	3.607E 01	1.438E-01	7.324E 00	5.506E-01	3.382E-02
1	203	1.932E 01	7.702E-02	7.324E 00	2.949E-01	1.812E-02
1	204	1.363E 01	5.434E-02	7.324E 00	2.081E-01	1.278E-02
1	205	1.037E 01	4.134E-02	7.324E 00	1.583E-01	9.723E-03
1	206	8.853E 00	3.529E-02	7.324E 00	1.351E-01	8.300E-03
1	207	7.985E 00	3.183E-02	7.324E 00	1.219E-01	7.486E-03
1	208	6.267E 00	2.498E-02	7.324E 00	9.567E-02	5.876E-03
1	209	5.845E 00	2.330E-02	7.324E 00	8.923E-02	5.481E-03
1	210	4.839E 00	1.929E-02	7.324E 00	7.387E-02	4.537E-03
1	211	4.455E 00	1.776E-02	7.324E 00	6.801E-02	4.177E-03
1	212	3.162E 01	1.260E-01	7.324E 00	4.826E-01	2.964E-02
1	213	2.072E 01	8.260E-02	7.324E 00	3.163E-01	1.943E-02
1	214	1.250E 01	4.983E-02	7.324E 00	1.908E-01	1.172E-02
1	215	8.133E 00	3.242E-02	7.324E 00	1.241E-01	7.625E-03
1	301	1.749E 02	6.972E-01	7.324E 00	2.670E 00	1.640E-01
1	302	6.576E 01	2.621E-01	7.324E 00	1.004E 00	6.165E-02
1	303	3.392E 01	1.352E-01	7.324E 00	5.177E-01	3.180E-02
1	304	2.254E 01	8.985E-02	7.324E 00	3.441E-01	2.113E-02
1	305	1.730E 01	6.897E-02	7.324E 00	2.641E-01	1.622E-02

Table 3 (CONTINUED)

RUN	GAGE	$\dot{q}_w$	C_h	$\dot{q}_o$	$\dot{q}_w / \dot{q}_o$	h
1	306	1.597E 01	6.367E-02	7.324E 00	2.438E-01	1.498E-02
1	307	1.358E 01	5.413E-02	7.324E 00	2.073E-01	1.273E-02
1	308	1.009E 01	4.024E-02	7.324E 00	1.541E-01	9.465E-03
1	309	9.898E 00	3.945E-02	7.324E 00	1.511E-01	9.280E-03
1	310	8.502E 00	3.389E-02	7.324E 00	1.298E-01	7.972E-03
1	311	7.847E 00	3.128E-02	7.324E 00	1.198E-01	7.357E-03
1	312	8.809E 01	3.511E-01	7.324E 00	1.345E 00	8.259E-02
1	313	5.652E 01	2.253E-01	7.324E 00	8.627E-01	5.299E-02
1	314	3.258E 01	1.299E-01	7.324E 00	4.973E-01	3.054E-02
1	315	1.597E 01	6.366E-02	7.324E 00	2.438E-01	1.497E-02
1	402	4.733E 01	1.886E-01	7.324E 00	7.224E-01	4.437E-02
1	403	2.241E 01	8.933E-02	7.324E 00	3.421E-01	2.101E-02
1	404	1.517E 01	6.048E-02	7.324E 00	2.316E-01	1.423E-02
1	406	9.807E 00	3.909E-02	7.324E 00	1.497E-01	9.195E-03
1	407	8.419E 00	3.356E-02	7.324E 00	1.285E-01	7.893E-03
1	408	6.941E 00	2.767E-02	7.324E 00	1.060E-01	6.508E-03
1	409	6.274E 00	2.501E-02	7.324E 00	9.577E-02	5.882E-03
1	412	3.366E 01	1.342E-01	7.324E 00	5.138E-01	3.156E-02
1	413	2.505E 01	9.983E-02	7.324E 00	3.823E-01	2.348E-02
1	501	1.051E 02	4.188E-01	7.324E 00	1.604E 00	9.850E-02
1	502	4.023E 01	1.604E-01	7.324E 00	6.142E-01	3.772E-02
1	504	1.638E 01	6.529E-02	7.324E 00	2.500E-01	1.536E-02
1	505	1.352E 01	5.388E-02	7.324E 00	2.063E-01	1.267E-02
1	506	1.059E 01	4.220E-02	7.324E 00	1.616E-01	9.927E-03
1	507	6.763E 00	2.696E-02	7.324E 00	1.032E-01	6.341E-03
1	508	8.399E 00	3.348E-02	7.324E 00	1.282E-01	7.874E-03
1	509	7.637E 00	3.044E-02	7.324E 00	1.166E-01	7.161E-03
1	510	7.992E 00	3.186E-02	7.324E 00	1.220E-01	7.493E-03
1	511	6.135E 00	2.445E-02	7.324E 00	9.365E-02	5.752E-03
1	512	3.705E 01	1.477E-01	7.324E 00	5.656E-01	3.474E-02
1	601	2.401E 00	9.570E-03	7.324E 00	3.665E-02	2.251E-03
1	602	3.502E 00	1.396E-02	7.324E 00	5.345E-02	3.283E-03
1	603	4.551E 00	1.814E-02	7.324E 00	6.946E-02	4.266E-03
1	609	6.192E 00	2.468E-02	7.324E 00	9.451E-02	5.805E-03
1	610	6.467E 00	2.578E-02	7.324E 00	9.872E-02	6.064E-03
1	611	6.280E 00	2.503E-02	7.324E 00	9.586E-02	5.888E-03
1	612	6.193E 00	2.468E-02	7.324E 00	9.453E-02	5.806E-03

Table 3 (CONTINUED)

RUN	GAGE	$\dot{q}_w$	C_h	$\dot{q}_o$	$\dot{q}_w / \dot{q}_o$	h
1	613	6.379E 00	2.543E-02	7.324E 00	9.737E-02	5.980E-03
1	701	4.351E-01	1.734E-03	7.324E 00	6.642E-03	4.080E-04
1	702	3.467E-01	1.382E-03	7.324E 00	5.292E-03	3.250E-04
1	703	3.144E-01	1.253E-03	7.324E 00	4.800E-03	2.948E-04
2	101	9.533E 01	2.893E-02	2.916E 01	3.655E-01	7.900E-02
2	102	1.578E 02	4.789E-02	2.916E 01	6.050E-01	1.308E-01
2	103	8.829E 01	2.680E-02	2.916E 01	3.385E-01	7.317E-02
2	104	8.647E 01	2.624E-02	2.916E 01	3.315E-01	7.166E-02
2	105	8.000E 01	2.428E-02	2.916E 01	3.067E-01	6.630E-02
2	106	7.530E 01	2.285E-02	2.916E 01	2.887E-01	6.240E-02
2	107	7.826E 01	2.375E-02	2.916E 01	3.000E-01	6.485E-02
2	108	6.154E 01	1.868E-02	2.916E 01	2.360E-01	5.100E-02
2	109	8.189E 01	2.485E-02	2.916E 01	3.140E-01	6.786E-02
2	110	6.078E 01	1.845E-02	2.916E 01	2.330E-01	5.037E-02
2	111	7.255E 01	2.202E-02	2.916E 01	2.782E-01	6.012E-02
2	112	2.155E 01	6.540E-03	2.916E 01	8.261E-02	1.786E-02
2	113	1.348E 01	4.091E-03	2.916E 01	5.168E-02	1.117E-02
2	114	7.790E 00	2.364E-03	2.916E 01	2.987E-02	6.456E-03
2	115	3.555E 00	1.079E-03	2.916E 01	1.363E-02	2.946E-03
2	202	3.017E 02	9.157E-02	2.916E 01	1.157E 00	2.500E-01
2	203	1.708E 02	5.185E-02	2.916E 01	6.549E-01	1.416E-01
2	204	1.266E 02	3.842E-02	2.916E 01	4.853E-01	1.049E-01
2	205	1.003E 02	3.045E-02	2.916E 01	3.846E-01	8.313E-02
2	206	8.138E 01	2.470E-02	2.916E 01	3.120E-01	6.744E-02
2	207	6.963E 01	2.113E-02	2.916E 01	2.670E-01	5.770E-02
2	208	5.907E 01	1.793E-02	2.916E 01	2.265E-01	4.895E-02
2	209	5.720E 01	1.736E-02	2.916E 01	2.193E-01	4.740E-02
2	210	4.504E 01	1.367E-02	2.916E 01	1.727E-01	3.732E-02
2	211	4.727E 01	1.435E-02	2.916E 01	1.812E-01	3.917E-02
2	212	1.391E 02	4.223E-02	2.916E 01	5.334E-01	1.153E-01
2	213	7.648E 01	2.321E-02	2.916E 01	2.932E-01	6.338E-02
2	214	3.803E 01	1.154E-02	2.916E 01	1.458E-01	3.151E-02
2	215	2.204E 01	6.689E-03	2.916E 01	8.450E-02	1.826E-02
2	301	5.096E 02	1.547E-01	2.916E 01	1.954E 00	4.223E-01
2	302	2.479E 02	7.523E-02	2.916E 01	9.504E-01	2.054E-01

Table 3 (CONTINUED)

RUN	GAGE	$\dot{q}_w$	C_h	$\dot{q}_o$	$\dot{q}_w / \dot{q}_o$	h
2	303	1.575E 02	4.780E-02	2.916E 01	6.038E-01	1.305E-01
2	304	1.069E 02	3.245E-02	2.916E 01	4.100E-01	8.861E-02
2	305	9.204E 01	2.794E-02	2.916E 01	3.529E-01	7.628E-02
2	306	7.469E 01	2.267E-02	2.916E 01	2.864E-01	6.190E-02
2	307	6.954E 01	2.110E-02	2.916E 01	2.666E-01	5.762E-02
2	308	6.100E 01	1.851E-02	2.916E 01	2.339E-01	5.055E-02
2	309	5.222E 01	1.585E-02	2.916E 01	2.002E-01	4.328E-02
2	310	5.264E 01	1.598E-02	2.916E 01	2.018E-01	4.362E-02
2	311	3.708E 01	1.125E-02	2.916E 01	1.422E-01	3.073E-02
2	312	1.528E 02	4.639E-02	2.916E 01	5.860E-01	1.267E-01
2	313	8.555E 01	2.596E-02	2.916E 01	3.280E-01	7.089E-02
2	314	3.958E 01	1.201E-02	2.916E 01	1.517E-01	3.280E-02
2	315	1.876E 01	5.694E-03	2.916E 01	7.193E-02	1.555E-02
2	402	2.847E 02	8.640E-02	2.916E 01	1.091E 00	2.359E-01
2	403	1.445E 02	4.387E-02	2.916E 01	5.541E-01	1.198E-01
2	404	9.453E 01	2.869E-02	2.916E 01	3.624E-01	7.833E-02
2	406	6.754E 01	2.050E-02	2.916E 01	2.590E-01	5.597E-02
2	407	5.592E 01	1.697E-02	2.916E 01	2.144E-01	4.634E-02
2	408	4.842E 01	1.470E-02	2.916E 01	1.856E-01	4.012E-02
2	409	4.305E 01	1.307E-02	2.916E 01	1.651E-01	3.567E-02
2	410	3.804E 01	1.154E-02	2.916E 01	1.458E-01	3.152E-02
2	411	3.466E 01	1.052E-02	2.916E 01	1.329E-01	2.872E-02
2	412	1.594E 02	4.838E-02	2.916E 01	6.111E-01	1.321E-01
2	413	9.008E 01	2.734E-02	2.916E 01	3.453E-01	7.465E-02
2	414	4.356E 01	1.322E-02	2.916E 01	1.670E-01	3.610E-02
2	415	1.875E 01	5.692E-03	2.916E 01	7.190E-02	1.554E-02
2	501	4.279E 02	1.299E-01	2.916E 01	1.640E 00	3.546E-01
2	502	2.390E 02	7.253E-02	2.916E 01	9.162E-01	1.980E-01
2	503	1.507E 02	4.572E-02	2.916E 01	5.776E-01	1.248E-01
2	504	1.118E 02	3.393E-02	2.916E 01	4.286E-01	9.265E-02
2	505	8.879E 01	2.695E-02	2.916E 01	3.404E-01	7.358E-02
2	506	7.479E 01	2.270E-02	2.916E 01	2.867E-01	6.198E-02
2	507	6.890E 01	2.091E-02	2.916E 01	2.642E-01	5.710E-02
2	508	6.135E 01	1.862E-02	2.916E 01	2.352E-01	5.084E-02
2	509	5.332E 01	1.618E-02	2.916E 01	2.044E-01	4.419E-02
2	510	4.792E 01	1.454E-02	2.916E 01	1.837E-01	3.971E-02

Table 3 (CONTINUED)

RUN	GAGE	$\dot{q}_w$	C_h	$\dot{q}_o$	$\dot{q}_w / \dot{q}_o$	h
2	511	3.497E 01	1.061E-02	2.916E 01	1.341E-01	2.898E-02
2	512	1.051E 02	3.189E-02	2.916E 01	4.028E-01	8.707E-02
2	513	4.976E 01	1.510E-02	2.916E 01	1.908E-01	4.124E-02
2	514	2.651E 01	8.047E-03	2.916E 01	1.017E-01	2.197E-02
2	515	2.087E 01	6.334E-03	2.916E 01	8.002E-02	1.729E-02
2	601	3.983E 01	1.209E-02	2.916E 01	1.527E-01	3.301E-02
2	602	4.355E 01	1.322E-02	2.916E 01	1.670E-01	3.609E-02
2	603	4.614E 01	1.400E-02	2.916E 01	1.769E-01	3.824E-02
2	604	5.358E 01	1.626E-02	2.916E 01	2.054E-01	4.440E-02
2	605	6.123E 01	1.858E-02	2.916E 01	2.348E-01	5.074E-02
2	606	8.031E 01	2.437E-02	2.916E 01	3.079E-01	6.655E-02
2	607	7.179E 01	2.179E-02	2.916E 01	2.752E-01	5.949E-02
2	608	3.850E 01	1.168E-02	2.916E 01	1.476E-01	3.190E-02
2	609	4.513E 01	1.370E-02	2.916E 01	1.730E-01	3.740E-02
2	610	4.356E 01	1.319E-02	2.916E 01	1.666E-01	3.601E-02
2	611	4.842E 01	1.470E-02	2.916E 01	1.856E-01	4.012E-02
2	612	4.268E 01	1.295E-02	2.916E 01	1.636E-01	3.537E-02
2	613	4.587E 01	1.392E-02	2.916E 01	1.759E-01	3.802E-02
2	701	9.232E 00	2.802E-03	2.916E 01	3.540E-02	7.651E-03
2	703	8.572E 00	2.602E-03	2.916E 01	3.286E-02	7.103E-03
3	101	1.307E 02	3.866E-02	3.027E 01	4.829E-01	1.059E-01
3	102	2.094E 02	6.192E-02	3.027E 01	7.734E-01	1.697E-01
3	103	1.646E 02	4.866E-02	3.027E 01	6.079E-01	1.333E-01
3	104	1.625E 02	4.804E-02	3.027E 01	6.001E-01	1.316E-01
3	105	1.625E 02	4.807E-02	3.027E 01	6.004E-01	1.317E-01
3	106	1.544E 02	4.567E-02	3.027E 01	5.705E-01	1.251E-01
3	107	1.572E 02	4.650E-02	3.027E 01	5.808E-01	1.274E-01
3	108	1.531E 02	4.528E-02	3.027E 01	5.656E-01	1.241E-01
3	109	1.381E 02	4.085E-02	3.027E 01	5.102E-01	1.119E-01
3	110	1.485E 02	4.392E-02	3.027E 01	5.486E-01	1.203E-01
3	111	1.178E 02	3.483E-02	3.027E 01	4.351E-01	9.544E-02
3	112	1.952E 01	5.771E-03	3.027E 01	7.209E-02	1.581E-02
3	113	1.696E 01	5.017E-03	3.027E 01	6.266E-02	1.375E-02
3	114	8.278E 00	2.448E-03	3.027E 01	3.058E-02	6.708E-03
3	115	3.715E 00	1.099E-03	3.027E 01	1.372E-02	3.010E-03

Table 3 (CONTINUED)

RUN	GAGE	$\dot{q}_w$	C_h	$\dot{q}_o$	$\dot{q}_w / \dot{q}_o$	h
3	202	3.096E 02	9.157E-02	3.027E 01	1.144E 00	2.509E-01
3	203	2.028E 02	5.996E-02	3.027E 01	7.490E-01	1.643E-01
3	204	1.506E 02	4.453E-02	3.027E 01	5.562E-01	1.220E-01
3	205	1.268E 02	3.750E-02	3.027E 01	4.685E-01	1.028E-01
3	206	1.060E 02	3.134E-02	3.027E 01	3.915E-01	8.589E-02
3	207	9.136E 01	2.702E-02	3.027E 01	3.374E-01	7.403E-02
3	208	8.437E 01	2.495E-02	3.027E 01	3.116E-01	6.837E-02
3	209	7.901E 01	2.336E-02	3.027E 01	2.918E-01	6.402E-02
3	210	7.071E 01	2.091E-02	3.027E 01	2.612E-01	5.730E-02
3	211	7.043E 01	2.083E-02	3.027E 01	2.602E-01	5.707E-02
3	212	8.450E 01	2.499E-02	3.027E 01	3.121E-01	6.847E-02
3	213	6.091E 01	1.801E-02	3.027E 01	2.250E-01	4.936E-02
3	214	3.685E 01	1.090E-02	3.027E 01	1.361E-01	2.986E-02
3	215	1.821E 01	5.383E-03	3.027E 01	6.725E-02	1.475E-02
3	301	1.963E 02	5.806E-02	3.027E 01	7.252E-01	1.591E-01
3	302	2.440E 02	7.216E-02	3.027E 01	9.013E-01	1.977E-01
3	303	1.893E 02	5.599E-02	3.027E 01	6.993E-01	1.534E-01
3	304	1.589E 02	4.698E-02	3.027E 01	5.868E-01	1.287E-01
3	305	1.492E 02	4.411E-02	3.027E 01	5.510E-01	1.209E-01
3	306	1.504E 02	4.446E-02	3.027E 01	5.554E-01	1.218E-01
3	307	1.503E 02	4.445E-02	3.027E 01	5.552E-01	1.218E-01
3	308	1.413E 02	4.178E-02	3.027E 01	5.218E-01	1.145E-01
3	309	1.325E 02	3.917E-02	3.027E 01	4.893E-01	1.073E-01
3	310	1.287E 02	3.806E-02	3.027E 01	4.754E-01	1.043E-01
3	311	1.078E 02	3.187E-02	3.027E 01	3.981E-01	8.734E-02
3	312	9.217E 01	2.725E-02	3.027E 01	3.404E-01	7.468E-02
3	313	5.496E 01	1.625E-02	3.027E 01	2.030E-01	4.453E-02
3	314	3.276E 01	9.688E-03	3.027E 01	1.210E-01	2.655E-02
3	315	2.367E 01	6.999E-03	3.027E 01	8.743E-02	1.918E-02
3	402	2.937E 02	8.684E-02	3.027E 01	1.085E 00	2.380E-01
3	403	1.675E 02	4.952E-02	3.027E 01	6.185E-01	1.357E-01
3	404	1.250E 02	3.696E-02	3.027E 01	4.617E-01	1.013E-01
3	406	9.113E 01	2.695E-02	3.027E 01	3.366E-01	7.384E-02
3	407	7.677E 01	2.270E-02	3.027E 01	2.836E-01	6.221E-02
3	408	7.034E 01	2.080E-02	3.027E 01	2.598E-01	5.700E-02

Table 3 (CONTINUED)

RUN	GAGE	$\dot{q}_w$	C_h	$\dot{q}_o$	$\dot{q}_w / \dot{q}_o$	h
3	409	6.160E 01	1.822E-02	3.027E 01	2.275E-01	4.991E-02
3	410	5.451E 01	1.612E-02	3.027E 01	2.013E-01	4.417E-02
3	411	5.214E 01	1.542E-02	3.027E 01	1.926E-01	4.225E-02
3	413	4.601E 01	1.360E-02	3.027E 01	1.699E-01	3.728E-02
3	414	2.330E 01	6.891E-03	3.027E 01	8.608E-02	1.888E-02
3	415	1.020E 01	3.016E-03	3.027E 01	3.768E-02	8.266E-03
3	501	3.049E 02	9.016E-02	3.027E 01	1.126E 00	2.471E-01
3	502	2.662E 02	7.872E-02	3.027E 01	9.833E-01	2.157E-01
3	503	1.914E 02	5.659E-02	3.027E 01	7.069E-01	1.551E-01
3	504	1.727E 02	5.106E-02	3.027E 01	6.378E-01	1.399E-01
3	505	1.174E 02	3.470E-02	3.027E 01	4.335E-01	9.509E-02
3	506	1.016E 02	3.005E-02	3.027E 01	3.754E-01	8.235E-02
3	508	7.485E 01	2.213E-02	3.027E 01	2.765E-01	6.065E-02
3	509	7.610E 01	2.250E-02	3.027E 01	2.811E-01	6.166E-02
3	510	7.170E 01	2.120E-02	3.027E 01	2.648E-01	5.810E-02
3	511	6.037E 01	1.785E-02	3.027E 01	2.230E-01	4.891E-02
3	512	5.364E 01	1.586E-02	3.027E 01	1.981E-01	4.346E-02
3	513	2.891E 01	8.548E-03	3.027E 01	1.068E-01	2.342E-02
3	514	1.378E 01	4.075E-03	3.027E 01	5.090E-02	1.117E-02
3	601	4.258E 01	1.259E-02	3.027E 01	1.573E-01	3.450E-02
3	602	6.689E 01	1.978E-02	3.027E 01	2.471E-01	5.420E-02
3	603	7.430E 01	2.197E-02	3.027E 01	2.745E-01	6.021E-02
3	604	7.711E 01	2.280E-02	3.027E 01	2.848E-01	6.248E-02
3	605	8.029E 01	2.374E-02	3.027E 01	2.966E-01	6.506E-02
3	606	8.178E 01	2.418E-02	3.027E 01	3.021E-01	6.627E-02
3	607	1.050E 02	3.104E-02	3.027E 01	3.877E-01	8.504E-02
3	608	6.066E 01	1.794E-02	3.027E 01	2.241E-01	4.915E-02
3	610	5.991E 01	1.772E-02	3.027E 01	2.213E-01	4.854E-02
3	611	7.051E 01	2.085E-02	3.027E 01	2.604E-01	5.713E-02
3	612	6.625E 01	1.959E-02	3.027E 01	2.447E-01	5.368E-02
3	613	6.872E 01	2.032E-02	3.027E 01	2.538E-01	5.569E-02
3	701	2.227E 01	6.585E-03	3.027E 01	8.226E-02	1.804E-02
3	702	2.033E 01	6.013E-03	3.027E 01	7.511E-02	1.648E-02
3	703	1.834E 01	5.425E-03	3.027E 01	6.776E-02	1.486E-02

Table 3 (CONTINUED)

RUN	GAGE	$\dot{q}_w$	C_h	$\dot{q}_o$	$\dot{q}_w / \dot{q}_o$	h
4	101	1.208E 02	3.773E-02	2.619E 01	5.158E-01	1.090E-01
4	102	2.623E 02	8.189E-02	2.619E 01	1.119E 00	2.365E-01
4	103	2.024E 02	6.319E-02	2.619E 01	8.639E-01	1.825E-01
4	104	2.033E 02	6.347E-02	2.619E 01	8.677E-01	1.833E-01
4	105	1.961E 02	6.124E-02	2.619E 01	8.371E-01	1.768E-01
4	106	1.757E 02	5.486E-02	2.619E 01	7.499E-01	1.584E-01
4	107	1.743E 02	5.443E-02	2.619E 01	7.440E-01	1.572E-01
4	108	1.636E 02	5.107E-02	2.619E 01	6.981E-01	1.475E-01
4	109	1.471E 02	4.594E-02	2.619E 01	6.280E-01	1.327E-01
4	110	1.534E 02	4.790E-02	2.619E 01	6.547E-01	1.383E-01
4	111	1.437E 02	4.486E-02	2.619E 01	6.132E-01	1.295E-01
4	112	1.984E 01	6.194E-03	2.619E 01	8.468E-02	1.789E-02
4	113	9.725E 00	3.037E-03	2.619E 01	4.151E-02	8.769E-03
4	114	4.928E 00	1.539E-03	2.619E 01	2.104E-02	4.444E-03
4	115	2.636E 00	8.230E-04	2.619E 01	1.125E-02	2.376E-03
4	202	2.432E 02	7.593E-02	2.619E 01	1.038E 00	2.193E-01
4	203	1.856E 02	5.795E-02	2.619E 01	7.921E-01	1.673E-01
4	204	1.469E 02	4.586E-02	2.619E 01	6.269E-01	1.324E-01
4	205	1.293E 02	4.037E-02	2.619E 01	5.519E-01	1.166E-01
4	206	1.136E 02	3.548E-02	2.619E 01	4.850E-01	1.025E-01
4	207	9.916E 01	3.096E-02	2.619E 01	4.233E-01	8.941E-02
4	208	8.517E 01	2.660E-02	2.619E 01	3.636E-01	7.680E-02
4	209	8.813E 01	2.752E-02	2.619E 01	3.762E-01	7.946E-02
4	210	7.461E 01	2.330E-02	2.619E 01	3.185E-01	6.727E-02
4	211	7.673E 01	2.396E-02	2.619E 01	3.275E-01	6.919E-02
4	212	6.270E 01	1.958E-02	2.619E 01	2.676E-01	5.654E-02
4	213	3.657E 01	1.142E-02	2.619E 01	1.561E-01	3.297E-02
4	214	1.899E 01	5.929E-03	2.619E 01	8.105E-02	1.712E-02
4	215	1.127E 01	3.518E-03	2.619E 01	4.809E-02	1.016E-02
4	301	2.160E 02	6.743E-02	2.619E 01	9.218E-01	1.947E-01
4	302	1.541E 02	4.813E-02	2.619E 01	6.579E-01	1.390E-01
4	303	1.028E 02	3.209E-02	2.619E 01	4.386E-01	9.265E-02
4	304	8.797E 01	2.747E-02	2.619E 01	3.755E-01	7.932E-02

Table 3 (CONTINUED)

RUN	GAGE	$\dot{q}_w$	C_h	$\dot{q}_o$	$\dot{q}_w / \dot{q}_o$	h
4	305	8.647E 01	2.700E-02	2.619E 01	3.691E-01	7.797E-02
4	306	6.872E 01	2.146E-02	2.619E 01	2.933E-01	6.196E-02
4	307	7.214E 01	2.253E-02	2.619E 01	3.079E-01	6.505E-02
4	308	6.024E 01	1.881E-02	2.619E 01	2.571E-01	5.432E-02
4	309	5.665E 01	1.769E-02	2.619E 01	2.418E-01	5.108E-02
4	310	5.348E 01	1.670E-02	2.619E 01	2.283E-01	4.822E-02
4	311	4.891E 01	1.527E-02	2.619E 01	2.088E-01	4.410E-02
4	312	9.301E 01	2.904E-02	2.619E 01	3.970E-01	8.387E-02
4	313	5.478E 01	1.710E-02	2.619E 01	2.338E-01	4.939E-02
4	314	2.953E 01	9.219E-03	2.619E 01	1.260E-01	2.662E-02
4	315	1.344E 01	4.198E-03	2.619E 01	5.738E-02	1.212E-02
4	402	1.698E 02	5.302E-02	2.619E 01	7.248E-01	1.531E-01
4	403	1.315E 02	4.107E-02	2.619E 01	5.614E-01	1.186E-01
4	404	9.999E 01	3.122E-02	2.619E 01	4.268E-01	9.016E-02
4	406	8.148E 01	2.544E-02	2.619E 01	3.478E-01	7.347E-02
4	407	7.198E 01	2.248E-02	2.619E 01	3.072E-01	6.490E-02
4	408	6.914E 01	2.159E-02	2.619E 01	2.951E-01	6.234E-02
4	409	6.212E 01	1.940E-02	2.619E 01	2.652E-01	5.602E-02
4	410	5.796E 01	1.810E-02	2.619E 01	2.474E-01	5.226E-02
4	411	5.589E 01	1.745E-02	2.619E 01	2.386E-01	5.040E-02
4	412	2.396E 01	7.480E-03	2.619E 01	1.023E-01	2.160E-02
4	413	1.363E 01	4.256E-03	2.619E 01	5.818E-02	1.229E-02
4	414	7.217E 00	2.253E-03	2.619E 01	3.080E-02	6.507E-03
4	415	2.524E 00	7.880E-04	2.619E 01	1.077E-02	2.276E-03
4	501	9.391E 01	2.932E-02	2.619E 01	4.008E-01	8.468E-02
4	502	1.567E 02	4.894E-02	2.619E 01	6.690E-01	1.413E-01
4	503	1.434E 02	4.479E-02	2.619E 01	6.122E-01	1.293E-01
4	504	1.264E 02	3.946E-02	2.619E 01	5.394E-01	1.139E-01
4	505	1.065E 02	3.326E-02	2.619E 01	4.547E-01	9.606E-02
4	506	9.341E 01	2.917E-02	2.619E 01	3.987E-01	8.423E-02
4	507	8.701E 01	2.717E-02	2.619E 01	3.714E-01	7.845E-02
4	508	7.809E 01	2.438E-02	2.619E 01	3.333E-01	7.042E-02
4	509	7.511E 01	2.345E-02	2.619E 01	3.206E-01	6.773E-02
4	510	7.216E 01	2.253E-02	2.619E 01	3.080E-01	6.507E-02

Table 3 (CONTINUED)

RUN	GAGE	$\dot{q}_w$	C_h	$\dot{q}_o$	$\dot{q}_w / \dot{q}_o$	h
4	511	5.936E 01	1.853E-02	2.619E 01	2.534E-01	5.352E-02
4	512	1.329E 01	4.151E-03	2.619E 01	5.674E-02	1.199E-02
4	513	7.824E 00	2.443E-03	2.619E 01	3.340E-02	7.055E-03
4	514	3.430E 00	1.071E-03	2.619E 01	1.464E-02	3.093E-03
4	515	3.221E 00	1.006E-03	2.619E 01	1.375E-02	2.904E-03
4	601	6.157E 01	1.922E-02	2.619E 01	2.628E-01	5.551E-02
4	602	7.139E 01	2.229E-02	2.619E 01	3.047E-01	6.437E-02
4	603	8.632E 01	2.695E-02	2.619E 01	3.685E-01	7.783E-02
4	604	7.892E 01	2.464E-02	2.619E 01	3.369E-01	7.116E-02
4	605	8.107E 01	2.532E-02	2.619E 01	3.461E-01	7.310E-02
4	606	9.658E 01	3.016E-02	2.619E 01	4.122E-01	8.708E-02
4	607	1.077E 02	3.362E-02	2.619E 01	4.595E-01	9.707E-02
4	608	6.548E 01	2.045E-02	2.619E 01	2.795E-01	5.905E-02
4	609	1.288E 02	4.023E-02	2.619E 01	5.500E-01	1.162E-01
4	610	8.630E 01	2.695E-02	2.619E 01	3.684E-01	7.782E-02
4	611	7.176E 01	2.241E-02	2.619E 01	3.063E-01	6.470E-02
4	612	6.798E 01	2.123E-02	2.619E 01	2.902E-01	6.130E-02
4	613	6.815E 01	2.128E-02	2.619E 01	2.909E-01	6.145E-02
4	701	2.077E 01	6.485E-03	2.619E 01	8.865E-02	1.873E-02
4	702	2.156E 01	6.731E-03	2.619E 01	9.202E-02	1.944E-02
4	703	2.156E 01	6.731E-03	2.619E 01	9.202E-02	1.944E-02
5	101	8.107E 01	2.543E-02	2.662E 01	3.405E-01	7.185E-02
5	102	2.003E 02	6.284E-02	2.662E 01	8.413E-01	1.775E-01
5	103	2.075E 02	6.509E-02	2.662E 01	8.714E-01	1.839E-01
5	104	2.194E 02	6.884E-02	2.662E 01	9.216E-01	1.945E-01
5	105	2.221E 02	6.967E-02	2.662E 01	9.327E-01	1.968E-01
5	106	2.073E 02	6.504E-02	2.662E 01	8.707E-01	1.837E-01
5	107	1.989E 02	6.240E-02	2.662E 01	8.354E-01	1.763E-01
5	108	1.948E 02	6.112E-02	2.662E 01	8.182E-01	1.727E-01
5	109	1.569E 02	4.924E-02	2.662E 01	6.592E-01	1.391E-01
5	110	1.651E 02	5.179E-02	2.662E 01	6.933E-01	1.463E-01
5	111	1.621E 02	5.087E-02	2.662E 01	6.810E-01	1.437E-01
5	112	9.703E 00	3.044E-03	2.662E 01	4.075E-02	8.600E-03
5	113	5.559E 00	1.744E-03	2.662E 01	2.335E-02	4.927E-03
5	114	3.015E 00	9.458E-04	2.662E 01	1.266E-02	2.672E-03

Table 3 (CONTINUED)

RUN	GAGE	$\dot{q}_w$	C_h	$\dot{q}_o$	$\dot{q}_w / \dot{q}_o$	h
5	115	1.918E 01	6.018E-03	2.662E 01	8.056E-02	1.700E-02
5	202	1.680E 02	5.269E-02	2.662E 01	7.054E-01	1.489E-01
5	203	1.401E 02	4.396E-02	2.662E 01	5.885E-01	1.242E-01
5	204	1.184E 02	3.714E-02	2.662E 01	4.972E-01	1.049E-01
5	205	1.068E 02	3.351E-02	2.662E 01	4.487E-01	9.468E-02
5	206	9.175E 01	2.878E-02	2.662E 01	3.853E-01	8.132E-02
5	207	8.467E 01	2.656E-02	2.662E 01	3.556E-01	7.504E-02
5	208	7.121E 01	2.234E-02	2.662E 01	2.991E-01	6.311E-02
5	209	6.989E 01	2.193E-02	2.662E 01	2.935E-01	6.194E-02
5	210	5.996E 01	1.881E-02	2.662E 01	2.518E-01	5.314E-02
5	211	6.131E 01	1.923E-02	2.662E 01	2.575E-01	5.434E-02
5	213	8.371E 00	2.626E-03	2.662E 01	3.516E-02	7.419E-03
5	214	4.938E 00	1.549E-03	2.662E 01	2.074E-02	4.377E-03
5	215	3.094E 00	9.708E-04	2.662E 01	1.300E-02	2.742E-03
5	301	1.883E 02	5.909E-02	2.662E 01	7.910E-01	1.669E-01
5	302	2.078E 02	6.520E-02	2.662E 01	8.728E-01	1.842E-01
5	303	1.767E 02	5.543E-02	2.662E 01	7.420E-01	1.566E-01
5	304	1.616E 02	5.071E-02	2.662E 01	6.789E-01	1.433E-01
5	305	1.790E 02	5.616E-02	2.662E 01	7.518E-01	1.586E-01
5	306	1.227E 02	3.850E-02	2.662E 01	5.155E-01	1.088E-01
5	307	1.122E 02	3.520E-02	2.662E 01	4.713E-01	9.945E-02
5	308	9.922E 01	3.113E-02	2.662E 01	4.167E-01	8.794E-02
5	309	8.583E 01	2.693E-02	2.662E 01	3.605E-01	7.607E-02
5	310	9.449E 01	2.964E-02	2.662E 01	3.969E-01	8.374E-02
5	311	8.084E 01	2.536E-02	2.662E 01	3.395E-01	7.165E-02
5	312	3.426E 01	1.075E-02	2.662E 01	1.439E-01	3.036E-02
5	313	1.653E 01	5.185E-03	2.662E 01	6.941E-02	1.465E-02
5	314	7.445E 00	2.336E-03	2.662E 01	3.127E-02	6.598E-03
5	315	3.680E 00	1.154E-03	2.662E 01	1.545E-02	3.261E-03
5	402	1.044E 02	3.275E-02	2.662E 01	4.384E-01	9.251E-02
5	403	9.860E 01	3.093E-02	2.662E 01	4.141E-01	8.739E-02
5	404	8.935E 01	2.803E-02	2.662E 01	3.753E-01	7.919E-02
5	406	8.183E 01	2.567E-02	2.662E 01	3.437E-01	7.252E-02
5	407	7.650E 01	2.400E-02	2.662E 01	3.213E-01	6.780E-02
5	408	7.612E 01	2.388E-02	2.662E 01	3.197E-01	6.746E-02
5	409	6.909E 01	2.167E-02	2.662E 01	2.902E-01	6.123E-02

Table 3 (CONTINUED)

RUN	GAGE	$\dot{q}_w$	C_h	$\dot{q}_o$	$\dot{q}_w / \dot{q}_o$	h
5	410	6.742E 01	2.115E-02	2. 62E 01	2.832E-01	5.976E-02
5	411	6.224E 01	1.953E-02	2.662E 01	2.614E-01	5.517E-02
5	412	7.623E 00	2.392E-03	2.662E 01	3.202E-02	6.756E-03
5	413	4.542E 00	1.425E-03	2.662E 01	1.908E-02	4.026E-03
5	414	2.960E 00	9.287E-04	2.662E 01	1.243E-02	2.624E-03
5	415	8.183E-01	2.567E-04	2.662E 01	3.437E-03	7.252E-04
5	501	2.818E 01	8.841E-03	2.662E 01	1.184E-01	2.498E-02
5	502	9.413E 01	2.953E-02	2.662E 01	3.954E-01	8.343E-02
5	503	9.929E 01	3.115E-02	2.662E 01	4.170E-01	8.799E-02
5	504	9.780E 01	3.068E-02	2.662E 01	4.108E-01	8.668E-02
5	505	8.649E 01	2.714E-02	2.662E 01	3.633E-01	7.666E-02
5	506	8.049E 01	2.525E-02	2.662E 01	3.381E-01	7.134E-02
5	507	7.770E 01	2.438E-02	2.662E 01	3.263E-01	6.886E-02
5	508	7.033E 01	2.206E-02	2.662E 01	2.954E-01	6.233E-02
5	509	7.424E 01	2.329E-02	2.662E 01	3.118E-01	6.579E-02
5	510	7.495E 01	2.351E-02	2.662E 01	3.148E-01	6.642E-02
5	511	6.048E 01	1.897E-02	2.662E 01	2.540E-01	5.360E-02
5	512	1.954E 00	6.130E-04	2.662E 01	8.206E-03	1.732E-03
5	513	2.215E 00	6.950E-04	2.662E 01	9.305E-03	1.963E-03
5	514	1.160E 00	3.640E-04	2.662E 01	4.873E-03	1.028E-03
5	515	1.346E 00	4.224E-04	2.662E 01	5.655E-03	1.193E-03
5	601	1.023E 02	3.208E-02	2.662E 01	4.295E-01	9.064E-02
5	602	8.031E 01	2.519E-02	2.662E 01	3.373E-01	7.118E-02
5	603	8.052E 01	2.526E-02	2.662E 01	3.382E-01	7.136E-02
5	604	7.006E 01	2.198E-02	2.662E 01	2.943E-01	6.210E-02
5	605	8.046E 01	2.524E-02	2.662E 01	3.379E-01	7.131E-02
5	606	9.460E 01	2.968E-02	2.662E 01	3.973E-01	8.384E-02
5	607	9.564E 01	3.001E-02	2.662E 01	4.017E-01	8.477E-02
5	608	1.118E 02	3.507E-02	2.662E 01	4.695E-01	9.908E-02
5	609	8.763E 01	2.749E-02	2.662E 01	3.680E-01	7.767E-02
5	610	8.231E 01	2.582E-02	2.662E 01	3.457E-01	7.295E-02
5	611	7.903E 01	2.479E-02	2.662E 01	3.319E-01	7.004E-02
5	612	7.879E 01	2.472E-02	2.662E 01	3.309E-01	6.983E-02
5	613	7.478E 01	2.346E-02	2.662E 01	3.141E-01	6.627E-02
5	701	2.751E 01	8.632E-03	2.662E 01	1.156E-01	2.439E-02
5	702	2.960E 01	9.286E-03	2.662E 01	1.243E-01	2.623E-02
5	703	2.558E 01	8.026E-03	2.662E 01	1.075E-01	2.267E-02

Table 3 (CONTINUED)

RUN	GAGE	$\dot{q}_w$	C_h	$\dot{q}_o$	$\dot{q}_w / \dot{q}_o$	h
6	101	5.868E 01	1.854E-02	2.816E 01	2.330E-01	4.927E-02
6	102	1.680E 02	5.309E-02	2.816E 01	6.670E-01	1.410E-01
6	103	2.094E 02	6.619E-02	2.816E 01	8.316E-01	1.759E-01
6	104	2.214E 02	6.996E-02	2.816E 01	8.790E-01	1.859E-01
6	105	2.178E 02	6.882E-02	2.816E 01	8.647E-01	1.829E-01
6	106	2.103E 02	6.645E-02	2.816E 01	8.348E-01	1.765E-01
6	107	2.075E 02	6.556E-02	2.816E 01	8.238E-01	1.742E-01
6	108	1.866E 02	5.896E-02	2.816E 01	7.408E-01	1.567E-01
6	109	1.689E 02	5.336E-02	2.816E 01	6.705E-01	1.418E-01
6	110	1.589E 02	5.023E-02	2.816E 01	6.310E-01	1.334E-01
6	111	1.665E 02	5.260E-02	2.816E 01	6.609E-01	1.398E-01
6	112	7.643E 00	2.415E-03	2.816E 01	3.034E-02	6.417E-03
6	113	3.477E 00	1.099E-03	2.816E 01	1.380E-02	2.919E-03
6	114	2.129E 00	6.728E-04	2.816E 01	8.453E-03	1.788E-03
6	115	1.063E 00	3.358E-04	2.816E 01	4.219E-03	8.923E-04
6	202	1.199E 02	3.788E-02	2.816E 01	4.760E-01	1.007E-01
6	203	1.080E 02	3.411E-02	2.816E 01	4.286E-01	9.064E-02
6	204	1.026E 02	3.243E-02	2.816E 01	4.074E-01	8.616E-02
6	205	9.729E 01	3.074E-02	2.816E 01	3.863E-01	8.169E-02
6	206	8.517E 01	2.692E-02	2.816E 01	3.382E-01	7.151E-02
6	207	8.052E 01	2.545E-02	2.816E 01	3.197E-01	6.761E-02
6	208	7.627E 01	2.410E-02	2.816E 01	3.028E-01	6.404E-02
6	209	7.437E 01	2.350E-02	2.816E 01	2.953E-01	6.245E-02
6	210	6.586E 01	2.081E-02	2.816E 01	2.615E-01	5.530E-02
6	211	6.860E 01	2.168E-02	2.816E 01	2.724E-01	5.760E-02
6	212	5.587E 00	1.766E-03	2.816E 01	2.218E-02	4.691E-03
6	213	2.701E 00	8.537E-04	2.816E 01	1.073E-02	2.268E-03
6	214	1.358E 00	4.293E-04	2.816E 01	5.393E-03	1.141E-03
6	215	9.286E-01	2.935E-04	2.816E 01	3.687E-03	7.797E-04
6	301	7.366E 01	2.328E-02	2.816E 01	2.925E-01	6.185E-02
6	302	1.129E 02	3.567E-02	2.816E 01	4.481E-01	9.477E-02
6	303	1.166E 02	3.686E-02	2.816E 01	4.632E-01	9.795E-02
6	304	1.068E 02	3.376E-02	2.816E 01	4.241E-01	8.969E-02
6	305	9.357E 01	2.957E-02	2.816E 01	3.715E-01	7.856E-02
6	306	8.877E 01	2.805E-02	2.816E 01	3.525E-01	7.454E-02
6	307	8.668E 01	2.739E-02	2.816E 01	3.442E-01	7.279E-02
6	308	7.655E 01	2.419E-02	2.816E 01	3.039E-01	6.427E-02

Table 3 (CONTINUED)

RUN	GAGE	$\dot{q}_w$	C_h	$\dot{q}_o$	$\dot{q}_w / \dot{q}_o$	h
6	309	6.824E 01	2.157E-02	2.816E 01	2.710E-01	5.730E-02
6	310	7.010E 01	2.215E-02	2.816E 01	2.783E-01	5.886E-02
6	311	7.281E 01	2.301E-02	2.816E 01	2.891E-01	6.114E-02
6	312	9.244E 00	2.921E-03	2.816E 01	3.670E-02	7.762E-03
6	313	3.883E 00	1.227E-03	2.816E 01	1.542E-02	3.260E-03
6	314	1.965E 00	6.210E-04	2.816E 01	7.803E-03	1.650E-03
6	315	1.323E 00	4.181E-04	2.816E 01	5.253E-03	1.111E-03
6	402	9.035E 01	2.855E-02	2.816E 01	3.587E-01	7.586E-02
6	403	9.268E 01	2.929E-02	2.816E 01	3.680E-01	7.782E-02
6	404	8.104E 01	2.561E-02	2.816E 01	3.218E-01	6.804E-02
6	406	7.477E 01	2.363E-02	2.816E 01	2.969E-01	6.278E-02
6	407	6.937E 01	2.192E-02	2.816E 01	2.754E-01	5.825E-02
6	408	6.686E 01	2.113E-02	2.816E 01	2.655E-01	5.614E-02
6	409	6.455E 01	2.040E-02	2.816E 01	2.563E-01	5.420E-02
6	410	6.040E 01	1.909E-02	2.816E 01	2.398E-01	5.072E-02
6	411	5.892E 01	1.862E-02	2.816E 01	2.339E-01	4.947E-02
6	412	3.565E 00	1.127E-03	2.816E 01	1.416E-02	2.994E-03
6	413	1.825E 00	5.766E-04	2.816E 01	7.245E-03	1.532E-03
6	414	1.350E 00	4.267E-04	2.816E 01	5.361E-03	1.134E-03
6	415	8.128E-01	2.569E-04	2.816E 01	3.227E-03	6.825E-04
6	501	1.789E 01	5.653E-03	2.816E 01	7.103E-02	1.502E-02
6	502	7.610E 01	2.405E-02	2.816E 01	3.021E-01	6.390E-02
6	503	8.474E 01	2.678E-02	2.816E 01	3.364E-01	7.115E-02
6	504	7.980E 01	2.522E-02	2.816E 01	3.168E-01	6.700E-02
6	505	7.773E 01	2.457E-02	2.816E 01	3.086E-01	6.527E-02
6	506	7.410E 01	2.342E-02	2.816E 01	2.942E-01	6.222E-02
6	507	7.153E 01	2.261E-02	2.816E 01	2.840E-01	6.006E-02
6	508	6.787E 01	2.145E-02	2.816E 01	2.695E-01	5.699E-02
6	509	7.496E 01	2.369E-02	2.816E 01	2.976E-01	6.294E-02
6	510	6.586E 01	2.081E-02	2.816E 01	2.615E-01	5.530E-02
6	511	5.643E 01	1.783E-02	2.816E 01	2.241E-01	4.738E-02
6	512	1.051E 00	3.322E-04	2.816E 01	4.174E-03	8.827E-04
6	513	2.030E 00	6.414E-04	2.816E 01	8.059E-03	1.704E-03
6	514	1.571E 00	4.964E-04	2.816E 01	6.236E-03	1.319E-03
6	515	1.704E 00	5.385E-04	2.816E 01	6.765E-03	1.431E-03
6	601	8.837E 01	2.793E-02	2.816E 01	3.509E-01	7.420E-02
6	602	7.618E 01	2.408E-02	2.816E 01	3.025E-01	6.397E-02

Table 3 (CONTINUED)

RUN	GAGE	$\dot{q}_w$	C_h	$\dot{q}_o$	$\dot{q}_w / \dot{q}_o$	h
6	603	9.026E 01	2.852E-02	2.816E 01	3.584E-01	7.578E-02
6	604	7.695E 01	2.432E-02	2.816E 01	3.055E-01	6.461E-02
6	605	7.085E 01	2.239E-02	2.816E 01	2.813E-01	5.949E-02
6	606	7.959E 01	2.515E-02	2.816E 01	3.160E-01	6.683E-02
6	607	7.446E 01	2.353E-02	2.816E 01	2.957E-01	6.252E-02
6	608	7.063E 01	2.232E-02	2.816E 01	2.805E-01	5.931E-02
6	609	6.679E 01	2.111E-02	2.816E 01	2.652E-01	5.608E-02
6	610	8.144E 01	2.574E-02	2.816E 01	3.234E-01	6.838E-02
6	611	6.862E 01	2.168E-02	2.816E 01	2.724E-01	5.762E-02
6	612	6.776E 01	2.141E-02	2.816E 01	2.690E-01	5.689E-02
6	613	7.179E 01	2.269E-02	2.816E 01	2.851E-01	6.028E-02
6	701	2.990E 01	9.449E-03	2.816E 01	1.187E-01	2.511E-02
6	702	3.627E 01	1.146E-02	2.816E 01	1.440E-01	3.046E-02
6	703	2.666E 01	8.424E-03	2.816E 01	1.058E-01	2.238E-02
7	101	1.350E 02	4.238E-02	2.775E 01	5.439E-01	1.151E-01
7	102	1.968E 02	6.178E-02	2.775E 01	7.928E-01	1.677E-01
7	103	1.545E 02	4.851E-02	2.775E 01	6.225E-01	1.317E-01
7	104	1.509E 02	4.739E-02	2.775E 01	6.082E-01	1.287E-01
7	105	1.505E 02	4.725E-02	2.775E 01	6.064E-01	1.283E-01
7	106	1.576E 02	4.948E-02	2.775E 01	6.350E-01	1.343E-01
7	107	1.556E 02	4.883E-02	2.775E 01	6.268E-01	1.326E-01
7	108	1.514E 02	4.755E-02	2.775E 01	6.102E-01	1.291E-01
7	109	1.415E 02	4.443E-02	2.775E 01	5.702E-01	1.206E-01
7	110	1.412E 02	4.432E-02	2.775E 01	5.688E-01	1.203E-01
7	111	1.379E 02	4.331E-02	2.775E 01	5.558E-01	1.176E-01
7	112	2.699E 01	8.474E-03	2.775E 01	1.088E-01	2.301E-02
7	113	1.506E 01	4.728E-03	2.775E 01	6.068E-02	1.284E-02
7	114	7.569E 00	2.376E-03	2.775E 01	3.050E-02	6.452E-03
7	115	3.729E 00	1.171E-03	2.775E 01	1.502E-02	3.178E-03
7	202	2.960E 02	9.293E-02	2.775E 01	1.193E 00	2.523E-01
7	203	1.919E 02	6.026E-02	2.775E 01	7.733E-01	1.636E-01
7	204	1.471E 02	4.619E-02	2.775E 01	5.928E-01	1.254E-01
7	205	1.207E 02	3.789E-02	2.775E 01	4.863E-01	1.029E-01
7	206	9.910E 01	3.111E-02	2.775E 01	3.993E-01	8.447E-02
7	207	8.924E 01	2.802E-02	2.775E 01	3.596E-01	7.607E-02

Table 3 (CONTINUED)

RUN	GAGE	$\dot{q}_w$	C_h	$\dot{q}_o$	$\dot{q}_w / \dot{q}_o$	h
7	208	7.770E 01	2.439E-02	2.775E 01	3.131E-01	6.623E-02
7	209	7.533E 01	2.365E-02	2.775E 01	3.035E-01	6.421E-02
7	210	6.532E 01	2.051E-02	2.775E 01	2.632E-01	5.568E-02
7	211	6.730E 01	2.113E-02	2.775E 01	2.712E-01	5.737E-02
7	212	9.827E 01	3.085E-02	2.775E 01	3.960E-01	8.377E-02
7	213	5.409E 01	1.698E-02	2.775E 01	2.179E-01	4.610E-02
7	214	2.866E 01	8.998E-03	2.775E 01	1.155E-01	2.443E-02
7	215	1.676E 01	5.262E-03	2.775E 01	6.754E-02	1.429E-02
7	301	2.993E 02	9.395E-02	2.775E 01	1.206E 00	2.551E-01
7	302	2.186E 02	6.863E-02	2.775E 01	8.808E-01	1.863E-01
7	303	1.504E 02	4.722E-02	2.775E 01	6.060E-01	1.282E-01
7	304	1.157E 02	3.633E-02	2.775E 01	4.663E-01	9.865E-02
7	305	1.002E 02	3.145E-02	2.775E 01	4.037E-01	8.540E-02
7	306	8.367E 01	2.627E-02	2.775E 01	3.371E-01	7.132E-02
7	307	8.355E 01	2.623E-02	2.775E 01	3.366E-01	7.122E-02
7	308	6.544E 01	2.055E-02	2.775E 01	2.637E-01	5.579E-02
7	309	4.544E 01	1.427E-02	2.775E 01	1.831E-01	3.874E-02
7	310	4.788E 01	1.503E-02	2.775E 01	1.929E-01	4.081E-02
7	311	3.813E 01	1.197E-02	2.775E 01	1.537E-01	3.251E-02
7	312	1.220E 02	3.830E-02	2.775E 01	4.916E-01	1.040E-01
7	313	7.689E 01	2.414E-02	2.775E 01	3.098E-01	6.554E-02
7	314	4.934E 01	1.549E-02	2.775E 01	1.988E-01	4.206E-02
7	315	2.805E 01	8.807E-03	2.775E 01	1.130E-01	2.391E-02
7	402	2.700E 02	8.476E-02	2.775E 01	1.088E 00	2.302E-01
7	403	1.612E 02	5.062E-02	2.775E 01	6.497E-01	1.375E-01
7	404	1.192E 02	3.743E-02	2.775E 01	4.804E-01	1.016E-01
7	406	8.930E 01	2.804E-02	2.775E 01	3.598E-01	7.612E-02
7	407	7.154E 01	2.246E-02	2.775E 01	2.882E-01	6.098E-02
7	408	6.759E 01	2.122E-02	2.775E 01	2.723E-01	5.762E-02
7	409	5.942E 01	1.866E-02	2.775E 01	2.394E-01	5.065E-02
7	410	5.427E 01	1.704E-02	2.775E 01	2.187E-01	4.626E-02
7	411	5.310E 01	1.667E-02	2.775E 01	2.140E-01	4.527E-02
7	412	8.704E 01	2.732E-02	2.775E 01	3.507E-01	7.419E-02
7	413	4.513E 01	1.417E-02	2.775E 01	1.818E-01	3.847E-02
7	414	2.257E 01	7.085E-03	2.775E 01	9.094E-02	1.924E-02
7	415	1.002E 01	3.145E-03	2.775E 01	4.037E-02	8.540E-03

Table 3 (CONTINUED)

RUN	GAGE	$\dot{q}_w$	C_h	$\dot{q}_o$	$\dot{q}_w / \dot{q}_o$	h
7	501	2.845E 02	8.931E-02	2.775E 01	1.146E 00	2.425E-01
7	502	2.564E 02	8.049E-02	2.775E 01	1.033E 00	2.186E-01
7	504	1.351E 02	4.242E-02	2.775E 01	5.445E-01	1.152E-01
7	505	1.110E 02	3.484E-02	2.775E 01	4.472E-01	9.460E-02
7	506	9.253E 01	2.905E-02	2.775E 01	3.728E-01	7.888E-02
7	507	8.367E 01	2.627E-02	2.775E 01	3.371E-01	7.132E-02
7	508	7.276E 01	2.284E-02	2.775E 01	2.932E-01	6.202E-02
7	509	7.117E 01	2.234E-02	2.775E 01	2.868E-01	6.067E-02
7	510	6.443E 01	2.023E-02	2.775E 01	2.596E-01	5.492E-02
7	511	5.548E 01	1.742E-02	2.775E 01	2.235E-01	4.729E-02
7	512	5.414E 01	1.700E-02	2.775E 01	2.181E-01	4.615E-02
7	513	2.906E 01	9.124E-03	2.775E 01	1.171E-01	2.477E-02
7	514	1.392E 01	4.372E-03	2.775E 01	5.611E-02	1.187E-02
7	515	1.096E 01	3.442E-03	2.775E 01	4.417E-02	9.345E-03
7	601	6.891E 01	2.163E-02	2.775E 01	2.776E-01	5.874E-02
7	602	6.152E 01	1.931E-02	2.775E 01	2.479E-01	5.244E-02
7	603	6.749E 01	2.119E-02	2.775E 01	2.719E-01	5.753E-02
7	604	7.274E 01	2.284E-02	2.775E 01	2.931E-01	6.200E-02
7	605	7.611E 01	2.389E-02	2.775E 01	3.067E-01	6.488E-02
7	606	1.106E 02	3.473E-02	2.775E 01	4.457E-01	9.429E-02
7	607	5.290E 01	1.661E-02	2.775E 01	2.131E-01	4.509E-02
7	608	7.250E 01	2.276E-02	2.775E 01	2.921E-01	6.180E-02
7	609	5.793E 01	1.819E-02	2.775E 01	2.334E-01	4.938E-02
7	610	5.850E 01	1.836E-02	2.775E 01	2.357E-01	4.986E-02
7	611	5.846E 01	1.835E-02	2.775E 01	2.356E-01	4.983E-02
7	612	6.304E 01	1.979E-02	2.775E 01	2.540E-01	5.374E-02
7	613	6.173E 01	1.938E-02	2.775E 01	2.487E-01	5.262E-02
7	701	1.221E 01	3.833E-03	2.775E 01	4.920E-02	1.041E-02
7	702	1.323E 01	4.154E-03	2.775E 01	5.331E-02	1.128E-02
7	703	1.255E 01	3.940E-03	2.775E 01	5.057E-02	1.070E-02
8	101	6.987E 01	2.242E-02	2.778E 01	2.812E-01	5.905E-02
8	102	1.815E 02	5.825E-02	2.778E 01	7.307E-01	1.534E-01
8	103	2.102E 02	6.744E-02	2.778E 01	8.459E-01	1.776E-01
8	104	2.128E 02	6.828E-02	2.778E 01	8.564E-01	1.798E-01
8	105	2.105E 02	6.755E-02	2.778E 01	8.472E-01	1.779E-01

Table 3 (CONTINUED)

RUN	GAGE	$\dot{q}_w$	C_h	$\dot{q}_o$	$\dot{q}_w / \dot{q}_o$	h
8	106	2.030E 02	6.514E-02	2.778E 01	8.170E-01	1.716E-01
8	107	1.957E 02	6.281E-02	2.778E 01	7.878E-01	1.654E-01
8	108	1.898E 02	6.091E-02	2.778E 01	7.640E-01	1.604E-01
8	109	1.705E 02	5.472E-02	2.778E 01	6.864E-01	1.441E-01
8	110	1.699E 02	5.452E-02	2.778E 01	6.838E-01	1.436E-01
8	111	1.633E 02	5.240E-02	2.778E 01	6.572E-01	1.380E-01
8	112	8.844E 00	2.838E-03	2.778E 01	3.560E-02	7.475E-03
8	113	4.459E 00	1.431E-03	2.778E 01	1.795E-02	3.768E-03
8	114	2.272E 00	7.290E-04	2.778E 01	9.143E-03	1.920E-03
8	115	1.572E 00	5.044E-04	2.778E 01	6.326E-03	1.328E-03
8	202	1.772E 02	5.686E-02	2.778E 01	7.132E-01	1.498E-01
8	203	1.426E 02	4.577E-02	2.778E 01	5.740E-01	1.205E-01
8	204	1.257E 02	4.033E-02	2.778E 01	5.059E-01	1.062E-01
8	205	1.140E 02	3.657E-02	2.778E 01	4.587E-01	9.631E-02
8	206	1.033E 02	3.314E-02	2.778E 01	4.157E-01	8.729E-02
8	207	9.105E 01	2.922E-02	2.778E 01	3.664E-01	7.694E-02
8	208	7.914E 01	2.539E-02	2.778E 01	3.185E-01	6.688E-02
8	209	7.831E 01	2.513E-02	2.778E 01	3.152E-01	6.618E-02
8	210	6.642E 01	2.131E-02	2.778E 01	2.673E-01	5.613E-02
8	211	6.603E 01	2.119E-02	2.778E 01	2.657E-01	5.580E-02
8	212	1.813E 01	5.819E-03	2.778E 01	7.299E-02	1.533E-02
8	213	1.031E 01	3.309E-03	2.778E 01	4.150E-02	8.714E-03
8	214	5.706E 00	1.831E-03	2.778E 01	2.297E-02	4.822E-03
8	215	3.403E 00	1.092E-03	2.778E 01	1.370E-02	2.876E-03
8	301	1.826E 02	5.859E-02	2.778E 01	7.349E-01	1.543E-01
8	302	2.102E 02	6.746E-02	2.778E 01	8.461E-01	1.777E-01
8	308	1.093E 02	3.507E-02	2.778E 01	4.398E-01	9.235E-02
8	309	9.242E 01	2.966E-02	2.778E 01	3.720E-01	7.810E-02
8	310	9.683E 01	3.107E-02	2.778E 01	3.897E-01	8.183E-02
8	311	8.986E 01	2.883E-02	2.778E 01	3.617E-01	7.594E-02
8	312	2.984E 01	9.576E-03	2.778E 01	1.201E-01	2.522E-02
8	313	1.472E 01	4.724E-03	2.778E 01	5.926E-02	1.244E-02
8	314	6.849E 00	2.198E-03	2.778E 01	2.757E-02	5.788E-03
8	315	3.481E 00	1.117E-03	2.778E 01	1.401E-02	2.942E-03
8	402	1.205E 02	3.868E-02	2.778E 01	4.851E-01	1.019E-01
8	403	1.052E 02	3.375E-02	2.778E 01	4.233E-01	8.888E-02
8	404	8.993E 01	2.886E-02	2.778E 01	3.620E-01	7.600E-02

Table 3 (CONTINUED)

RUN	GAGE	$\dot{q}_w$	C_h	$\dot{q}_o$	$\dot{q}_w / \dot{q}_o$	h
8	406	8.286E 01	2.659E-02	2.778E 01	3.335E-01	7.003E-02
8	407	7.606E 01	2.441E-02	2.778E 01	3.061E-01	6.428E-02
8	410	6.734E 01	2.161E-02	2.778E 01	2.710E-01	5.691E-02
8	411	6.664E 01	2.138E-02	2.778E 01	2.682E-01	5.632E-02
8	412	8.669E 00	2.782E-03	2.778E 01	3.489E-02	7.326E-03
8	413	4.450E 00	1.428E-03	2.778E 01	1.791E-02	3.761E-03
8	414	1.846E 00	5.923E-04	2.778E 01	7.429E-03	1.560E-03
8	415	1.658E 00	5.320E-04	2.778E 01	6.672E-03	1.401E-03
8	501	2.849E 01	9.141E-03	2.778E 01	1.147E-01	2.408E-02
8	502	9.660E 01	3.100E-02	2.778E 01	3.888E-01	8.164E-02
8	504	9.170E 01	2.943E-02	2.778E 01	3.691E-01	7.750E-02
8	505	8.423E 01	2.703E-02	2.778E 01	3.390E-01	7.119E-02
8	506	8.141E 01	2.612E-02	2.778E 01	3.277E-01	6.880E-02
8	507	7.819E 01	2.509E-02	2.778E 01	3.147E-01	6.608E-02
8	508	7.002E 01	2.247E-02	2.778E 01	2.818E-01	5.918E-02
8	509	7.304E 01	2.344E-02	2.778E 01	2.940E-01	6.173E-02
8	510	7.146E 01	2.293E-02	2.778E 01	2.876E-01	6.039E-02
8	511	5.461E 01	1.752E-02	2.778E 01	2.198E-01	4.615E-02
8	512	3.360E 00	1.078E-03	2.778E 01	1.352E-02	2.839E-03
8	513	2.303E 00	7.391E-04	2.778E 01	9.270E-03	1.946E-03
8	514	1.986E 00	6.373E-04	2.778E 01	7.994E-03	1.678E-03
8	515	1.467E 00	4.709E-04	2.778E 01	5.906E-03	1.240E-03
8	601	1.064E 02	3.413E-02	2.778E 01	4.281E-01	8.989E-02
8	602	7.922E 01	2.542E-02	2.778E 01	3.188E-01	6.695E-02
8	603	6.915E 01	2.219E-02	2.778E 01	2.783E-01	5.844E-02
8	604	7.288E 01	2.339E-02	2.778E 01	2.933E-01	6.159E-02
8	605	8.557E 01	2.746E-02	2.778E 01	3.444E-01	7.232E-02
8	606	9.568E 01	3.070E-02	2.778E 01	3.851E-01	8.086E-02
8	607	1.016E 02	3.261E-02	2.778E 01	4.090E-01	8.587E-02
8	608	8.483E 01	2.722E-02	2.778E 01	3.414E-01	7.169E-02
8	609	8.344E 01	2.677E-02	2.778E 01	3.358E-01	7.052E-02
8	610	7.787E 01	2.499E-02	2.778E 01	3.134E-01	6.581E-02
8	611	7.651E 01	2.455E-02	2.778E 01	3.079E-01	6.466E-02
8	612	6.958E 01	2.233E-02	2.778E 01	2.801E-01	5.881E-02
8	613	7.833E 01	2.514E-02	2.778E 01	3.153E-01	6.620E-02
8	701	5.020E 01	1.611E-02	2.778E 01	2.020E-01	4.242E-02
8	702	2.629E 01	8.436E-03	2.778E 01	1.058E-01	2.222E-02
8	703	2.268E 01	7.277E-03	2.778E 01	9.127E-02	1.917E-02

Table 3 (CONTINUED)

RUN	GAGE	$\dot{q}_w$	C_h	$\dot{q}_o$	$\dot{q}_w / \dot{q}_o$	h
10	101	2.516E 01	1.222E-02	6.572E 00	4.280E-01	9.144E-02
10	102	5.996E 01	2.912E-02	6.572E 00	1.020E 00	2.179E-01
10	103	6.579E 01	3.196E-02	6.572E 00	1.119E 00	2.391E-01
10	104	6.389E 01	3.103E-02	6.572E 00	1.087E 00	2.322E-01
10	105	5.549E 01	2.695E-02	6.572E 00	9.439E-01	2.017E-01
10	106	5.392E 01	2.619E-02	6.572E 00	9.173E-01	1.960E-01
10	107	5.002E 01	2.430E-02	6.572E 00	8.509E-01	1.818E-01
10	108	4.675E 01	2.271E-02	6.572E 00	7.952E-01	1.699E-01
10	109	4.104E 01	1.993E-02	6.572E 00	6.981E-01	1.492E-01
10	110	4.164E 01	2.022E-02	6.572E 00	7.083E-01	1.513E-01
10	111	3.641E 01	1.768E-02	6.572E 00	6.193E-01	1.323E-01
10	112	2.988E 00	1.452E-03	6.572E 00	5.083E-02	1.086E-02
10	113	1.313E 00	6.377E-04	6.572E 00	2.233E-02	4.772E-03
10	114	5.744E-01	2.790E-04	6.572E 00	9.771E-03	2.088E-03
10	115	0.0	0.0	6.572E 00	0.0	0.0
10	202	5.758E 01	2.797E-02	6.572E 00	9.795E-01	2.093E-01
10	203	4.337E 01	2.107E-02	6.572E 00	7.378E-01	1.576E-01
10	204	3.491E 01	1.696E-02	6.572E 00	5.938E-01	1.269E-01
10	205	2.968E 01	1.442E-02	6.572E 00	5.049E-01	1.079E-01
10	206	2.597E 01	1.261E-02	6.572E 00	4.417E-01	9.438E-02
10	207	2.304E 01	1.119E-02	6.572E 00	3.920E-01	8.376E-02
10	208	1.977E 01	9.602E-03	6.572E 00	3.363E-01	7.185E-02
10	209	2.041E 01	9.917E-03	6.572E 00	3.473E-01	7.420E-02
10	210	1.888E 01	9.169E-03	6.572E 00	3.211E-01	6.861E-02
10	211	2.003E 01	9.730E-03	6.572E 00	3.407E-01	7.280E-02
10	212	1.255E 01	6.096E-03	6.572E 00	2.135E-01	4.561E-02
10	213	6.727E 00	3.268E-03	6.572E 00	1.144E-01	2.445E-02
10	214	3.427E 00	1.665E-03	6.572E 00	5.830E-02	1.246E-02
10	215	1.901E 00	9.235E-04	6.572E 00	3.234E-02	6.910E-03
10	301	7.822E 01	3.800E-02	6.572E 00	1.331E 00	2.843E-01
10	302	9.408E 01	4.570E-02	6.572E 00	1.600E 00	3.420E-01
10	303	6.756E 01	3.282E-02	6.572E 00	1.149E 00	2.456E-01
10	304	5.607E 01	2.723E-02	6.572E 00	9.537E-01	2.038E-01
10	305	4.375E 01	2.125E-02	6.572E 00	7.443E-01	1.590E-01
10	306	3.766E 01	1.830E-02	6.572E 00	6.407E-01	1.369E-01
10	307	3.091E 01	1.501E-02	6.572E 00	5.258E-01	1.123E-01

Table 3 (CONTINUED)

RUN	GAGE	$\dot{q}_w$	C_h	$\dot{q}_o$	$\dot{q}_w / \dot{q}_o$	h
10	308	2.743E 01	1.332E-02	6.572E 00	4.666E-01	9.969E-02
10	309	2.543E 01	1.235E-02	6.572E 00	4.326E-01	9.244E-02
10	310	2.322E 01	1.128E-02	6.572E 00	3.950E-01	8.439E-02
10	311	2.137E 01	1.038E-02	6.572E 00	3.635E-01	7.767E-02
10	312	1.392E 01	6.761E-03	6.572E 00	2.368E-01	5.059E-02
10	313	8.028E 00	3.900E-03	6.572E 00	1.366E-01	2.918E-02
10	314	3.880E 00	1.884E-03	6.572E 00	6.599E-02	1.410E-02
10	315	1.538E 00	7.469E-04	6.572E 00	2.616E-02	5.589E-03
10	402	4.098E 01	1.991E-02	6.572E 00	6.971E-01	1.490E-01
10	403	4.314E 01	2.095E 02	6.572E 00	7.338E-01	1.568E-01
10	404	3.457E 01	1.679E-02	6.572E 00	5.881E-01	1.257E-01
10	406	3.169E 01	1.539E-02	6.572E 00	5.390E-01	1.152E-01
10	407	3.049E 01	1.481E-02	6.572E 00	5.187E-01	1.108E-01
10	408	3.265E 01	1.586E-02	6.572E 00	5.554E-01	1.187E-01
10	409	3.146E 01	1.528E-02	6.572E 00	5.351E-01	1.143E-01
10	410	3.121E 01	1.516E-02	6.572E 00	5.309E-01	1.134E-01
10	411	3.053E 01	1.483E-02	6.572E 00	5.194E-01	1.110E-01
10	412	4.275E 00	2.076E-03	6.572E 00	7.271E-02	1.554E-02
10	413	2.326E 00	1.130E-03	6.572E 00	3.957E-02	8.454E-03
10	414	8.339E-01	4.051E-04	6.572E 00	1.419E-02	3.031E-03
10	415	4.789E-01	2.326E-04	6.572E 00	8.147E-03	1.741E-03
10	501	1.981E 01	9.620E-03	6.572E 00	3.369E-01	7.198E-02
10	502	3.743E 01	1.818E-02	6.572E 00	6.368E-01	1.361E-01
10	504	2.829E 01	1.374E-02	6.572E 00	4.813E-01	1.028E-01
10	505	2.409E 01	1.170E-02	6.572E 00	4.097E-01	8.754E-02
10	506	2.225E 01	1.081E-02	6.572E 00	3.785E-01	8.087E-02
10	507	2.058E 01	9.995E-03	6.572E 00	3.500E-01	7.479E-02
10	508	1.763E 01	8.565E-03	6.572E 00	2.999E-01	6.408E-02
10	509	1.840E 01	8.939E-03	6.572E 00	3.130E-01	6.689E-02
10	510	1.712E 01	8.318E-03	6.572E 00	2.913E-01	6.224E-02
10	511	1.368E 01	6.644E-03	6.572E 00	2.327E-01	4.971E-02
10	512	1.986E 00	9.647E-04	6.572E 00	3.378E-02	7.218E-03
10	513	1.494E 00	7.255E-04	6.572E 00	2.541E-02	5.429E-03
10	514	5.003E-01	2.430E-04	6.572E 00	8.510E-03	1.818E-03
10	515	9.582E-01	4.655E-04	6.572E 00	1.630E-02	3.483E-03
10	601	1.847E 01	8.971E-03	6.572E 00	3.142E-01	6.712E-02

Table 3 (CONTINUED)

RUN	GAGE	$\dot{q}_w$	C_h	$\dot{q}_o$	$\dot{q}_w / \dot{q}_o$	h
10	602	1.532E 01	7.442E-03	6.572E 00	2.606E-01	5.568E-02
10	603	1.939E 01	9.417E-03	6.572E 00	3.298E-01	7.046E-02
10	604	2.321E 01	1.127E-02	6.572E 00	3.948E-01	8.436E-02
10	605	1.896E 01	9.211E-03	6.572E 00	3.226E-01	6.892E-02
10	606	1.566E 01	7.607E-03	6.572E 00	2.664E-01	5.692E-02
10	607	5.157E 01	2.505E-02	6.572E 00	8.772E-01	1.874E-01
10	608	2.381E 01	1.156E-02	6.572E 00	4.050E-01	8.653E-02
10	609	1.441E 01	6.999E-03	6.572E 00	2.451E-01	5.237E-02
10	610	2.733E 01	1.328E-02	6.572E 00	4.650E-01	9.935E-02
10	611	2.103E 01	1.022E-02	6.572E 00	3.578E-01	7.644E-02
10	612	3.164E 01	1.537E-02	6.572E 00	5.382E-01	1.150E-01
10	613	2.846E 01	1.383E-02	6.572E 00	4.842E-01	1.035E-01
10	701	3.967E 00	1.927E-03	6.572E 00	6.749E-02	1.442E-02
10	702	3.971E 00	1.929E-03	6.572E 00	6.754E-02	1.443E-02
10	703	4.442E 00	2.158E-03	6.572E 00	7.557E-02	1.615E-02
11	101	1.494E 01	5.581E-03	7.762E 00	2.152E-01	5.176E-02
11	102	5.366E 01	2.004E-02	7.762E 00	7.729E-01	1.859E-01
11	103	6.723E 01	2.511E-02	7.762E 00	9.684E-01	2.329E-01
11	104	7.206E 01	2.691E-02	7.762E 00	1.038E 00	2.496E-01
11	105	7.107E 01	2.654E-02	7.762E 00	1.024E 00	2.462E-01
11	106	6.383E 01	2.384E-02	7.762E 00	9.194E-01	2.211E-01
11	107	6.413E 01	2.395E-02	7.762E 00	9.237E-01	2.221E-01
11	108	6.457E 01	2.411E-02	7.762E 00	9.299E-01	2.237E-01
11	109	5.651E 01	2.111E-02	7.762E 00	8.140E-01	1.958E-01
11	110	5.789E 01	2.162E-02	7.762E 00	8.338E-01	2.005E-01
11	111	5.199E 01	1.942E-02	7.762E 00	7.488E-01	1.801E-01
11	112	1.709E 00	6.383E-04	7.762E 00	2.461E-02	5.920E-03
11	113	7.697E-01	2.875E-04	7.762E 00	1.109E-02	2.666E-03
11	114	3.608E-01	1.348E-04	7.762E 00	5.197E-03	1.250E-03
11	115	0.0	0.0	7.762E 00	0.0	0.0
11	202	4.042E 01	1.510E-02	7.762E 00	5.822E-01	1.400E-01
11	203	3.750E 01	1.401E-02	7.762E 00	5.401E-01	1.299E-01
11	204	3.228E 01	1.206E-02	7.762E 00	4.650E-01	1.118E-01
11	205	2.922E 01	1.091E-02	7.762E 00	4.209E-01	1.012E-01
11	206	2.512E 01	9.383E-03	7.762E 00	3.619E-01	8.703E-02
11	207	2.391E 01	8.931E-03	7.762E 00	3.444E-01	8.233E-02

Table 3 (CONTINUED)

RUN	GAGE	$\dot{q}_w$	C_h	$\dot{q}_o$	$\dot{q}_w / \dot{q}_o$	h
11	208	2.203E 01	8.229E-03	7.762E 00	3.173E-01	7.632E-02
11	209	2.372E 01	8.859E-03	7.762E 00	3.416E-01	8.216E-02
11	210	2.253E 01	8.416E-03	7.762E 00	3.246E-01	7.806E-02
11	211	2.351E 01	8.782E-03	7.762E 00	3.387E-01	8.145E-02
11	212	2.799E 00	1.045E-03	7.762E 00	4.031E-02	9.696E-03
11	213	1.323E 00	4.941E-04	7.762E 00	1.905E-02	4.582E-03
11	214	5.325E-01	1.989E-04	7.762E 00	7.669E-03	1.844E-03
11	215	0.0	0.0	7.762E 00	0.0	0.0
11	301	3.614E 01	1.350E-02	7.762E 00	5.206E-01	1.252E-01
11	302	6.137E 01	2.292E-02	7.762E 00	8.839E-01	2.126E-01
11	303	5.106E 01	1.907E-02	7.762E 00	7.354E-01	1.769E-01
11	304	4.395E 01	1.641E-02	7.762E 00	6.330E-01	1.522E-01
11	305	3.785E 01	1.414E-02	7.762E 00	5.451E-01	1.311E-01
11	306	3.551E 01	1.326E-02	7.762E 00	5.115E-01	1.230E-01
11	307	3.176E 01	1.186E-02	7.762E 00	4.575E-01	1.100E-01
11	308	3.018E 01	1.127E-02	7.762E 00	4.347E-01	1.046E-01
11	309	2.879E 01	1.075E-02	7.762E 00	4.147E-01	9.974E-02
11	310	2.693E 01	1.006E-02	7.762E 00	3.879E-01	9.330E-02
11	311	2.480E 01	9.263E-03	7.762E 00	3.572E-01	8.592E-02
11	312	2.985E 00	1.115E-03	7.762E 00	4.300E-02	1.034E-02
11	313	1.431E 00	5.345E-04	7.762E 00	2.061E-02	4.957E-03
11	314	6.539E-01	2.442E-04	7.762E 00	9.418E-03	2.265E-03
11	315	0.0	0.0	7.762E 00	0.0	0.0
11	402	3.260E 01	1.218E-02	7.762E 00	4.696E-01	1.129E-01
11	403	3.041E 01	1.136E-02	7.762E 00	4.380E-01	1.053E-01
11	404	2.885E 01	1.078E-02	7.762E 00	4.156E-01	9.995E-02
11	406	2.483E 01	9.275E-03	7.762E 00	3.577E-01	8.603E-02
11	407	2.411E 01	9.006E-03	7.762E 00	3.473E-01	8.353E-02
11	408	2.464E 01	9.202E-03	7.762E 00	3.549E-01	8.534E-02
11	409	2.176E 01	8.127E-03	7.762E 00	3.134E-01	7.537E-02
11	410	2.218E 01	8.283E-03	7.762E 00	3.194E-01	7.682E-02
11	411	1.713E 01	6.397E-03	7.762E 00	2.467E-01	5.933E-02
11	412	1.773E 00	6.622E-04	7.762E 00	2.554E-02	6.142E-03
11	413	6.157E-01	2.300E-04	7.762E 00	8.868E-03	2.133E-03
11	414	3.530E-01	1.319E-04	7.762E 00	5.085E-03	1.223E-03
11	415	0.0	0.0	7.762E 00	0.0	0.0
11	501	7.475E 00	2.792E-03	7.762E 00	1.077E-01	2.589E-02

Table 3 (CONTINUED)

RUN	GAGE	$\dot{q}_w$	C_h	$\dot{q}_o$	$\dot{q}_w / \dot{q}_o$	h
11	502	3.377E 01	1.261E-02	7.762E 00	4.864E-01	1.170E-01
11	504	3.426E 01	1.280E-02	7.762E 00	4.935E-01	1.187E-01
11	505	3.388E 01	1.265E-02	7.762E 00	4.879E-01	1.173E-01
11	506	3.173E 01	1.185E-02	7.762E 00	4.570E-01	1.099E-01
11	507	3.058E 01	1.142E-02	7.762E 00	4.405E-01	1.059E-01
11	508	3.094E 01	1.156E-02	7.762E 00	4.457E-01	1.072E-01
11	509	3.124E 01	1.167E-02	7.762E 00	4.499E-01	1.082E-01
11	510	3.124E 01	1.167E-02	7.762E 00	4.499E-01	1.082E-01
11	511	2.618E 01	9.777E-03	7.762E 00	3.770E-01	9.068E-02
11	512	5.194E-01	1.940E-04	7.762E 00	7.480E-03	1.799E-03
11	513	3.078E-01	1.149E-04	7.762E 00	4.433E-03	1.066E-03
11	514	2.103E-01	7.855E-05	7.762E 00	3.029E-03	7.286E-04
11	515	4.547E-01	1.698E-04	7.762E 00	6.549E-03	1.575E-03
11	601	3.758E 01	1.404E-02	7.762E 00	5.413E-01	1.302E-01
11	602	2.709E 01	1.012E-02	7.762E 00	3.901E-01	9.383E-02
11	603	2.341E 01	8.743E-03	7.762E 00	3.372E-01	8.109E-02
11	604	2.233E 01	8.342E-03	7.762E 00	3.217E-01	7.737E-02
11	605	2.154E 01	8.044E-03	7.762E 00	3.102E-01	7.461E-02
11	606	2.251E 01	8.407E-03	7.762E 00	3.242E-01	7.797E-02
11	607	2.404E 01	8.978E-03	7.762E 00	3.462E-01	8.327E-02
11	608	2.452E 01	9.157E-03	7.762E 00	3.531E-01	8.493E-02
11	609	2.435E 01	9.093E-03	7.762E 00	3.507E-01	8.433E-02
11	610	2.153E 01	8.042E-03	7.762E 00	3.101E-01	7.458E-02
11	611	1.881E 01	7.024E-03	7.762E 00	2.709E-01	6.515E-02
11	612	1.910E 01	7.133E-03	7.762E 00	2.751E-01	6.616E-02
11	613	1.837E 01	6.862E-03	7.762E 00	2.646E-01	6.364E-02
11	701	1.333E 01	4.979E-03	7.762E 00	1.920E-01	4.618E-02
12	101	1.126E 01	4.936E-03	7.119E 00	1.768E-01	3.934E-02
12	102	4.639E 01	2.033E-02	7.119E 00	7.285E-01	1.621E-01
12	103	6.031E 01	2.643E-02	7.119E 00	9.471E-01	2.107E-01
12	104	6.309E 01	2.765E-02	7.119E 00	9.907E-01	2.204E-01
12	105	6.008E 01	2.634E-02	7.119E 00	9.436E-01	2.099E-01
12	106	5.556E 01	2.435E-02	7.119E 00	8.725E-01	1.941E-01
12	107	5.596E 01	2.453E-02	7.119E 00	8.789E-01	1.955E-01
12	108	4.792E 01	2.101E-02	7.119E 00	7.526E-01	1.674E-01
12	109	4.500E 01	1.973E-02	7.119E 00	7.067E-01	1.572E-01

Table 3 (CONTINUED)

RUN	GAGE	$\dot{q}_w$	C_h	$\dot{q}_o$	$\dot{q}_w / \dot{q}_o$	h
12	110	4.576E 01	2.006E-02	7.119E 00	7.186E-01	1.599E-01
12	111	4.215E 01	1.847E-02	7.119E 00	6.619E-01	1.473E-01
12	112	1.001E 00	4.389E-04	7.119E 00	1.572E-02	3.499E-03
12	113	4.587E-01	2.011E-04	7.119E 00	7.203E-03	1.603E-03
12	114	0.0	0.0	7.119E 00	0.0	0.0
12	115	0.0	0.0	7.119E 00	0.0	0.0
12	202	2.523E 01	1.106E-02	7.119E 00	3.962E-01	8.814E-02
12	203	2.587E 01	1.134E-02	7.119E 00	4.063E-01	9.039E-02
12	204	2.384E 01	1.045E-02	7.119E 00	3.744E-01	8.331E-02
12	205	2.288E 01	1.003E-02	7.119E 00	3.593E-01	7.995E-02
12	206	1.993E 01	8.734E-03	7.119E 00	3.129E-01	6.962E-02
12	207	1.982E 01	8.688E-03	7.119E 00	3.113E-01	6.925E-02
12	208	1.796E 01	7.874E-03	7.119E 00	2.821E-01	6.276E-02
12	209	1.872E 01	8.205E-03	7.119E 00	2.940E-01	6.540E-02
12	210	1.735E 01	7.604E-03	7.119E 00	2.724E-01	6.062E-02
12	211	1.811E 01	7.937E-03	7.119E 00	2.843E-01	6.327E-02
12	212	4.411E-01	1.933E-04	7.119E 00	6.927E-03	1.541E-03
12	213	0.0	0.0	7.119E 00	0.0	0.0
12	214	0.0	0.0	7.119E 00	0.0	0.0
12	215	0.0	0.0	7.119E 00	0.0	0.0
12	301	1.209E 01	5.297E-03	7.119E 00	1.898E-01	4.223E-02
12	302	3.031E 01	1.329E-02	7.119E 00	4.760E-01	1.059E-01
12	303	3.009E 01	1.319E-02	7.119E 00	4.725E-01	1.051E-01
12	304	2.676E 01	1.173E-02	7.119E 00	4.203E-01	9.351E-02
12	305	2.514E 01	1.102E-02	7.119E 00	3.948E-01	8.784E-02
12	306	2.353E 01	1.032E-02	7.119E 00	3.696E-01	8.223E-02
12	307	2.116E 01	9.277E-03	7.119E 00	3.324E-01	7.395E-02
12	308	2.140E 01	9.379E-03	7.119E 00	3.360E-01	7.476E-02
12	309	2.022E 01	8.862E-03	7.119E 00	3.175E-01	7.064E-02
12	310	1.961E 01	8.594E-03	7.119E 00	3.079E-01	6.851E-02
12	311	1.904E 01	8.345E-03	7.119E 00	2.990E-01	6.652E-02
12	312	5.666E-01	2.483E-04	7.119E 00	8.897E-03	1.980E-03
12	313	0.0	0.0	7.119E 00	0.0	0.0
12	314	0.0	0.0	7.119E 00	0.0	0.0
12	315	0.0	0.0	7.119E 00	0.0	0.0
12	402	2.233E 01	9.787E-03	7.119E 00	3.507E-01	7.802E-02
12	403	2.291E 01	1.004E-02	7.119E 00	3.598E-01	8.006E-02

Table 3 (CONTINUED)

RUN	GAGE	$\dot{q}_w$	C_h	$\dot{q}_o$	$\dot{q}_w / \dot{q}_o$	h
12	404	2.053E 01	9.001E-03	7.119E 00	3.225E-01	7.175E-02
12	406	1.809E 01	7.931E-03	7.119E 00	2.841E-01	6.322E-02
12	407	1.733E 01	7.596E-03	7.119E 00	2.721E-01	6.055E-02
12	408	1.686E 01	7.389E-03	7.119E 00	2.647E-01	5.890E-02
12	409	1.634E 01	7.163E-03	7.119E 00	2.566E-01	5.710E-02
12	410	1.567E 01	6.869E-03	7.119E 00	2.461E-01	5.476E-02
12	411	1.528E 01	6.697E-03	7.119E 00	2.399E-01	5.339E-02
12	412	4.246E-01	1.861E-04	7.119E 00	6.668E-03	1.484E-03
12	413	3.847E-01	1.686E-04	7.119E 00	6.042E-03	1.344E-03
12	414	0.0	0.0	7.119E 00	0.0	0.0
12	415	1.333E-01	5.845E-05	7.119E 00	2.094E-03	4.659E-04
12	501	3.420E 00	1.499E-03	7.119E 00	5.371E-02	1.195E-02
12	502	1.987E 01	8.709E-03	7.119E 00	3.120E-01	6.943E-02
12	504	2.091E 01	9.165E-03	7.119E 00	3.283E-01	7.306E-02
12	505	2.029E 01	8.893E-03	7.119E 00	3.186E-01	7.089E-02
12	506	1.955E 01	8.567E-03	7.119E 00	3.069E-01	6.829E-02
12	507	1.963E 01	8.603E-03	7.119E 00	3.082E-01	6.858E-02
12	508	1.771E 01	7.764E-03	7.119E 00	2.781E-01	6.189E-02
12	509	1.763E 01	7.726E-03	7.119E 00	2.768E-01	6.158E-02
12	510	1.760E 01	7.714E-03	7.119E 00	2.764E-01	6.149E-02
12	511	1.541E 01	6.753E-03	7.119E 00	2.420E-01	5.383E-02
12	512	8.710E-02	3.818E-05	7.119E 00	1.368E-03	3.043E-04
12	513	9.992E-01	4.380E-04	7.119E 00	1.569E-02	3.491E-03
12	514	2.613E-01	1.145E-04	7.119E 00	4.103E-03	9.129E-04
12	515	7.652E-01	3.354E-04	7.119E 00	1.202E-02	2.674E-03
12	601	2.436E 01	1.068E-02	7.119E 00	3.826E-01	8.512E-02
12	602	1.904E 01	8.345E-03	7.119E 00	2.990E-01	6.652E-02
12	603	1.753E 01	7.685E-03	7.119E 00	2.753E-01	6.126E-02
12	604	1.718E 01	7.531E-03	7.119E 00	2.698E-01	6.003E-02
12	605	1.758E 01	7.707E-03	7.119E 00	2.761E-01	6.144E-02
12	606	2.086E 01	9.144E-03	7.119E 00	3.276E-01	7.289E-02
12	607	1.814E 01	7.953E-03	7.119E 00	2.849E-01	6.340E-02
12	608	1.791E 01	7.850E-03	7.119E 00	2.812E-01	6.257E-02
12	609	2.284E 01	1.001E-02	7.119E 00	3.587E-01	7.981E-02
12	610	1.672E 01	7.328E-03	7.119E 00	2.625E-01	5.841E-02
12	613	1.618E 01	7.091E-03	7.119E 00	2.541E-01	5.653E-02
12	701	9.936E 00	4.355E-03	7.119E 00	1.560E-01	3.472E-02
12	702	1.170E 01	5.128E-03	7.119E 00	1.837E-01	4.088E-02
12	703	1.076E 01	4.715E-03	7.119E 00	1.689E-01	3.758E-02

Table 3 (CONTINUED)

RUN	GAGE	$\dot{q}_w$	C_h	$\dot{q}_o$	$\dot{q}_w / \dot{q}_o$	h
13	101	5.320E 01	9.758E-03	1.188E 01	5.005E-01	1.674E-01
13	102	7.927E 01	1.454E-02	1.188E 01	7.458E-01	2.495E-01
13	103	5.940E 01	1.090E-02	1.188E 01	5.589E-01	1.870E-01
13	104	5.630E 01	1.033E-02	1.188E 01	5.297E-01	1.772E-01
13	105	4.748E 01	8.710E-03	1.188E 01	4.467E-01	1.494E-01
13	106	4.618E 01	8.471E-03	1.188E 01	4.345E-01	1.453E-01
13	107	4.595E 01	8.428E-03	1.188E 01	4.323E-01	1.446E-01
13	108	4.592E 01	8.423E-03	1.188E 01	4.320E-01	1.445E-01
13	109	4.413E 01	8.095E-03	1.188E 01	4.152E-01	1.389E-01
13	110	4.201E 01	7.706E-03	1.188E 01	3.953E-01	1.322E-01
13	111	3.869E 01	7.097E-03	1.188E 01	3.640E-01	1.218E-01
13	112	8.862E 00	1.626E-03	1.188E 01	8.339E-02	2.789E-02
13	113	4.622E 00	8.479E-04	1.188E 01	4.349E-02	1.455E-02
13	114	2.234E 00	4.098E-04	1.188E 01	2.102E-02	7.031E-03
13	115	6.585E-01	1.208E-04	1.188E 01	6.196E-03	2.072E-03
13	202	1.084E 02	1.989E-02	1.188E 01	1.020E 00	3.412E-01
13	203	7.858E 01	1.441E-02	1.188E 01	7.393E-01	2.473E-01
13	204	5.976E 01	1.096E-02	1.188E 01	5.623E-01	1.881E-01
13	205	4.409E 01	8.038E-03	1.188E 01	4.148E-01	1.388E-01
13	206	3.864E 01	7.088E-03	1.188E 01	3.635E-01	1.216E-01
13	207	3.571E 01	6.550E-03	1.188E 01	3.360E-01	1.124E-01
13	208	2.923E 01	5.362E-03	1.188E 01	2.750E-01	9.200E-02
13	209	2.877E 01	5.278E-03	1.188E 01	2.707E-01	9.056E-02
13	210	2.597E 01	4.763E-03	1.188E 01	2.443E-01	8.172E-02
13	211	2.647E 01	4.856E-03	1.188E 01	2.491E-01	8.331E-02
13	212	3.398E 01	6.233E-03	1.188E 01	3.197E-01	1.069E-01
13	213	1.983E 01	3.637E-03	1.188E 01	1.866E-01	6.241E-02
13	214	9.658E 00	1.772E-03	1.188E 01	9.087E-02	3.039E-02
13	215	5.449E 00	9.995E-04	1.188E 01	5.127E-02	1.715E-02
13	301	1.883E 02	3.454E-02	1.188E 01	1.771E 00	5.925E-01
13	302	1.729E 02	3.173E-02	1.188E 01	1.627E 00	5.443E-01
13	303	1.373E 02	2.518E-02	1.188E 01	1.292E 00	4.321E-01
13	304	1.213E 02	2.225E-02	1.188E 01	1.141E 00	3.817E-01
13	305	1.167E 02	2.140E-02	1.188E 01	1.098E 00	3.672E-01
13	306	1.135E 02	2.081E-02	1.188E 01	1.068E 00	3.571E-01
13	307	1.029E 02	1.888E-02	1.188E 01	9.684E-01	3.239E-01
13	308	9.215E 01	1.690E-02	1.188E 01	8.670E-01	2.900E-01

Table 3 (CONTINUED)

RUN	GAGE	$\dot{q}_w$	c_h	$\dot{q}_o$	$\dot{q}_w / \dot{q}_o$	h
13	309	8.127E 01	1.491E-02	1.188E 01	7.647E-01	2.558E-01
13	310	7.227E 01	1.326E-02	1.188E 01	6.800E-01	2.275E-01
13	311	7.010E 01	1.286E-02	1.188E 01	6.596E-01	2.206E-01
13	312	5.602E 01	1.028E-02	1.188E 01	5.271E-01	1.763E-01
13	313	3.333E 01	6.114E-03	1.188E 01	3.136E-01	1.049E-01
13	314	1.693E 01	3.106E-03	1.188E 01	1.593E-01	5.330E-02
13	315	9.043E 00	1.659E-03	1.188E 01	8.508E-02	2.846E-02
13	402	1.096E 02	2.011E-02	1.188E 01	1.031E 00	3.450E-01
13	403	7.009E 01	1.286E-02	1.188E 01	6.633E-01	2.205E-01
13	404	4.964E 01	9.106E-03	1.188E 01	4.671E-01	1.562E-01
13	406	3.620E 01	6.640E-03	1.188E 01	3.406E-01	1.139E-01
13	407	3.069E 01	5.631E-03	1.188E 01	2.888E-01	9.660E-02
13	408	2.738E 01	5.022E-03	1.188E 01	2.576E-01	8.616E-02
13	409	2.364E 01	4.336E-03	1.188E 01	2.224E-01	7.440E-02
13	410	1.857E 01	3.406E-03	1.188E 01	1.747E-01	5.843E-02
13	411	1.576E 01	2.891E-03	1.188E 01	1.483E-01	4.961E-02
13	412	3.462E 01	6.350E-03	1.188E 01	3.257E-01	1.090E-01
13	413	1.863E 01	3.417E-03	1.188E 01	1.753E-01	5.863E-02
13	414	8.364E 00	1.534E-03	1.188E 01	7.869E-02	2.632E-02
13	415	3.208E 00	5.884E-04	1.188E 01	3.018E-02	1.009E-02
13	501	1.217E 02	2.232E-02	1.188E 01	1.145E 00	3.830E-01
13	502	1.094E 02	2.007E-02	1.188E 01	1.030E 00	3.444E-01
13	504	5.869E 01	1.077E-02	1.188E 01	5.522E-01	1.847E-01
13	505	4.572E 01	8.386E-03	1.188E 01	4.302E-01	1.439E-01
13	506	4.072E 01	7.469E-03	1.188E 01	3.831E-01	1.281E-01
13	507	3.615E 01	6.631E-03	1.188E 01	3.401E-01	1.138E-01
13	508	3.012E 01	5.525E-03	1.188E 01	2.834E-01	9.479E-02
13	509	2.838E 01	5.206E-03	1.188E 01	2.671E-01	8.933E-02
13	510	2.629E 01	4.822E-03	1.188E 01	2.473E-01	8.273E-02
13	511	1.902E 01	3.488E-03	1.188E 01	1.789E-01	5.985E-02
13	512	2.111E 01	3.872E-03	1.188E 01	1.986E-01	6.643E-02
13	513	1.039E 01	1.906E-03	1.188E 01	9.775E-02	3.270E-02
13	514	4.962E 00	9.102E-04	1.188E 01	4.668E-02	1.562E-02
13	515	3.666E 00	6.725E-04	1.188E 01	3.449E-02	1.154E-02
13	601	2.339E 01	4.291E-03	1.188E 01	2.201E-01	7.363E-02
13	602	2.507E 01	4.600E-03	1.188E 01	2.359E-01	7.891E-02
13	603	2.652E 01	4.866E-03	1.188E 01	2.496E-01	8.348E-02

Table 3 (CONTINUED)

RUN	GAGE	$\dot{q}_w$	C_h	$\dot{q}_o$	$\dot{q}_w / \dot{q}_o$	h
13	604	2.684E 01	4.923E-03	1.188E 01	2.525E-01	8.446E-02
13	605	2.599E 01	4.768E-03	1.188E 01	2.445E-01	8.180E-02
13	606	2.693E 01	4.940E-03	1.188E 01	2.534E-01	8.475E-02
13	607	3.063E 01	5.620E-03	1.188E 01	2.882E-01	9.641E-02
13	608	5.539E 01	1.016E-02	1.188E 01	5.212E-01	1.743E-01
13	609	2.368E 01	4.344E-03	1.188E 01	2.228E-01	7.453E-02
13	610	3.445E 01	6.319E-03	1.188E 01	3.241E-01	1.084E-01
13	611	4.594E 01	8.428E-03	1.188E 01	4.323E-01	1.446E-01
13	612	2.519E 01	4.620E-03	1.188E 01	2.370E-01	7.927E-02
13	613	2.289E 01	4.199E-03	1.188E 01	2.154E-01	7.205E-02
13	701	1.480E 01	2.716E-03	1.188E 01	1.393E-01	4.659E-02
13	703	1.383E 01	2.536E-03	1.188E 01	1.301E-01	4.352E-02
14	101	1.190E 01	4.963E-03	6.930E 00	1.920E-01	4.467E-02
14	102	4.477E 01	1.867E-02	6.930E 00	7.223E-01	1.681E-01
14	103	5.225E 01	2.179E-02	6.930E 00	8.429E-01	1.961E-01
14	104	5.613E 01	2.341E-02	6.930E 00	9.055E-01	2.107E-01
14	105	5.798E 01	2.419E-02	6.930E 00	9.355E-01	2.177E-01
14	106	5.354E 01	2.233E-02	6.930E 00	8.637E-01	2.010E-01
14	107	5.139E 01	2.144E-02	6.930E 00	8.291E-01	1.929E-01
14	108	4.892E 01	2.041E-02	6.930E 00	7.892E-01	1.836E-01
14	109	4.648E 01	1.939E-02	6.930E 00	7.498E-01	1.745E-01
14	110	4.701E 01	1.961E-02	6.930E 00	7.584E-01	1.765E-01
14	111	4.585E 01	1.912E-02	6.930E 00	7.397E-01	1.721E-01
14	112	1.180E 00	4.924E-04	6.930E 00	1.904E-02	4.431E-03
14	113	5.309E-01	2.215E-04	6.930E 00	8.566E-03	1.993E-03
14	114	0.0	0.0	6.930E 00	0.0	0.0
14	115	0.0	0.0	6.930E 00	0.0	0.0
14	202	3.439E 01	1.435E-02	6.930E 00	5.548E-01	1.291E-01
14	203	2.948E 01	1.230E-02	6.930E 00	4.756E-01	1.107E-01
14	204	2.918E 01	1.217E-02	6.930E 00	4.708E-01	1.096E-01
14	205	2.592E 01	1.081E-02	6.930E 00	4.181E-01	9.730E-02
14	206	2.319E 01	9.675E-03	6.930E 00	3.742E-01	8.707E-02
14	207	2.190E 01	9.136E-03	6.930E 00	3.534E-01	8.222E-02

Table 3 (CONTINUED)

RUN	GAGE	$\dot{q}_w$	C_h	$\dot{q}_o$	$\dot{q}_w / \dot{q}_o$	h
14	208	2.052E 01	8.560E-03	6.930E 00	3.311E-01	7.704E-02
14	209	2.107E 01	8.788E-03	6.930E 00	3.399E-01	7.909E-02
14	210	2.013E 01	8.397E-03	6.930E 00	3.248E-01	7.557E-02
14	211	2.023E 01	8.438E-03	6.930E 00	3.263E-01	7.594E-02
14	212	1.810E 00	7.550E-04	6.930E 00	2.920E-02	6.795E-03
14	213	8.282E-01	3.454E-04	6.930E 00	1.336E-02	3.109E-03
14	214	0.0	0.0	6.930E 00	0.0	0.0
14	215	0.0	0.0	6.930E 00	0.0	0.0
14	301	1.938E 01	8.084E-03	6.930E 00	3.127E-01	7.275E-02
14	302	3.800E 01	1.585E-02	6.930E 00	6.130E-01	1.426E-01
14	303	3.494E 01	1.457E-02	6.930E 00	5.636E-01	1.312E-01
14	304	3.303E 01	1.378E-02	6.930E 00	5.328E-01	1.240E-01
14	305	2.860E 01	1.193E-02	6.930E 00	4.614E-01	1.074E-01
14	306	2.766E 01	1.154E-02	6.930E 00	4.462E-01	1.038E-01
14	307	2.634E 01	1.099E-02	6.930E 00	4.250E-01	9.889E-02
14	308	2.538E 01	1.059E-02	6.930E 00	4.095E-01	9.528E-02
14	309	2.530E 01	1.055E-02	6.930E 00	4.082E-01	9.499E-02
14	310	2.498E 01	1.042E-02	6.930E 00	4.030E-01	9.376E-02
14	311	2.384E 01	9.943E-03	6.930E 00	3.846E-01	8.949E-02
14	312	1.542E 00	6.431E-04	6.930E 00	2.487E-02	5.788E-03
14	313	6.897E-01	2.877E-04	6.930E 00	1.113E-02	2.589E-03
14	314	0.0	0.0	6.930E 00	0.0	0.0
14	315	0.0	0.0	6.930E 00	0.0	0.0
14	402	3.461E 01	1.444E-02	6.930E 00	5.584E-01	1.299E-01
14	403	2.875E 01	1.199E-02	6.930E 00	4.653E-01	1.079E-01
14	404	2.110E 01	8.802E-03	6.930E 00	3.404E-01	7.921E-02
14	406	2.040E 01	8.511E-03	6.930E 00	3.292E-01	7.659E-02
14	407	1.837E 01	7.664E-03	6.930E 00	2.964E-01	6.897E-02
14	408	1.640E 01	6.839E-03	6.930E 00	2.645E-01	6.155E-02
14	409	1.565E 01	6.529E-03	6.930E 00	2.525E-01	5.875E-02
14	410	1.713E 01	7.146E-03	6.930E 00	2.764E-01	6.431E-02
14	411	1.449E 01	6.043E-03	6.930E 00	2.337E-01	5.439E-02
14	412	4.474E 00	1.866E-03	6.930E 00	7.218E-02	1.680E-02
14	413	2.112E 00	8.810E-04	6.930E 00	3.407E-02	7.928E-03
14	414	8.860E-01	3.696E-04	6.930E 00	1.429E-02	3.326E-03
14	415	4.001E-01	1.669E-04	6.930E 00	6.456E-03	1.502E-03

Table 3 (CONTINUED)

RUN	GAGE	$\dot{q}_w$	C_h	$\dot{q}_o$	$\dot{q}_w / \dot{q}_o$	h
14	501	5.697E 00	2.376E-03	6.930E 00	9.191E-02	2.139E-02
14	502	2.649E 01	1.105E-02	6.930E 00	4.273E-01	9.943E-02
14	504	2.630E 01	1.097E-02	6.930E 00	4.242E-01	9.872E-02
14	505	2.584E 01	1.078E-02	6.930E 00	4.169E-01	9.701E-02
14	506	2.374E 01	9.904E-03	6.930E 00	3.831E-01	8.914E-02
14	507	2.366E 01	9.870E-03	6.930E 00	3.817E-01	8.882E-02
14	508	2.217E 01	9.248E-03	6.930E 00	3.577E-01	8.323E-02
14	509	2.213E 01	9.230E-03	6.930E 00	3.570E-01	8.307E-02
14	510	2.195E 01	9.155E-03	6.930E 00	3.541E-01	8.239E-02
14	511	1.862E 01	7.768E-03	6.930E 00	3.004E-01	6.991E-02
14	513	0.0	0.0	6.930E 00	0.0	0.0
14	514	1.050E-01	4.379E-05	6.930E 00	1.694E-03	3.941E-04
14	515	2.381E-01	9.934E-05	6.930E 00	3.842E-03	8.940E-04
14	601	2.770E 01	1.156E-02	6.930E 00	4.469E-01	1.040E-01
14	602	2.220E 01	9.261E-03	6.930E 00	3.582E-01	8.334E-02
14	603	2.224E 01	9.278E-03	6.930E 00	3.588E-01	8.350E-02
14	604	1.948E 01	8.126E-03	6.930E 00	3.143E-01	7.314E-02
14	605	2.040E 01	8.509E-03	6.930E 00	3.291E-01	7.657E-02
14	606	2.180E 01	9.092E-03	6.930E 00	3.517E-01	8.183E-02
14	607	2.029E 01	8.465E-03	6.930E 00	3.274E-01	7.618E-02
14	608	1.762E 01	7.352E-03	6.930E 00	2.843E-01	6.616E-02
14	609	2.232E 01	9.312E-03	6.930E 00	3.602E-01	8.381E-02
14	610	1.476E 01	6.155E-03	6.930E 00	2.381E-01	5.539E-02
14	611	1.539E 01	6.419E-03	6.930E 00	2.483E-01	5.777E-02
14	612	1.926E 01	8.033E-03	6.930E 00	3.107E-01	7.230E-02
14	613	2.483E 01	1.036E-02	6.930E 00	4.005E-01	9.320E-02
14	701	1.120E 01	4.672E-03	6.930E 00	1.807E-01	4.205E-02
14	702	1.195E 01	4.985E-03	6.930E 00	1.928E-01	4.486E-02
14	703	1.118E 01	4.664E-03	6.930E 00	1.804E-01	4.197E-02
15	101	1.694E 02	5.145E-02	2.176E 01	8.704E-01	1.762E-01
15	102	7.528E 01	2.287E-02	2.176E 01	3.869E-01	7.830E-02
15	103	3.637E 01	1.105E-02	2.176E 01	1.869E-01	3.783E-02
15	104	3.126E 01	9.497E-03	2.176E 01	1.607E-01	3.252E-02
15	105	2.222E 01	6.749E-03	2.176E 01	1.142E-01	2.311E-02
15	106	1.960E 01	5.955E-03	2.176E 01	1.007E-01	2.039E-02

Table 3 (CONTINUED)

RUN	GAGE	$\dot{q}_w$	C_h	$\dot{q}_o$	$\dot{q}_w / \dot{q}_o$	h
15	107	1.994E 01	6.056E-03	2.176E 01	1.025E-01	2.074E-02
15	108	1.715E 01	5.209E-03	2.176E 01	8.812E-02	1.784E-02
15	109	1.379E 01	4.188E-03	2.176E 01	7.085E-02	1.434E-02
15	110	1.326E 01	4.028E-03	2.176E 01	6.815E-02	1.379E-02
15	111	1.222E 01	3.712E-03	2.176E 01	6.280E-02	1.271E-02
15	112	6.915E 01	2.101E-02	2.176E 01	3.554E-01	7.192E-02
15	113	5.603E 01	1.702E-02	2.176E 01	2.879E-01	5.828E-02
15	114	2.979E 01	9.050E-03	2.176E 01	1.531E-01	3.099E-02
15	115	2.009E 01	6.103E-03	2.176E 01	1.032E-01	2.089E-02
15	202	1.360E 02	4.131E-02	2.176E 01	6.989E-01	1.415E-01
15	203	7.759E 01	2.357E-02	2.176E 01	3.987E-01	8.070E-02
15	204	4.968E 01	1.509E-02	2.176E 01	2.553E-01	5.167E-02
15	205	3.657E 01	1.111E-02	2.176E 01	1.879E-01	3.803E-02
15	206	3.070E 01	9.326E-03	2.176E 01	1.578E-01	3.193E-02
15	207	2.623E 01	7.966E-03	2.176E 01	1.348E-01	2.728E-02
15	208	2.085E 01	6.334E-03	2.176E 01	1.072E-01	2.169E-02
15	209	2.058E 01	6.252E-03	2.176E 01	1.058E-01	2.141E-02
15	210	1.725E 01	5.240E-03	2.176E 01	8.865E-02	1.794E-02
15	211	1.628E 01	4.945E-03	2.176E 01	8.365E-02	1.693E-02
15	212	1.272E 02	3.864E-02	2.176E 01	6.538E-01	1.323E-01
15	213	7.887E 01	2.396E-02	2.176E 01	4.053E-01	8.204E-02
15	214	4.538E 01	1.379E-02	2.176E 01	2.332E-01	4.720E-02
15	215	2.752E 01	8.359E-03	2.176E 01	1.414E-01	2.862E-02
15	301	4.622E 02	1.404E-01	2.176E 01	2.375E 00	4.807E-01
15	302	1.994E 02	6.058E-02	2.176E 01	1.025E 00	2.074E-01
15	303	9.401E 01	2.855E-02	2.176E 01	4.831E-01	9.778E-02
15	304	6.477E 01	1.967E-02	2.176E 01	3.329E-01	6.737E-02
15	305	4.895E 01	1.487E-02	2.176E 01	2.516E-01	5.091E-02
15	306	4.017E 01	1.220E-02	2.176E 01	2.064E-01	4.178E-02
15	307	3.266E 01	9.921E-03	2.176E 01	1.678E-01	3.397E-02
15	308	2.943E 01	8.939E-03	2.176E 01	1.512E-01	3.061E-02
15	309	2.681E 01	8.144E-03	2.176E 01	1.378E-01	2.788E-02
15	310	2.452E 01	7.448E-03	2.176E 01	1.260E-01	2.550E-02
15	311	2.275E 01	6.910E-03	2.176E 01	1.169E-01	2.366E-02
15	312	1.931E 02	5.865E-02	2.176E 01	9.922E-01	2.008E-01
15	313	1.245E 02	3.783E-02	2.176E 01	6.401E-01	1.295E-01
15	314	7.527E 01	2.286E-02	2.176E 01	3.868E-01	7.828E-02
15	315	4.216E 01	1.281E-02	2.176E 01	2.166E-01	4.385E-02

Table 3 (CONTINUED)

RUN	GAGE	$\dot{q}_w$	C_h	$\dot{q}_o$	$\dot{q}_w / \dot{q}_o$	h
15	402	1.696E 02	5.153E-02	2.176E 01	8.718E-01	1.764E-01
15	403	7.460E 01	2.267E-02	2.176E 01	3.839E 01	7.758E-02
15	404	4.706E 01	1.429E-02	2.176E 01	2.418E-01	4.895E-02
15	406	2.993E 01	9.092E-03	2.176E 01	1.538E-01	3.113E-02
15	407	2.439E 01	7.409E-03	2.176E 01	1.253E-01	2.537E-02
15	408	2.136E 01	6.488E-03	2.176E 01	1.098E-01	2.221E-02
15	409	1.917E 01	5.825E-03	2.176E 01	9.854E-02	1.994E-02
15	410	1.678E 01	5.098E-03	2.176E 01	8.624E-02	1.745E-02
15	411	1.448E 01	4.399E-03	2.176E 01	7.443E-02	1.506E-02
15	412	1.735E 02	5.269E-02	2.176E 01	8.914E-01	1.804E-01
15	413	1.072E 02	3.257E-02	2.176E 01	5.510E-01	1.115E-01
15	414	5.560E 01	1.689E-02	2.176E 01	2.857E-01	5.783E-02
15	415	2.085E 01	6.332E-03	2.176E 01	1.071E-01	2.168E-02
15	501	3.293E 02	1.000E-01	2.176E 01	1.692E 00	3.425E-01
15	502	1.532E 02	4.655E-02	2.176E 01	7.875E-01	1.594E-01
15	504	5.277E 01	1.603E-02	2.176E 01	2.712E-01	5.488E-02
15	505	3.873E 01	1.177E-02	2.176E 01	1.990E-01	4.028E-02
15	506	3.327E 01	1.011E-02	2.176E 01	1.710E-01	3.460E-0
15	507	2.772E 01	8.420E-03	2.176E 01	1.425E-01	2.883E-0
15	508	2.119E 01	6.437E-03	2.176E 01	1.089E-01	2.204E-02
15	509	2.042E 01	6.203E-03	2.176E 01	1.049E-01	2.124E-02
15	510	1.912E 01	5.808E-03	2.176E 01	9.825E-02	1.989E-02
15	511	1.469E 01	4.462E-03	2.176E 01	7.549E-02	1.528E-02
15	512	1.233E 02	3.746E-02	2.176E 01	6.338E-01	1.283E-01
15	513	7.536E 01	2.289E-02	2.176E 01	3.872E-01	7.838E-02
15	514	3.863E 01	1.173E-02	2.176E 01	1.985E-01	4.018E-02
15	515	2.749E 01	8.350E-03	2.176E 01	1.413E-01	2.859E-02
15	601	1.416E 01	4.302E-03	2.176E 01	7.277E-02	1.473E-02
15	602	1.387E 01	4.214E-03	2.176E 01	7.128E-02	1.443E-02
15	603	1.497E 01	4.548E-03	2.176E 01	7.694E-02	1.557E-02
15	604	1.664E 01	5.054E-03	2.176E 01	8.550E-02	1.730E-02
15	605	1.923E 01	5.842E-03	2.176E 01	9.884E-02	2.000E-02
15	606	1.916E 01	5.820E-03	2.176E 01	9.845E-02	1.993E-02
15	607	1.979E 01	6.011E-03	2.176E 01	1.017E-01	2.058E-02
15	608	2.069E 01	6.284E-03	2.176E 01	1.063E-01	2.152E-02

Table 3 (CONTINUED)

RUN	GAGE	$\dot{q}_w$	C_h	$\dot{q}_o$	$\dot{q}_w / \dot{q}_o$	h
15	609	2.212E 01	6.718E-03	2.176E 01	1.137E-01	2.300E-02
15	610	1.539E 01	4.676E-03	2.176E 01	7.911E-02	1.601E-02
15	611	1.793E 01	5.447E-03	2.176E 01	9.214E-02	1.865E-02
15	612	1.690E 01	5.133E-03	2.176E 01	8.684E-02	1.757E-02
15	613	1.764E 01	5.359E-03	2.176E 01	9.067E-02	1.835E-02
15	701	1.083E 00	3.290E-04	2.176E 01	5.566E-03	1.127E-03
15	702	8.029E-01	2.439E-04	2.176E 01	4.126E-03	8.351E-04
15	703	5.154E-01	1.566E-04	2.176E 01	2.649E-03	5.360E-04
16	101	6.746E 01	5.594E-03	1.735E 01	4.346E-01	2.180E-01
16	102	1.182E 02	9.799E-03	1.735E 01	7.614E-01	3.818E-01
16	103	9.558E 01	7.926E-03	1.735E 01	6.158E-01	3.089E-01
16	104	8.455E 01	7.011E-03	1.735E 01	5.447E-01	2.732E-01
16	105	7.080E 01	5.871E-03	1.735E 01	4.562E-01	2.288E-01
16	106	6.506E 01	5.395E-03	1.735E 01	4.192E-01	2.102E-01
16	107	6.166E 01	5.113E-03	1.735E 01	3.972E-01	1.992E-01
16	108	5.699E 01	4.726E-03	1.735E 01	3.672E-01	1.842E-01
16	109	5.112E 01	4.239E-03	1.735E 01	3.293E-01	1.652E-01
16	110	4.766E 01	3.952E-03	1.735E 01	3.071E-01	1.540E-01
16	111	3.890E 01	3.226E-03	1.735E 01	2.506E-01	1.257E-01
16	112	1.280E 01	1.061E-03	1.735E 01	8.246E-02	4.136E-02
16	113	8.651E 00	7.174E-04	1.735E 01	5.574E-02	2.795E-02
16	114	7.464E 00	6.190E-04	1.735E 01	4.809E-02	2.412E-02
16	115	5.178E 00	4.294E-04	1.735E 01	3.336E-02	1.673E-02
16	202	1.543E 02	1.279E-02	1.735E 01	9.940E-01	4.985E-01
16	204	7.280E 01	6.037E-03	1.735E 01	4.691E-01	2.352E-01
16	205	5.349E 01	4.436E-03	1.735E 01	3.446E-01	1.728E-01
16	206	4.442E 01	3.683E-03	1.735E 01	2.862E-01	1.435E-01
16	207	3.905E 01	3.238E-03	1.735E 01	2.516E-01	1.262E-01
16	208	3.494E 01	2.898E-03	1.735E 01	2.251E-01	1.129E-01
16	209	3.342E 01	2.771E-03	1.735E 01	2.153E-01	1.080E-01
16	210	3.301E 01	2.737E-03	1.735E 01	2.127E-01	1.067E-01
16	211	3.418E 01	2.834E-03	1.735E 01	2.202E-01	1.104E-01
16	212	7.682E 01	6.370E-03	1.735E 01	4.949E-01	2.482E-01
16	213	4.310E 01	3.574E-03	1.735E 01	2.777E-01	1.393E-01
16	214	2.127E 01	1.764E-03	1.735E 01	1.371E-01	6.874E-02
16	215	1.207E 01	1.001E-03	1.735E 01	7.775E-02	3.899E-02

Table 3 (CONTINUED)

RUN	GAGE	$\dot{q}_w$	C_h	$\dot{q}_o$	$\dot{q}_w/\dot{q}_o$	h
16	301	2.630E 02	2.181E-02	1.735E 01	1.694E 00	8.498E-01
16	302	1.950E 02	1.617E-02	1.735E 01	1.257E 00	6.302E-01
16	303	1.496. 02	1.240E-02	1.735E 01	9.636E-01	4.833E-01
16	304	1.167E 02	9.681E-03	1.735E 01	7.522E-01	3.772E-01
16	305	1.045E 02	8.667E-03	1.735E 01	6.734E-01	3.377E-01
16	306	9.469E 01	7.852E-03	1.735E 01	6.100E-01	3.060E-01
16	307	9.482E 01	7.863E-03	1.735E 01	6.109E-01	3.064E-01
16	308	7.190E 01	5.962E-03	1.735E 01	4.633E-01	2.323E-01
16	309	6.970E 01	5.780E-03	1.735E 01	4.491E-01	2.252E-01
16	310	8.354E 01	6.928E-03	1.735E 01	5.383E-01	2.699E-01
16	311	6.159E 01	5.107E-03	1.735E 01	3.968E-01	1.990E-01
16	312	1.003E 02	8.318E-03	1.735E 01	6.463E-01	3.241E-01
16	313	7.541E 01	6.253E-03	1.735E 01	4.859E-01	2.437E-01
16	314	4.491E 01	3.724E-03	1.735E 01	2.894E-01	1.451E-01
16	315	2.327E 01	1.930E-03	1.735E 01	1.499E-01	7.519E-02
16	402	1.764E 02	1.463E-02	1.735E 01	1.137E 00	5.701E-01
16	403	8.721E 01	7.232E-03	1.735E 01	5.693E-01	2.818E-01
16	404	6.251E 01	5.183E-03	1.735E 01	4.027E-01	2.020E-01
16	406	4.202E 01	3.485E-03	1.735E 01	2.707E-01	1.358E-01
16	407	3.532E 01	2.929E-03	1.735E 01	2.276E-01	1.141E-01
16	408	2.986E 01	2.476E-03	1.735E 01	1.924E-01	9.648E-02
16	409	2.701E 01	2.240E-03	1.735E 01	1.740E-01	8.727E-02
16	410	2.248E 01	1.864E-03	1.735E 01	1.448E-01	7.263E-02
16	411	1.533E 01	1.271E-03	1.735E 01	9.876E-02	4.953E-02
16	412	1.056E 02	8.759E-03	1.735E 01	6.805E-01	3.413E-01
16	413	5.723E 01	4.746E-03	1.735E 01	3.687E-01	1.849E-01
16	414	2.595E 01	2.152E-03	1.735E 01	1.672E-01	8.384E-02
16	415	1.010E 01	8.374E-04	1.735E 01	6.506E-02	3.263E-02
16	501	2.655E 02	2.202E-02	1.735E 01	1.711E 00	8.580E-01
16	502	1.573E 02	1.305E-02	1.735E 01	1.014F 00	5.083E-01
16	504	6.887E 01	5.711E-03	1.735E 01	4.437E-01	2.225E-01
16	505	5.447E 01	4.517E-03	1.735E 01	3.509E-01	1.760E-01
16	506	4.662E 01	3.866E-03	1.735E 01	3.004E-01	1.506E-01
16	509	3.125E 01	2.591E-03	1.735E 01	2.013E-01	1.010E-01
16	510	2.839E 01	2.354E-03	1.735E 01	1.829E-01	9.172E-02
16	511	2.151E 01	1.784E-03	1.735E 01	1.386E-01	6.951E-02

Table 3 (CONCLUDED)

RUN	GAGE	$\dot{q}_w$	c_h	$\dot{q}_o$	$\dot{q}_w / \dot{q}_o$	h
16	512	6.403E 01	5.310E-03	1.735E 01	4.125E-01	2.069E-01
16	513	3.390E 01	2.811E-03	1.735E 01	2.184E-01	1.095E-01
16	514	1.506E 01	1.249E-03	1.735E 01	9.704E-02	4.867E-02
16	515	8.469E 00	7.022E-04	1.735E 01	5.456E-02	2.736E-02
16	601	3.507E 01	2.908E-03	1.735E 01	2.260E-01	1.133E-01
16	602	2.080E 01	1.724E-03	1.735E 01	1.340E-01	6.720E-02
16	603	2.178E 01	1.806E-03	1.735E 01	1.404E-01	7.039E-02
16	604	2.991E 01	2.480E-03	1.735E 01	1.927E-01	9.665E-02
16	605	2.927E 01	2.427E-03	1.735E 01	1.886E-01	9.458E-02
16	606	2.799E 01	2.321E-03	1.735E 01	1.803E-01	9.044E-02
16	607	2.762E 01	2.291E-03	1.735E 01	1.780E-01	8.926E-02
16	608	2.316E 01	1.920E-03	1.735E 01	1.492E-01	7.483E-02
16	609	2.933E 01	2.432E-03	1.735E 01	1.890E-01	9.477E-02
16	610	2.243E 01	1.860E-03	1.735E 01	1.445E-01	7.249E-02
16	611	2.149E 01	1.782E-03	1.735E 01	1.385E-01	6.945E-02
16	612	2.343E 01	1.943E-03	1.735E 01	1.510E-01	7.571E-02
16	613	2.309E 01	1.914E-03	1.735E 01	1.487E-01	7.460E-02
16	701	1.610E 01	1.335E-03	1.735E 01	1.038E-01	5.204E-02
16	703	1.063E 01	8.815E-04	1.735E 01	6.849E-02	3.435E-02

FIGURE INDEX

1. Basic Components of the CAL Hypersonic Shock Tunnel 96" High Energy Leg

2. 1/80 Scale NASA 12.5K Straight Wing Orbiter

3. (a) Bottom View of 1/80 Scale NASA 12.5K Straight Wing Orbiter with CAL Thin Film Heat Transfer Gages

   (b) Top View of 1/80 Scale NASA 12.5K Straight Wing Orbiter with CAL Thin Film Heat Transfer Gages

4. Installation Drawing of 1/80 Scale NASA 12.5K Straight Wing Orbiter in CAL 96-Inch Hypersonic Shock Tunnel

5. Installation Photograph of 1/80 Scale NASA 12.5K Straight Wing Orbiter in CAL 96-Inch Hypersonic Shock Tunnel with Mach 16 Nozzle

6. Nominal Heat Transfer Gage Locations - 1/80 Scale Orbiter Wing

7. Photograph of Windward Side of Leading Edge Heat Transfer Gages for 1/80 Scale NASA 12.5K Straight Wing Orbiter

8. Close-up Photograph of Leading Edge Heat Transfer Gages with Lead Wires Attached

9. Photograph of 1/80 Scale NASA Wing with Heat Transfer Gages and Lead Wires Installed

10-24. (a) Full Scale Normalized Chordwise Heating Distribution

10-24. (b) Full Scale Normalized Spanwise Heating Distribution

25. Schlieren Photographs of 1/80 Scale NASA 12.5K Straight Wing Orbiter

26. Leading Edge Heating versus Angle of Attack - Insert 1

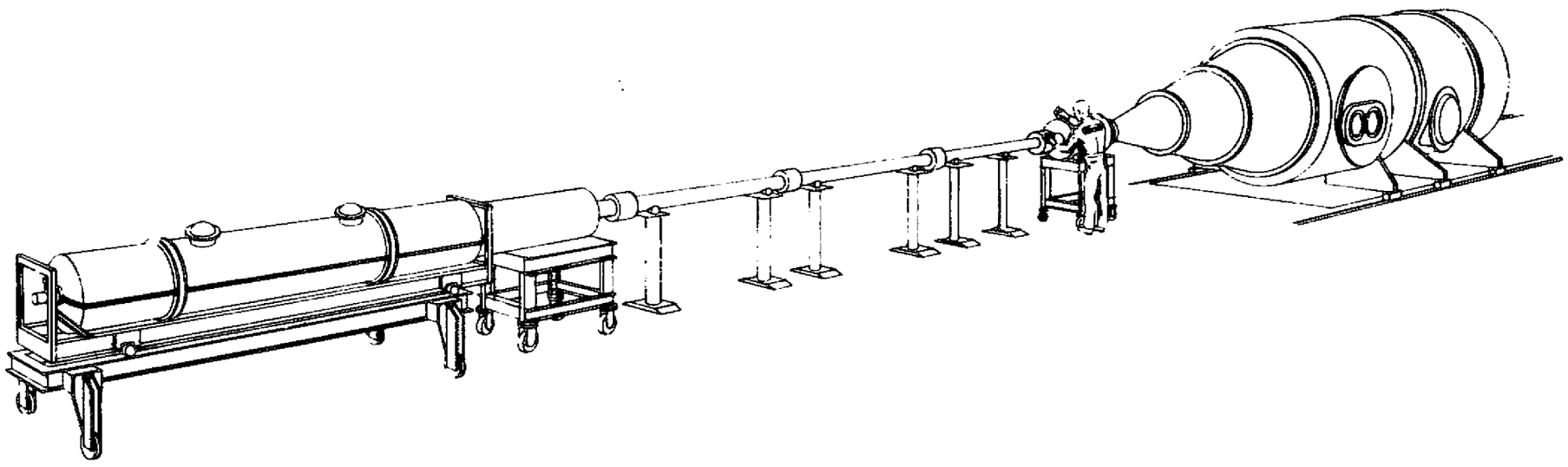
27. 17% Chord Heating versus Angle of Attack - Insert 1

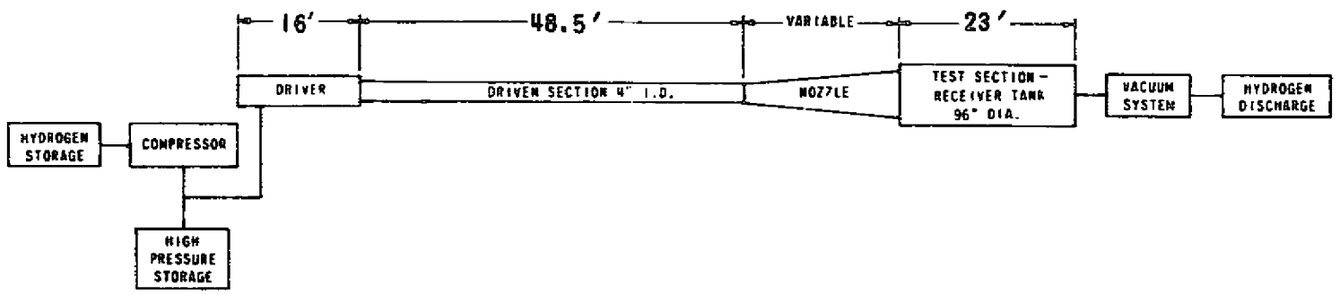
28. Leading Edge Heating versus Angle of Attack - Insert 3

29. Leading Edge Heating versus Angle of Attack - Insert 3

30. Full Scale Normalized Chordwise Heating Distribution in Non-perturbed Region of Wing

31. Temperature and Heat Transfer Rate Traces from Insert 3





3416

Figure 1 BASIC COMPONENTS OF THE CAL 96" LEG HYPERSONIC SHOCK TUNNEL

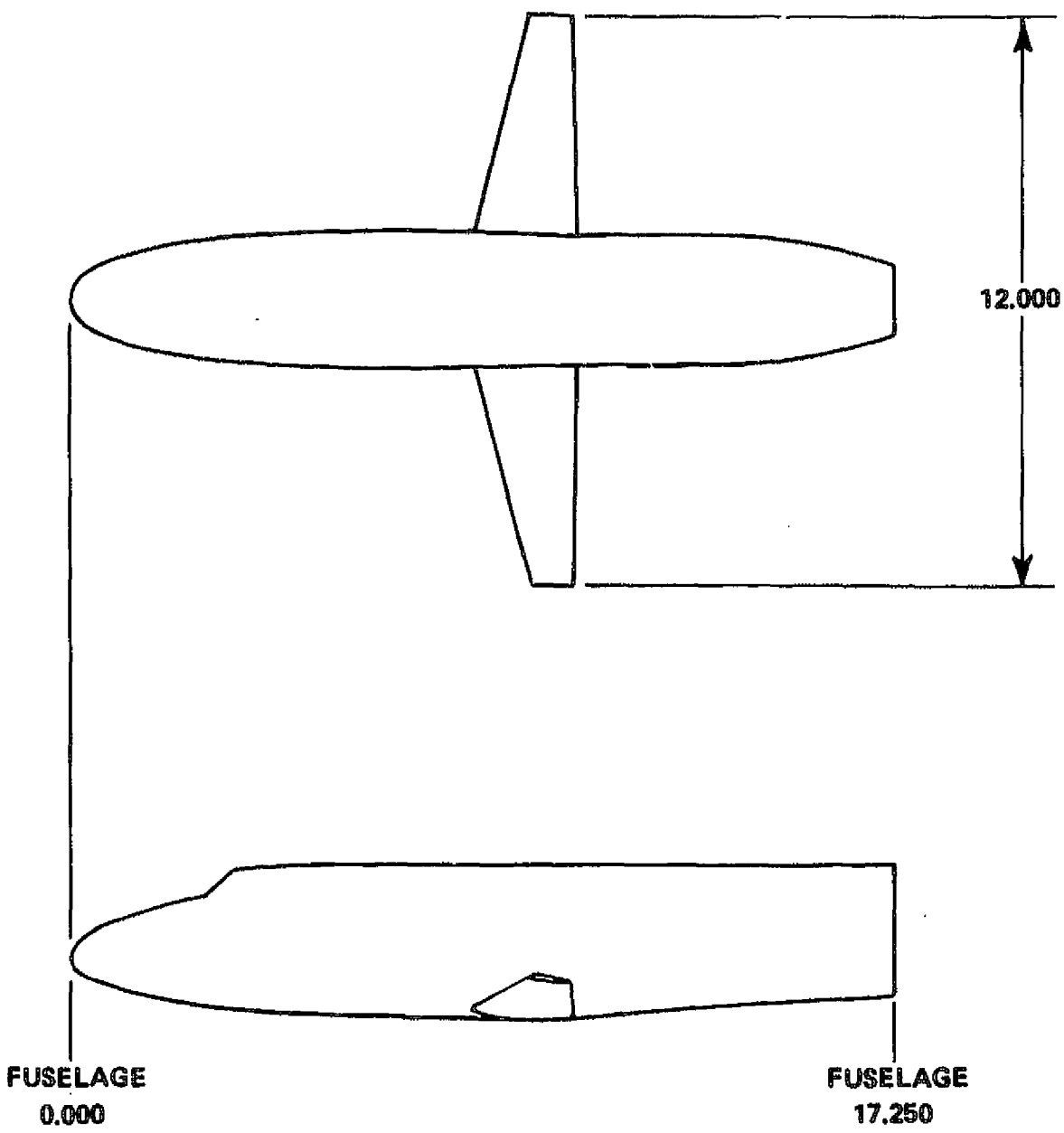


Figure 2 1/80 SCALE NASA 12.5K STRAIGHT WING ORBITER

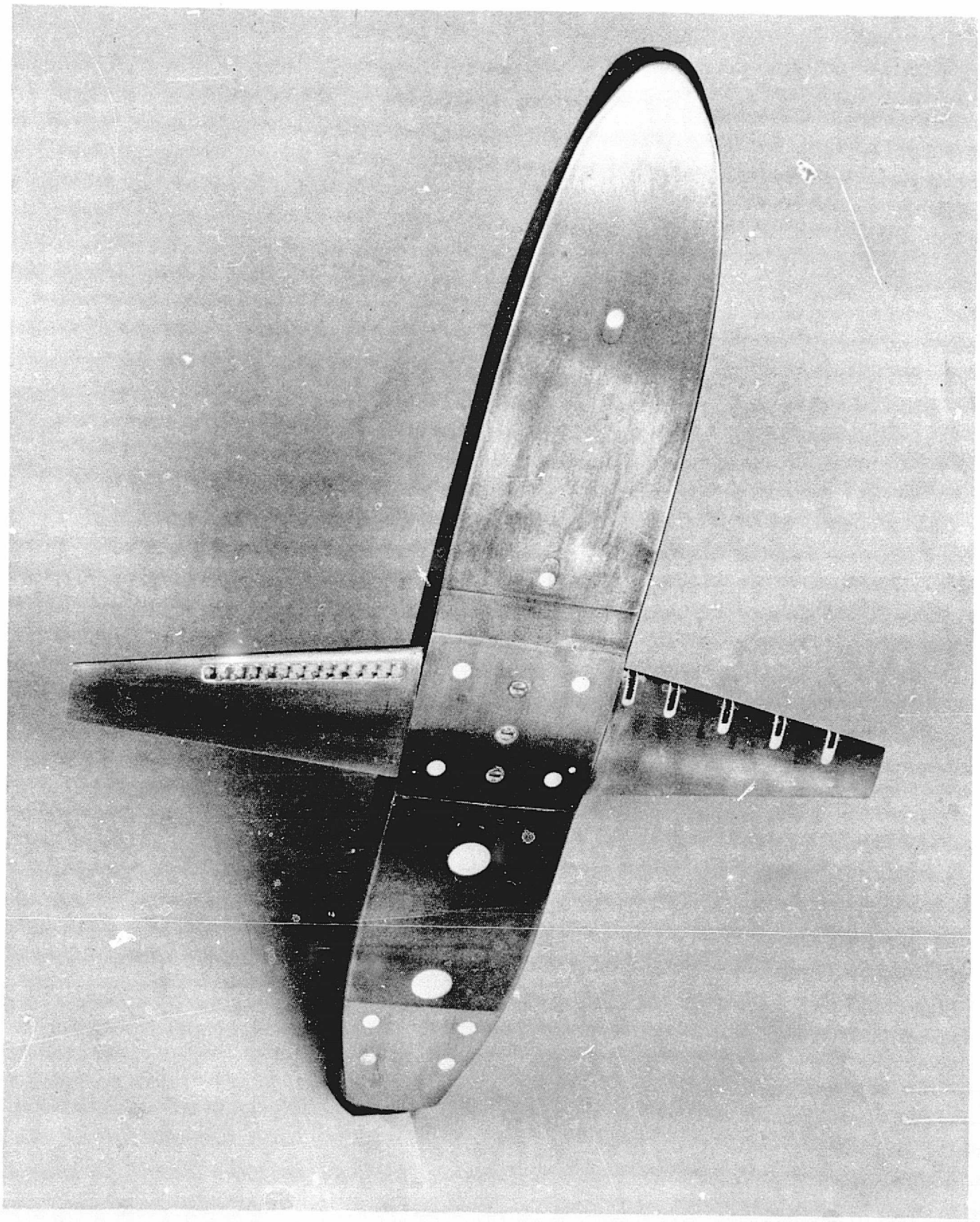


Figure 3 (a) BOTTOM VIEW OF 1/80 SCALE NASA 12.5K STRAIGHT WING ORBITER WITH CAL THIN FILM HEAT TRANSFER GAGES

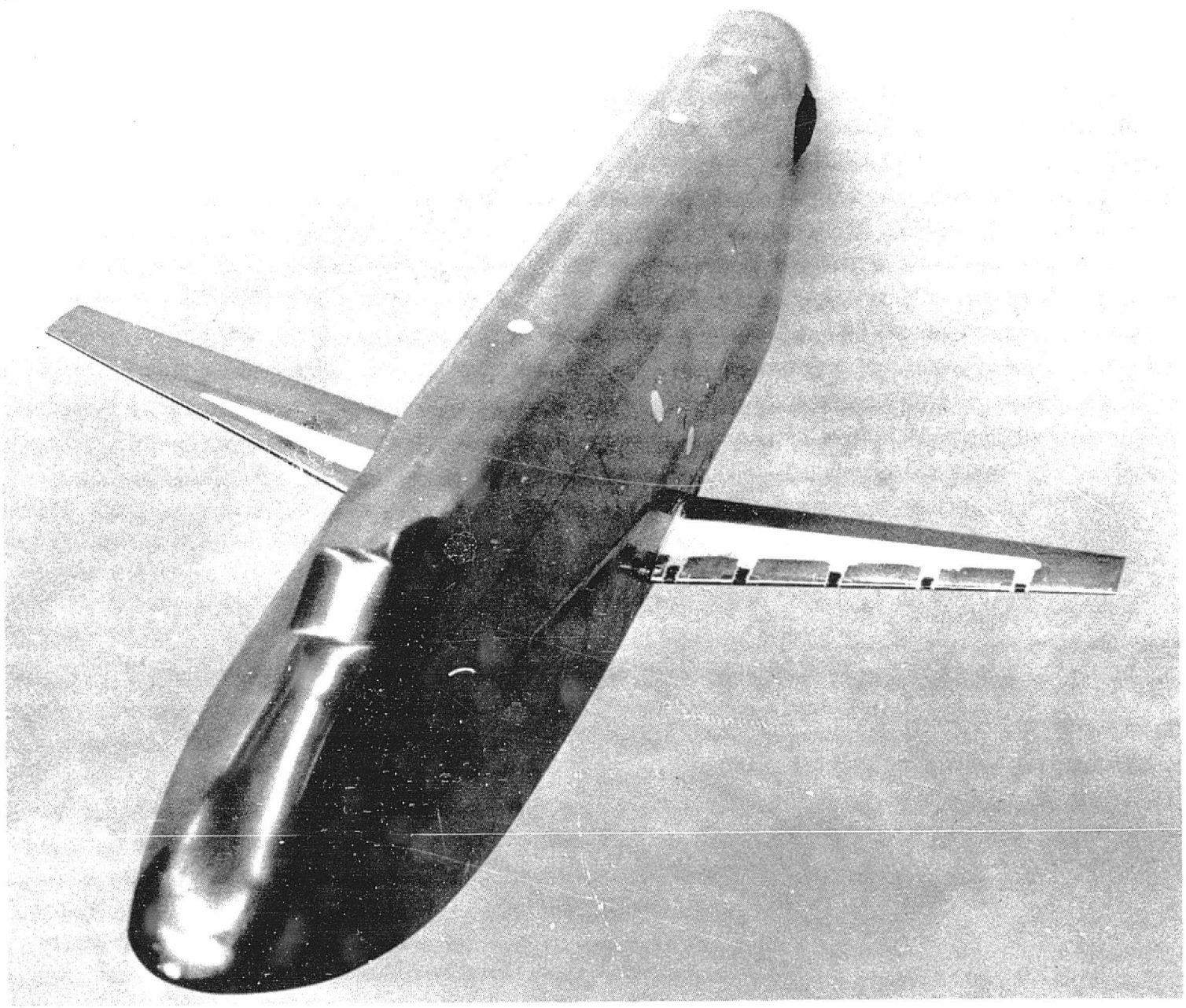


Figure 3(b) TOP VIEW OF 1/80 SCALE NASA 12.5K STRAIGHT WING ORBITER WITH CAL THIN FILM HEAT TRANSFER GAGES

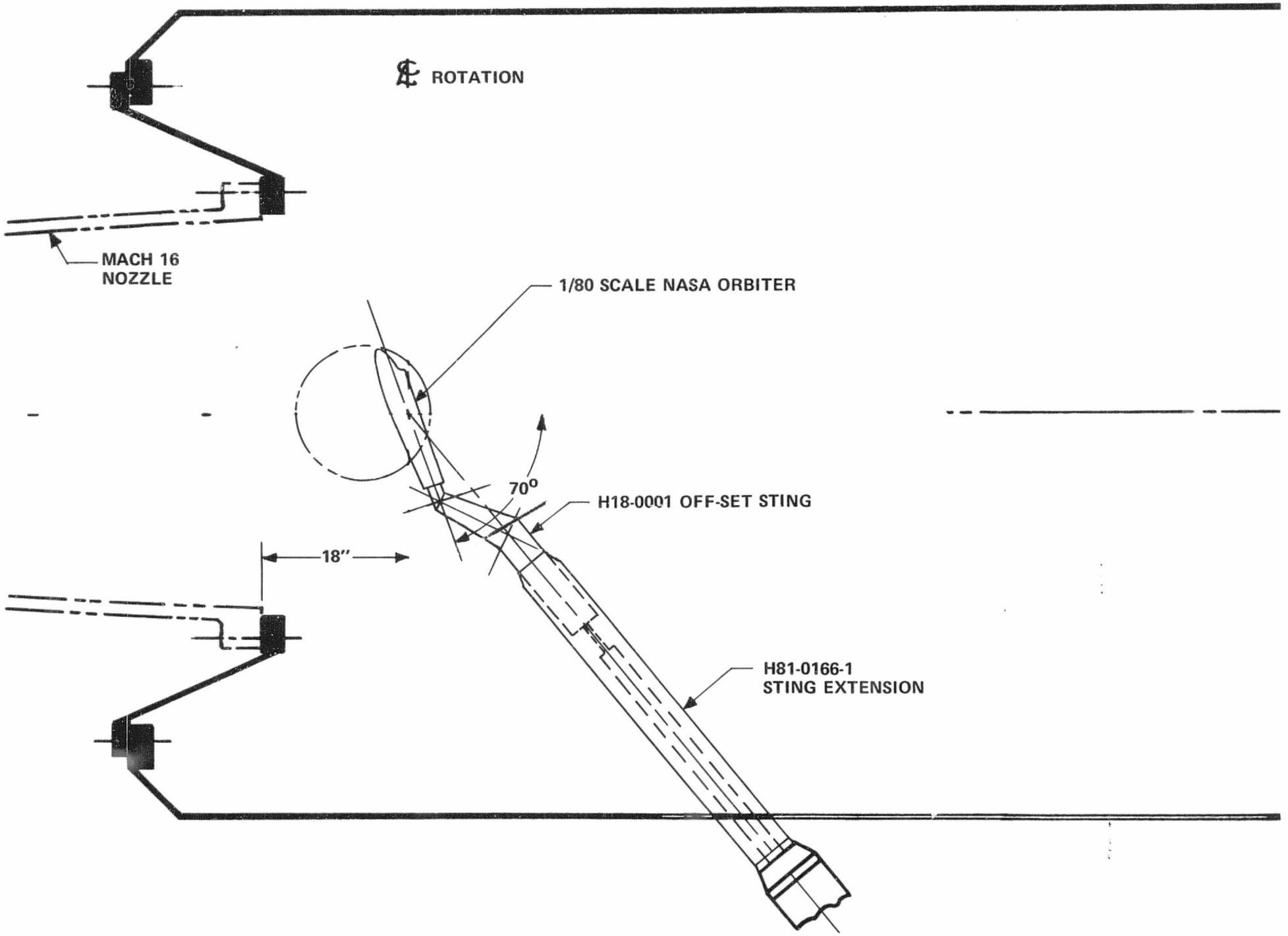


Figure 4 INSTALLATION DRAWING OF 1/80 SCALE NASA 12.5K STRAIGHT WING ORBITER IN CAL 96-INCH HYPERSONIC SHOCK TUNNEL

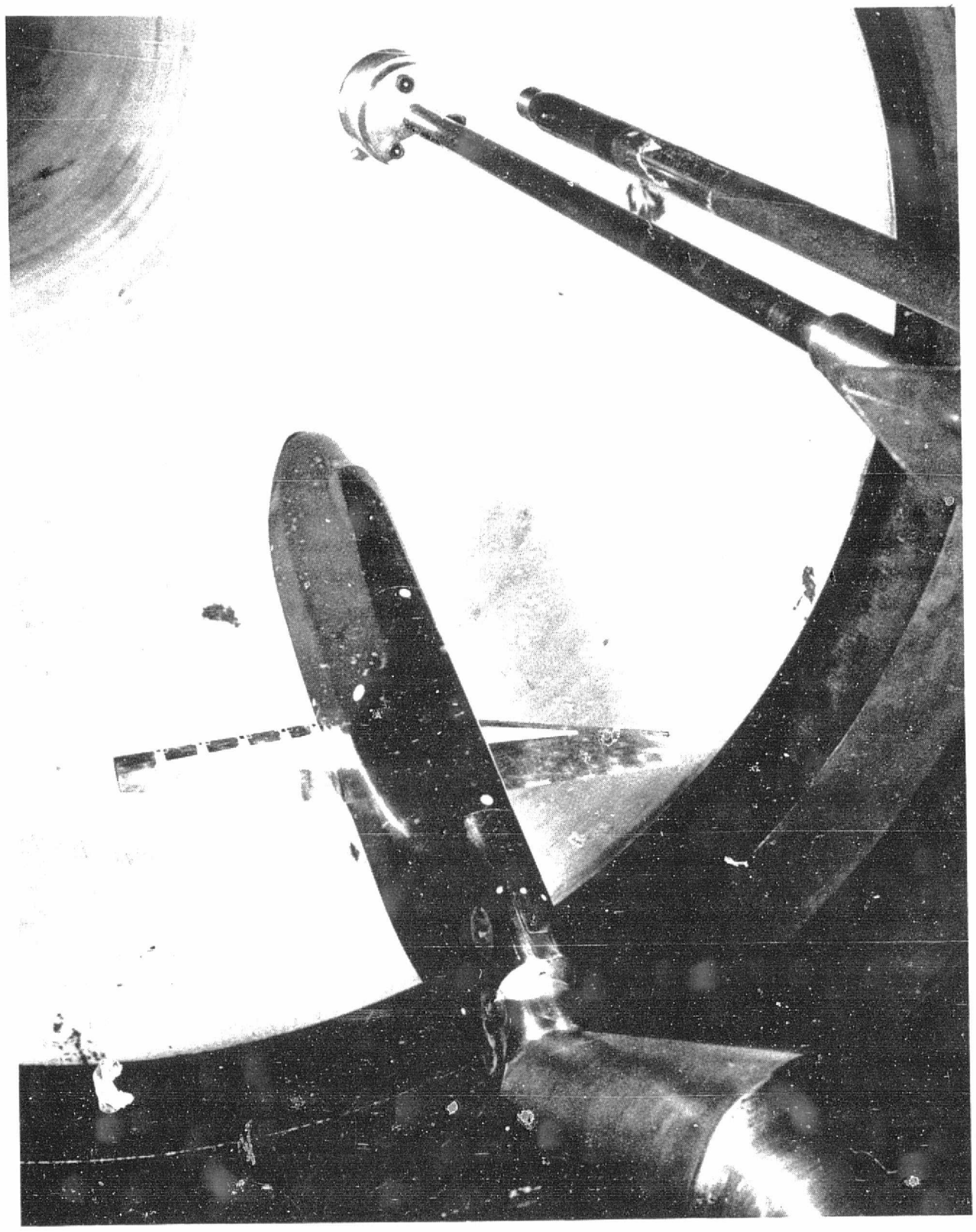
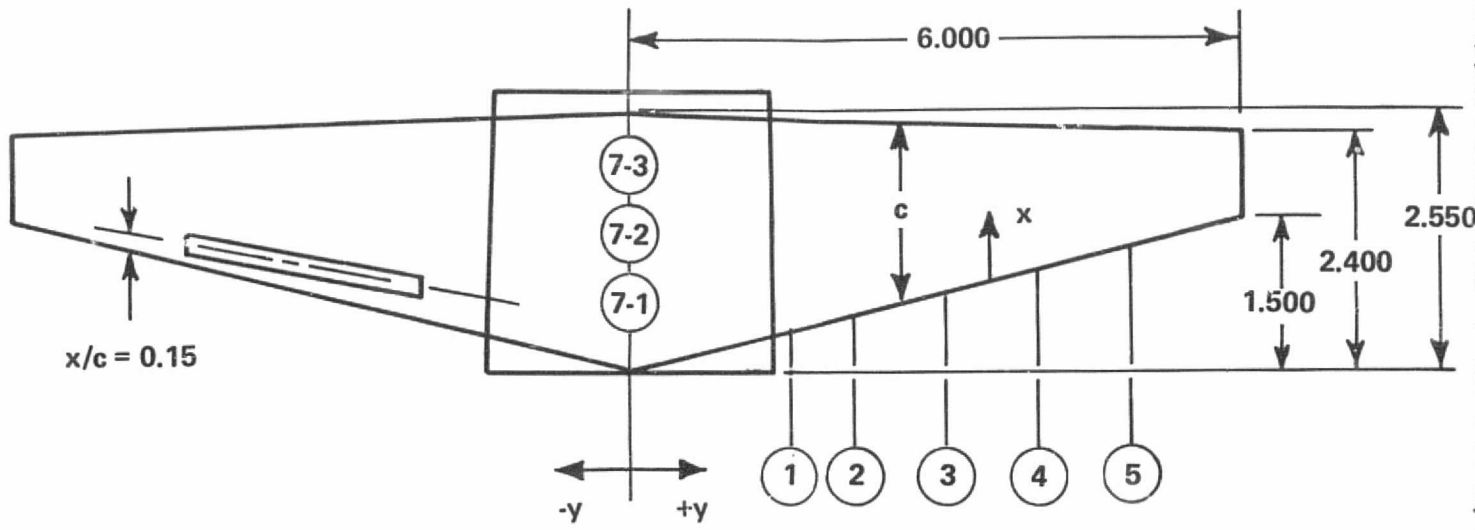


Figure 5 INSTALLATION OF 1/80 SCALE NASA 12.5K STRAIGHT WING ORBITER IN CAL 96-INCH HYPERSONIC SHOCK TUNNEL WITH MACH 16 NOZZLE



TOP VIEW

SPANWISE GAGES
(WINDWARD SIDE OF RIGHT WING)

GAGE	y (in)	y/½S	GAGE	y (in)	y/½S
6-1	-1.8	-0.300	6-8	-3.2	-0.533
6-2	-2.0	-0.333	6-9	-3.4	-0.567
6-3	-2.2	-0.367	6-10	-3.6	-0.600
6-4	-2.4	-0.400	6-11	-3.8	-0.633
6-5	-2.6	-0.433	6-12	-4.0	-0.667
6-6	-2.8	-0.467	6-13	-4.2	-0.700
6-7	-3.0	-0.500			

CENTER OF GAGES LOCATED AT x/c = 15

SPANWISE LOCATION

STATION	y (in)	c (in)	y/½S
1	1.64	2.10	0.273
2	2.33	1.91	0.388
3	3.25	1.66	0.542
4	4.16	1.41	0.693
5	5.08	1.15	0.847

BODY CENTERLINE GAGES

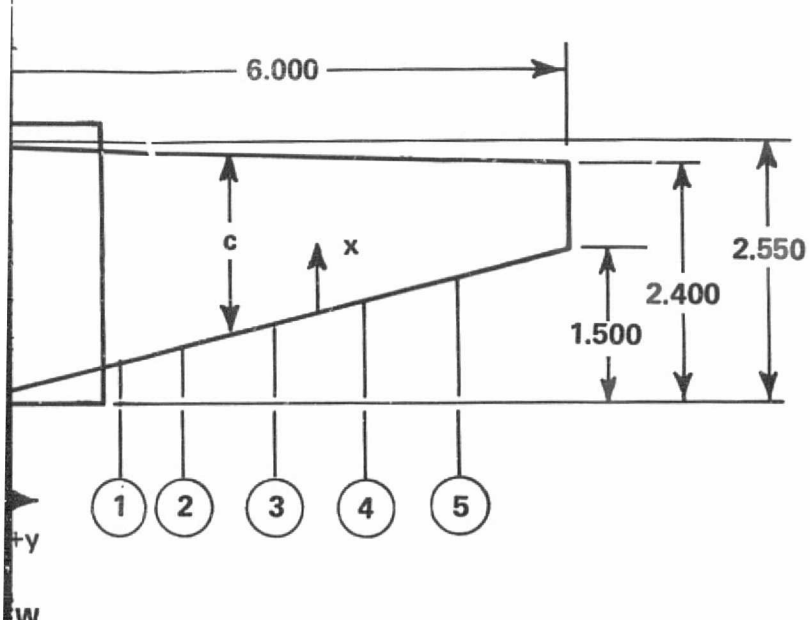
STATION	x	x/c
7-1	0.750	0.518
7-2	1.50	0.561
7-3	2.25	0.605

LEADING EDGE
(LEFT WING

G

*ST

FOLDOUT FRAME 1



LEADING EDGE GAGES
(LEFT WING)

SPANWISE LOCATION

STATION	y (in)	c (in)	y/½ S
1	1.64	2.10	0.273
2	2.33	1.91	0.388
3	3.25	1.66	0.542
4	4.16	1.41	0.693
5	5.08	1.15	0.847

CHORDWISE LOCATIONS ON EACH INSERT

WINDWARD		LEEWARD	
GAGE*	x/c	GAGE	x/c
ST01	0	ST12	0.01
ST02	0.01	ST13	0.02
ST03	0.03	ST14	0.04
ST04	0.05	ST 15	0.08
ST05	0.07		
ST06	0.09		
ST07	0.11		
ST08	0.14		
ST09	0.16		
ST10	0.18		
ST11	0.20		

*ST REPRESENTS STATION

RLINE GAGES

x	x/c
.750	0.518
.50	0.561
.25	0.605

Figure 6 NOMINAL HEAT TRANSFER GAGE LOCATIONS - 1/80 SCALE ORBITER WING (91 GAGES, TOTAL)

FOLDOUT FRAME 2

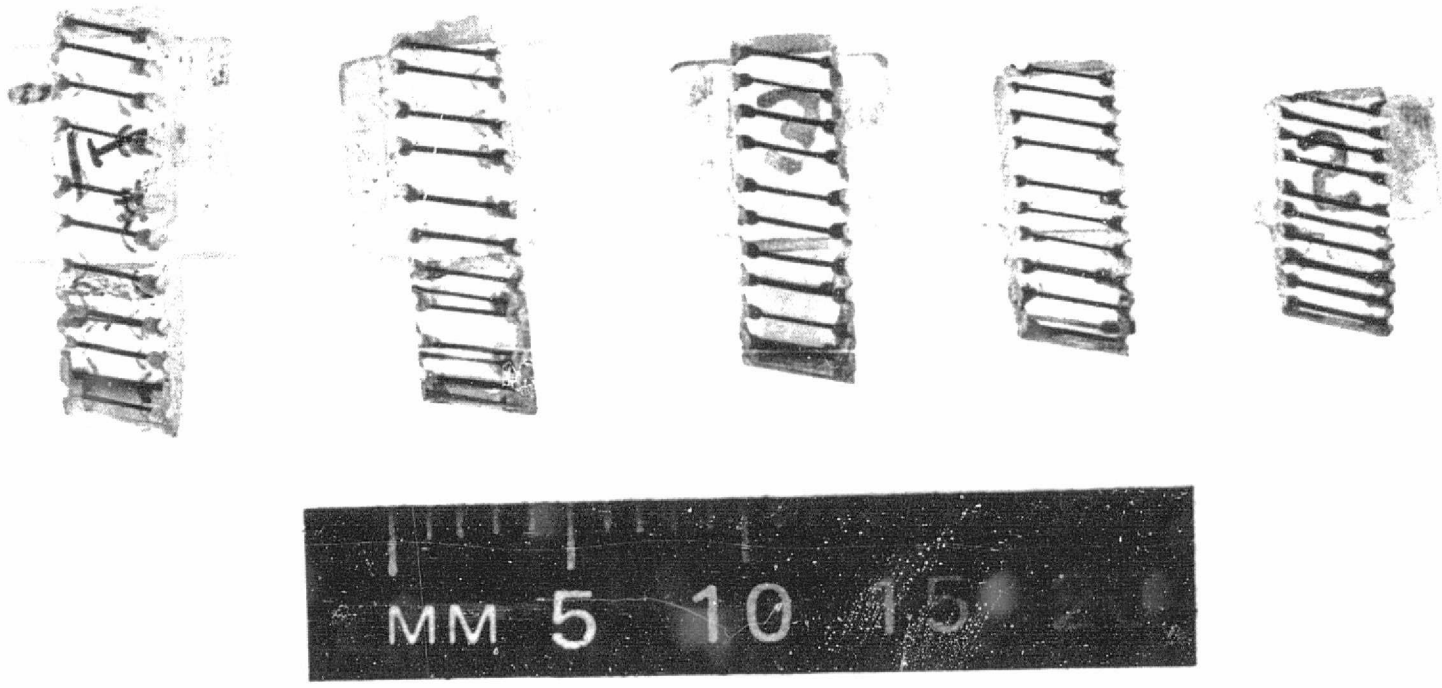


Figure 7 PHOTOGRAPH OF WINDWARD SIDE OF LEADING EDGE HEAT TRANSFER GAGES FOR 1/80 SCALE NASA 12.5K STRAIGHT WING ORBITER

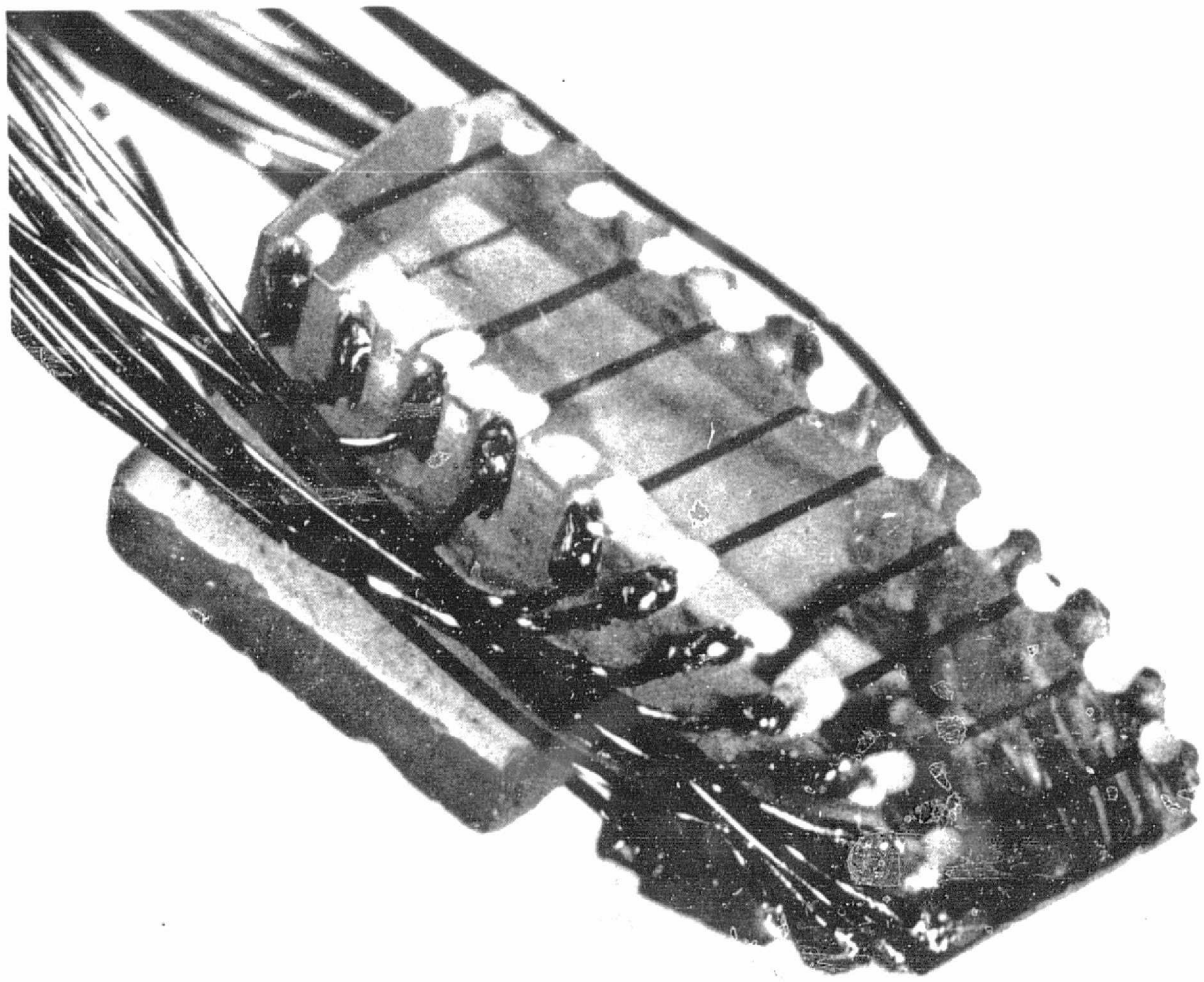


Figure 8 CLOSE-UP PHOTOGRAPH OF LEADING EDGE HEAT TRANSFER GAGES WITH LEAD WIRES ATTACHED

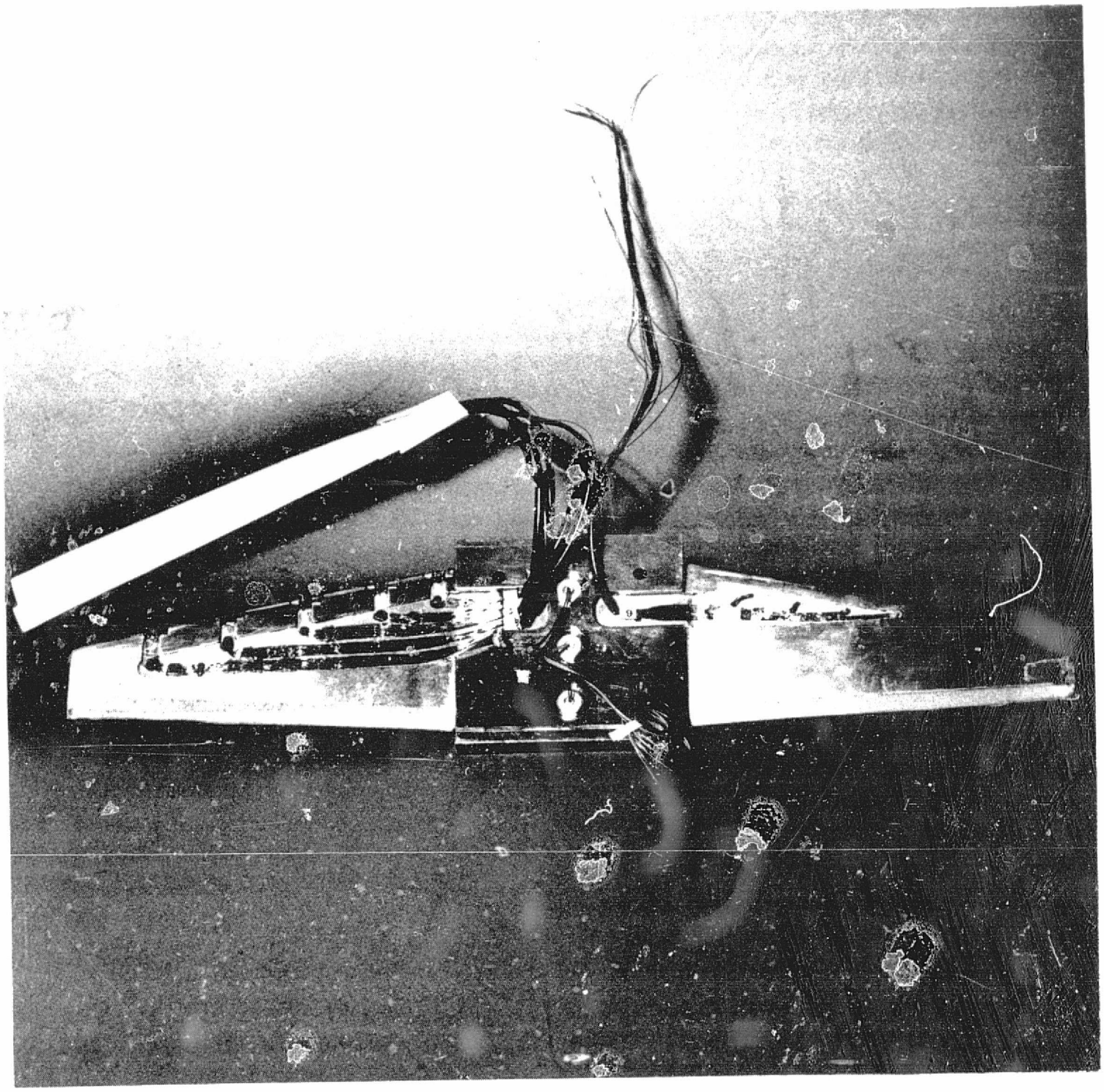


Figure 9 PHOTOGRAPH OF 1/80 SCALE NASA STRAIGHT WING WITH HEAT TRANSFER GAGES AND LEAD WIRES INSTALLED

FIGURE 10a

FULL SCALE NORMALIZED CHORDWISE HEATING DISTRIBUTION

NASA/MSC SPACE SHUTTLE

1/80 SCALE

STA ____

RUN 15 M_∞ = 7.58 $Re/_{FT}$ = 3.75×10^5 α = 0°

$\dot{q}_{D_{TR}}$ $_{R=1'}$ = 21.8

SYM	INSERT
○	1
□	2
◇	3
⏢	4
▽	5

LEEWARD GAGES FLAGGED

— — ESTIMATE (REF. 13)

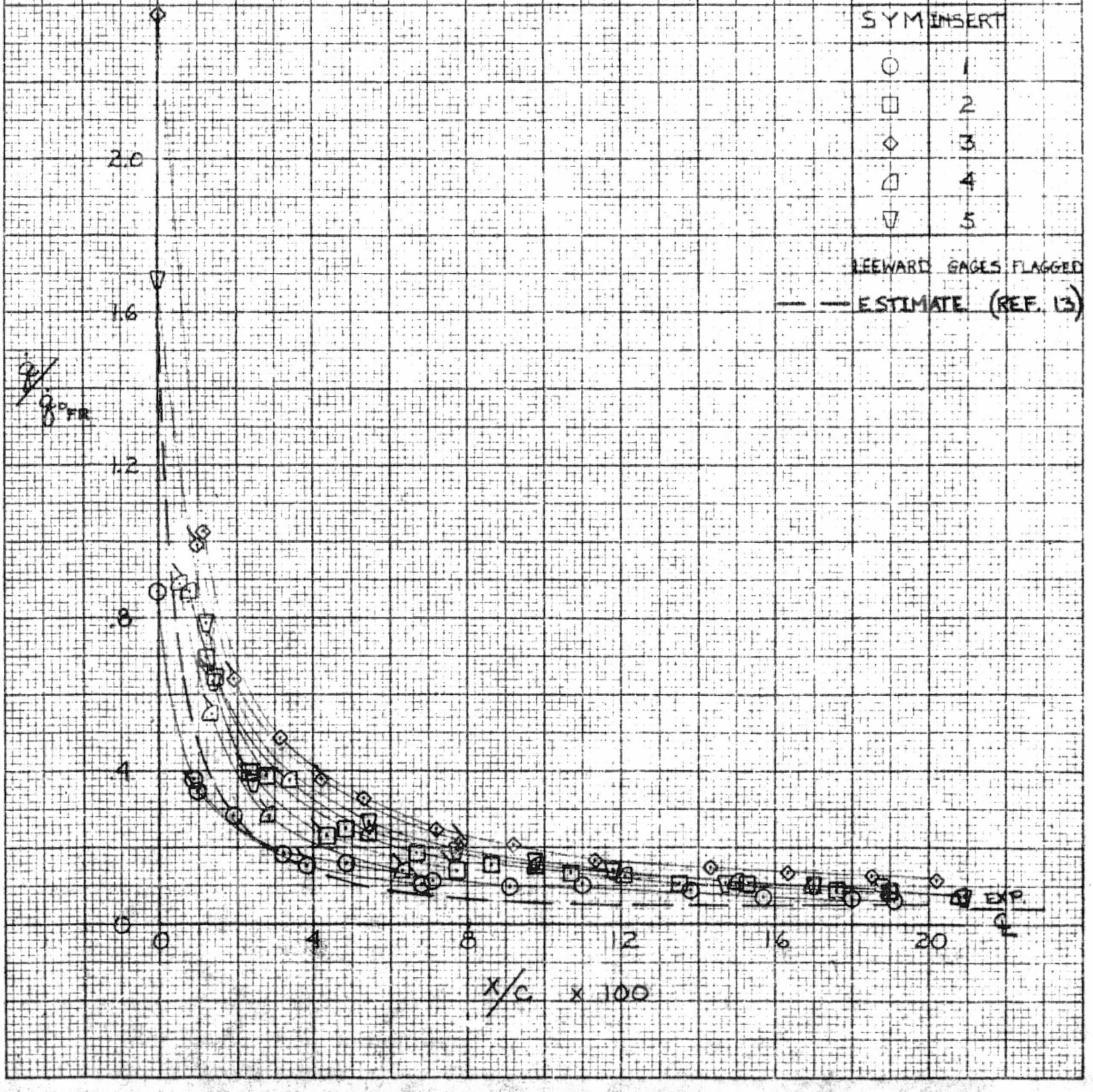


FIGURE 10 b

FULL SCALE NORMALIZED SPANWISE HEATING DISTRIBUTION

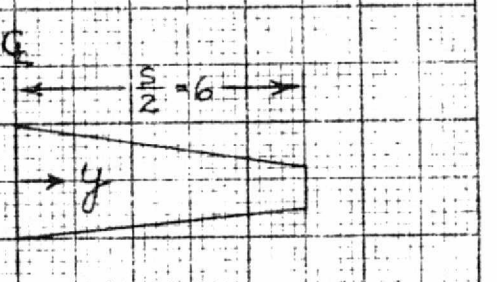
WINDWARD SIDE $X/C = .17$

NASA/MSC SPACE SHUTTLE

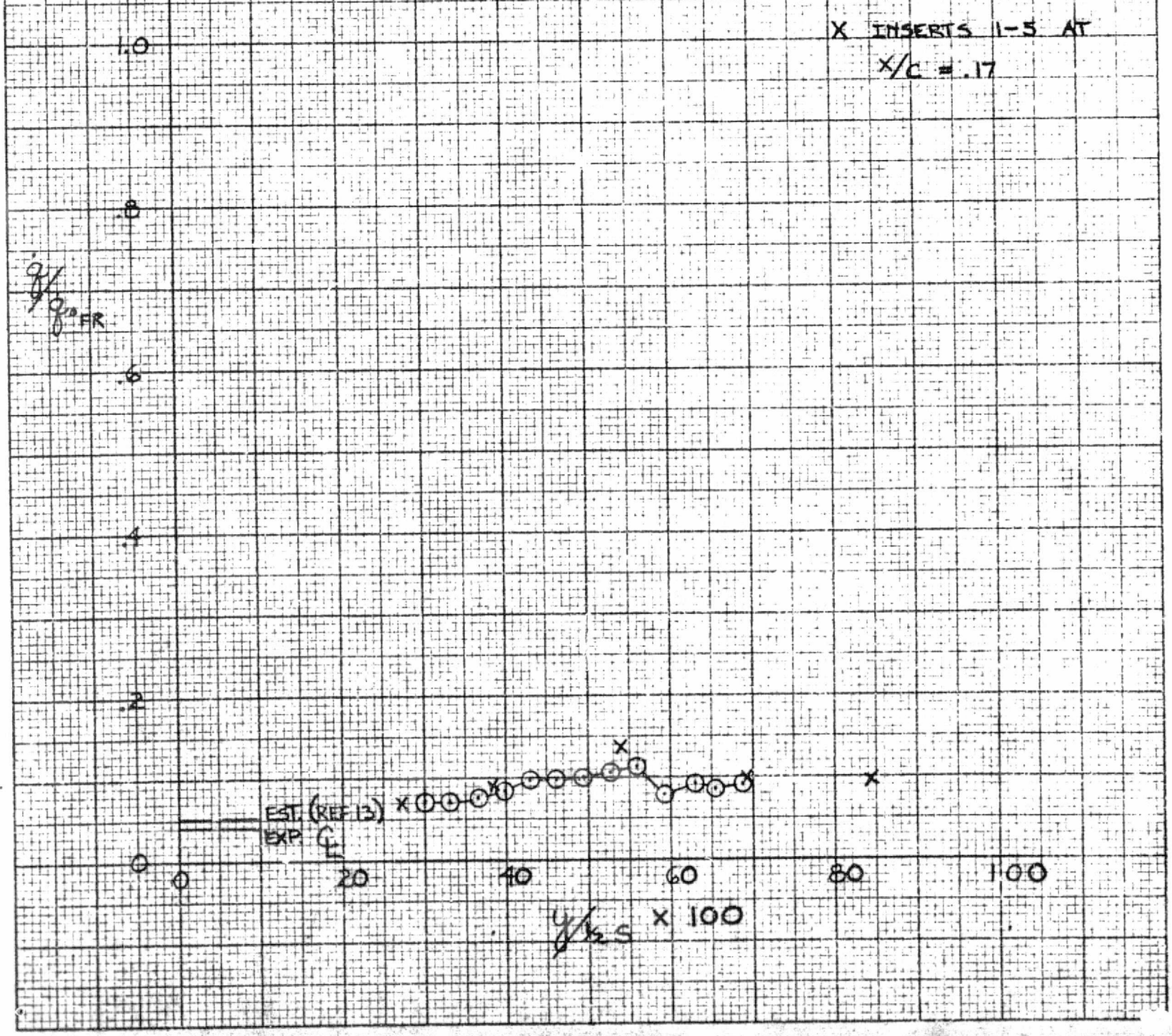
1/80 SCALE

RUN 15 $M_\infty = 7.58$ $Re/_{FT} = 3.75 \times 10^5$ $\alpha = 0°$

$\frac{q'_0}{q'_{0_{FR}}}_{R=1'} = 2.18$



X INSERTS 1-5 AT $X/C = .17$



7 X 10 INCHES MADE IN U.S.A.
KEUFFEL & ESSER CO.

FIGURE 11 a

FULL SCALE NORMALIZED CHORDWISE HEATING DISTRIBUTION

NASA/MSC SPACE SHUTTLE

1/80 SCALE

STA ____

RUN 16 M_∞ = 7.97 $Re/_{FT}$ = 1.08×10^7 α = 15°

$\dot{q}_{0_{FR_{R=1'}}}$ = 17.4

SYM	INSERT
○	1
□	2
◇	3
△	4
▽	5

LEEWARD GAGES FLAGGED

— — ESTIMATE (REF. 13)

$\dot{q}/\dot{q}_{0_{FR}}$

2.0
1.6
1.2
.8
.4

4 8 12 16 20

EXP. $\dot{q}_L$

X/C x 100

KEUFFEL & ESSER CO. MADE IN U.S.A. 7 X 10 INCHES

FIGURE 11 b

FULL SCALE NORMALIZED SPANWISE HEATING DISTRIBUTION

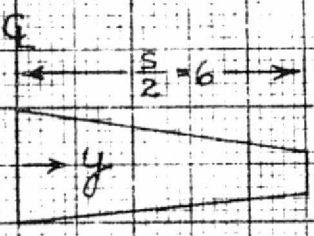
WINDWARD SIDE $x/c = .17$

NASA / MSC SPACE SHUTTLE

1/80 SCALE

RUN 16 M_∞ = 7.97 $Re/_{FT}$ = 1.08×10^7 α = 15°

$\dot{q}_{FR_{R=1'}}$ = 17.4



X INSERTS 1-5 AT $x/c = .17$

7 X 10 INCHES
KEUFFEL & ESSER CO.

FIGURE 12 a

FULL SCALE NORMALIZED CHORDWISE HEATING DISTRIBUTION

NASA/MSC SPACE SHUTTLE

1/80 SCALE

STA ____

RUN 13 M_∞ = 7.85 $Re/FT = 4.55 \times 10^6$ α = 30°

$\dot{q}_{D_{TR_{R=1'}}}$ = 11.9

SYM	INSERT
○	1
□	2
◇	3
◁	4
▽	5

LEEWARD GAGES FLAGGED

— — ESTIMATE (REF. 13)

$\dot{q}/\dot{q}_{D_{TR}}$

2.0
1.6
1.2
.8
.4

4 8 12 16 20

EXP C_L

X/C x 100

KEUFFEL & ESSER CO. MADE IN U.S.A.

FIGURE 12 b

FULL SCALE NORMALIZED SPANWISE HEATING DISTRIBUTION

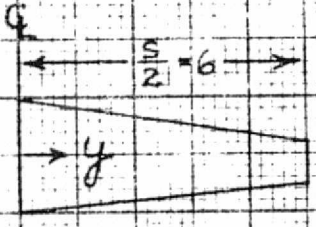
WINDWARD SIDE X/C = .17

NASA/MSC SPACE SHUTTLE

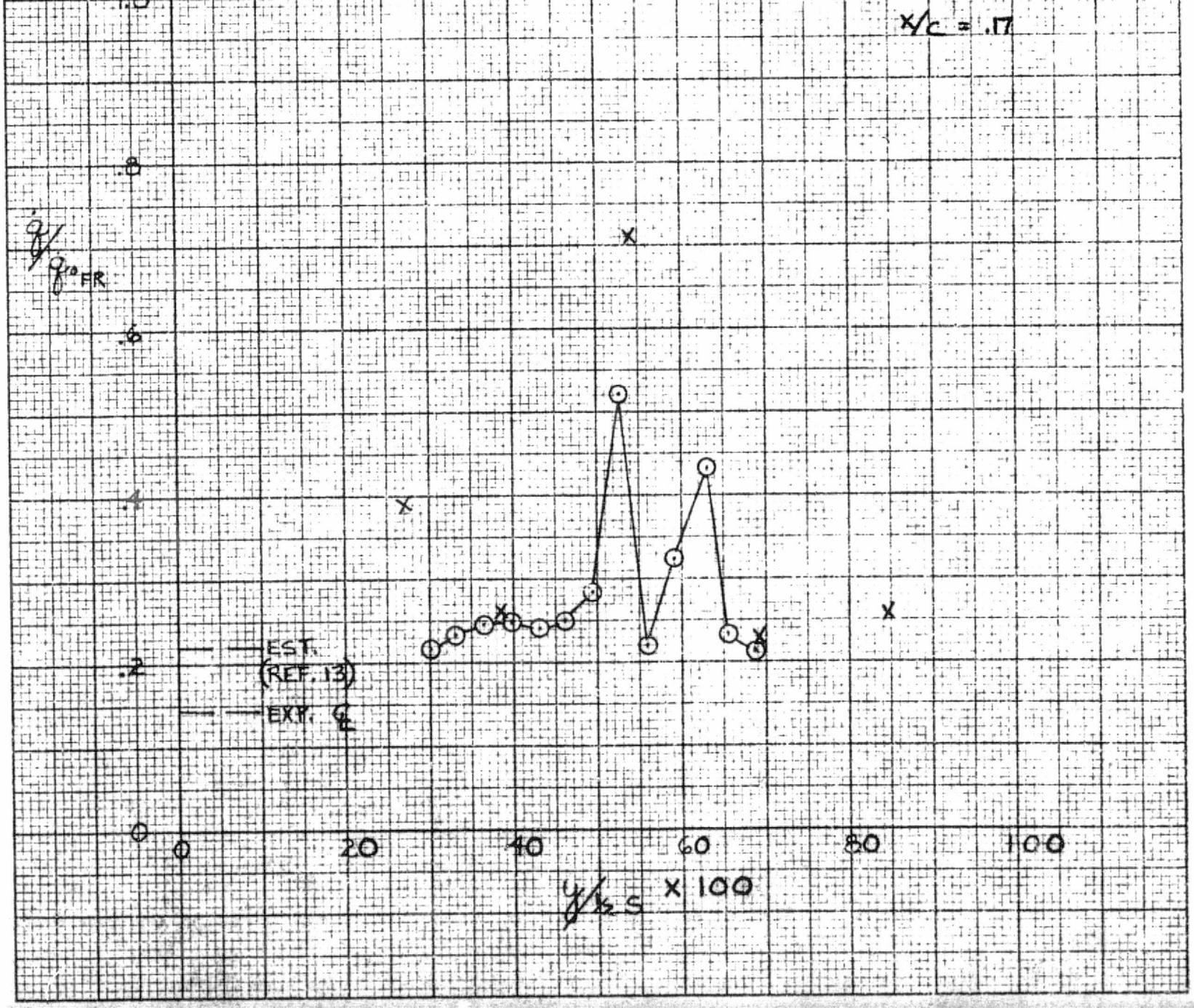
1/80 SCALE

RUN 13 M_∞ = 7.85 $Re/_{FT}$ = 4.55×10^6 α = 30°

$\dot{q}_{\dot{q}_{FR_{R=1'}}}$ = 11.9



X INSERTS 1-5 AT X/C = .17



K&E 7 X 10 INCHES
KEUFFEL & ESSER CO.

FIGURE 13a

FULL SCALE NORMALIZED CHORDWISE HEATING DISTRIBUTION

NASA/MSC SPACE SHUTTLE

1/80 SCALE

STA ____

RUN 10 M_∞ = 7.73 $Re/_{FT}$ = 2.13×10^6 α = 45°

$\frac{\dot{q}}{\dot{q}_{R_{ref}}}$ = 6.57

SYM	INSERT
○	1
□	2
◇	3
⏢	4
▽	5

LEEWARD GAGES FLAGGED

——— ESTIMATE (REF. 13)

$\frac{\dot{q}}{\dot{q}_{FR}}$

2.0
1.6
1.2
.8
.4
0

0 4 8 12 16 20

X/C x 100

EXP. / CF

11" x 8½" 7 X 10 INCHES MADE IN U.S.A.
KEUFFEL & ESSER CO

FIGURE 13 b

FULL SCALE NORMALIZED SPANWISE HEATING DISTRIBUTION

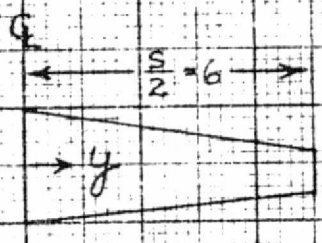
WINDWARD SIDE $X/C = .17$

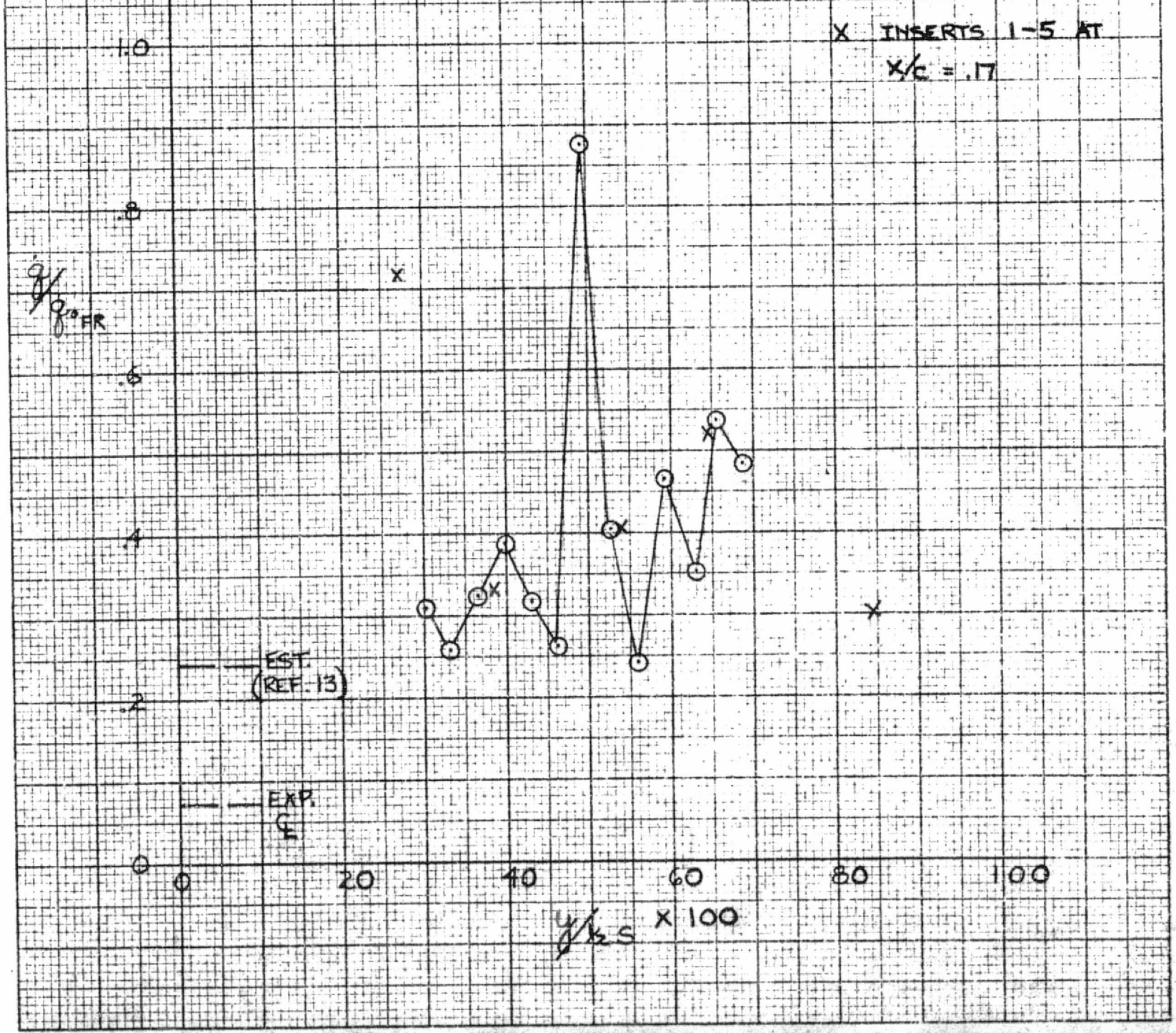
NASA / MSC SPACE SHUTTLE

1/80 SCALE

RUN 10 $M_\infty = 7.73$ $Re/_{FT} = 2.13 \times 10^6$ $\alpha = 45°$

$\dot{q}_{\infty_{FR}} = 6.57$ $R = 1'$





7 X 10 INCHES MADE IN U.S.A. KEUFFEL & ESSER CO.

FIGURE 14a

FULL SCALE NORMALIZED CHORDWISE HEATING DISTRIBUTION

NASA/MSC SPACE SHUTTLE

1/80 SCALE

STA ____

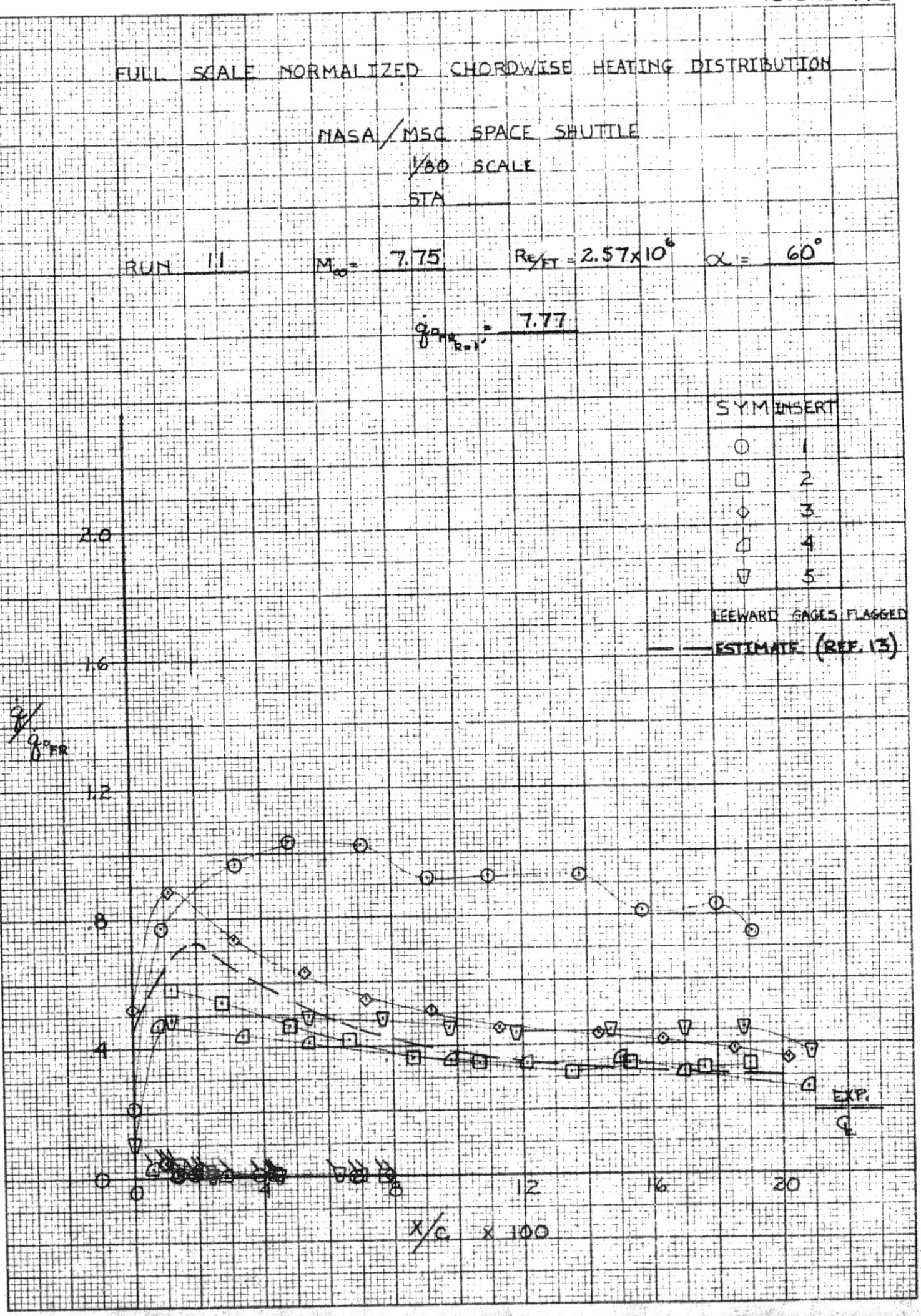
RUN 11 M_∞ = 7.75 $R_{e/FT}$ = 2.57×10^6 α = 60°

$\dot{q}_{0_{FR}}$ = 7.77

SYM	INSERT
○	1
□	2
◇	3
⏢	4
▽	5

LEEWARD GAGES FLAGGED

— — ESTIMATE (REF. 13)



7 X 10 INCHES MADE IN U.S.A.
KEUFFEL & ESSER CO.

FIGURE 14 b

FULL SCALE NORMALIZED SPANWISE HEATING DISTRIBUTION

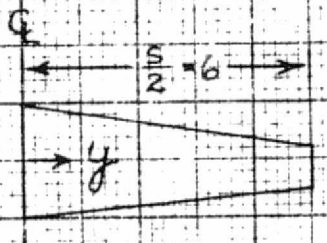
WINDWARD SIDE $X/C = .17$

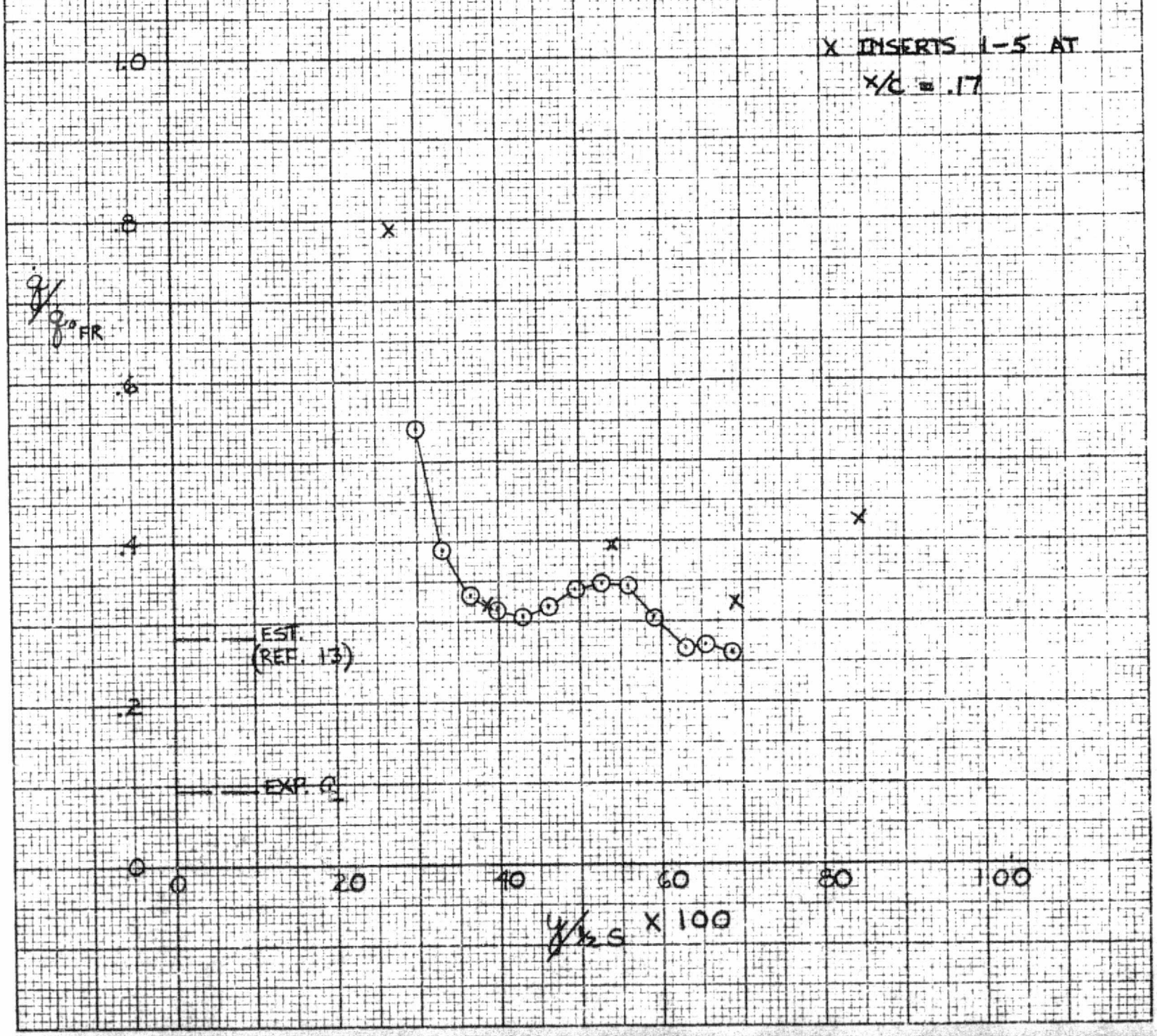
NASA / MSC SPACE SHUTTLE

1/80 SCALE

RUN 11 $M_\infty = 7.75$ $Re/FT = 2.57 \times 10^6$ $\alpha = 60°$

$\dot{q}_{\infty_{FR_{R=1'}}} = 7.77$





KE 7 X 10 INCHES
KEUFFEL & ESSER CO.

FIGURE 15a

FULL SCALE NORMALIZED CHORDWISE HEATING DISTRIBUTION

NASA/MSC SPACE SHUTTLE

1/80 SCALE

STA ____

RUN 14 M_∞ = 7.76 $Re/_{FT}$ = 2.64×10^6 α = 60°

β = +3°

$\dot{q}_{STR_{R=1'}}$ = 6.93

SYM	INSERT
○	1
□	2
◇	3
◁	4
▽	5

LEEWARD GAGES FLAGGED

— — ESTIMATE (REF. 13)

$\dot{q}/\dot{q}_{STR}$

2.0
1.6
1.2
.8
.4
0

4 8 12 16 20

X/C x 100

EXP. $\bar{c}_L$

KEUFFEL & ESSER CO

FIGURE 15 b

FULL SCALE NORMALIZED SPANWISE HEATING DISTRIBUTION

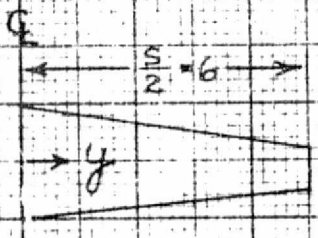
WINDWARD SIDE $X/C = .17$

NASA / MSC SPACE SHUTTLE

1/80 SCALE

RUN 14 $M_\infty = 7.76$ $Re/FT = 2.64 \times 10^6$ $\alpha = 60°$ $\beta = +3°$

$\dot{q}_{0_{FR_{R=1'}}} = 6.93$



X INSERTS 1-5 AT $X/C = .17$

7 X 10 INCHES
KEUFFEL & ESSER CO
MADE IN U.S.A.

FIGURE 16a

FULL SCALE NORMALIZED CHORDWISE HEATING DISTRIBUTION

NASA/MSC SPACE SHUTTLE

1/80 SCALE

STA ____

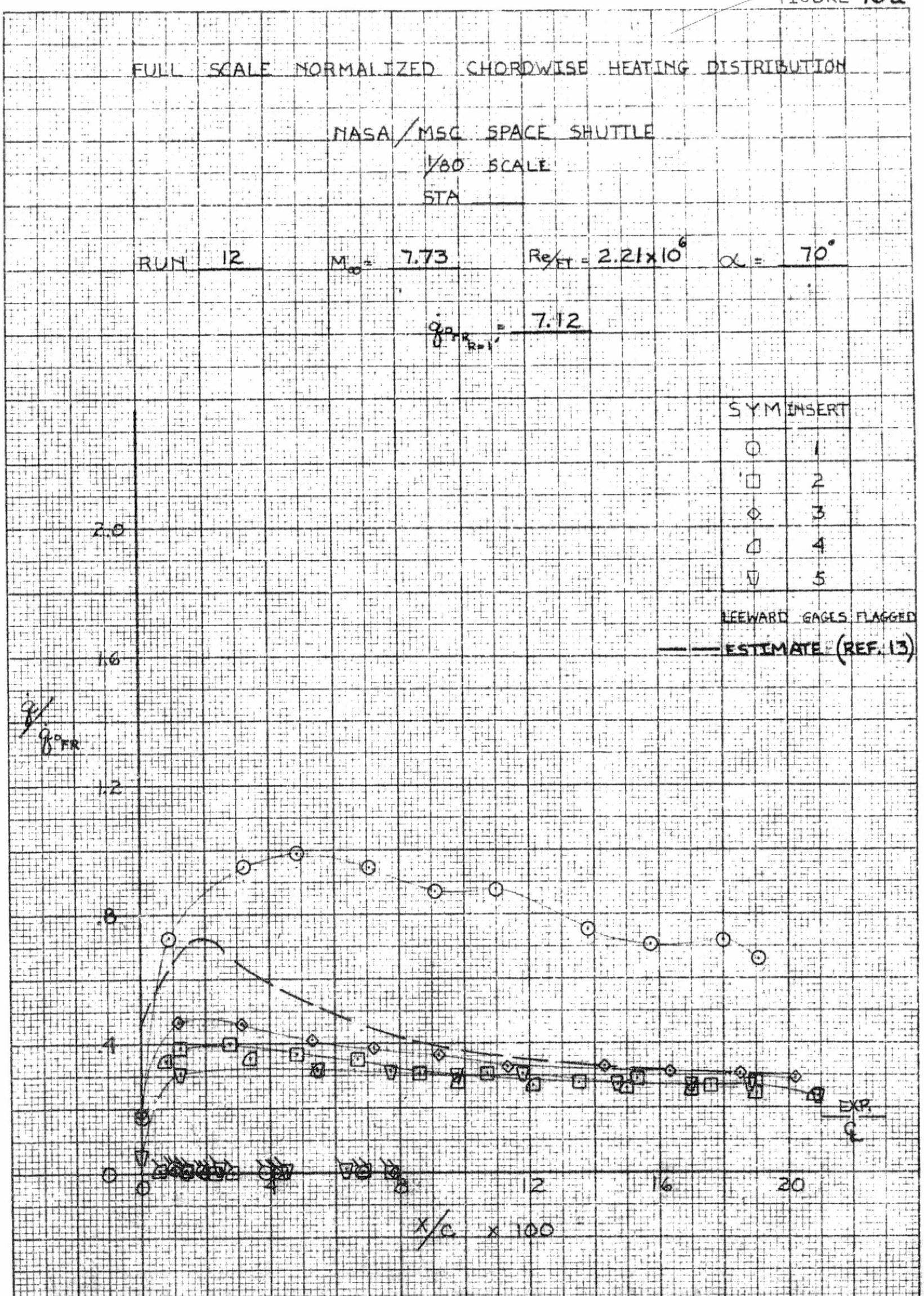
RUN 12 M_∞ = 7.73 $Re_{/FT}$ = 2.21×10^6 α = 70°

$\dot{q}_{R_N=R_{R=1'}}$ = 7.12

SYM	INSERT
○	1
□	2
◇	3
◁	4
▽	5

LEEWARD GAGES FLAGGED

—— ESTIMATE (REF. 13)



KEUFFEL & ESSER CO

FIGURE 16b

FULL SCALE NORMALIZED SPANWISE HEATING DISTRIBUTION

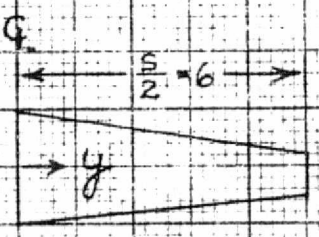
WINDWARD SIDE $x/c = .17$

NASA/MSC SPACE SHUTTLE

1/80 SCALE

RUN 12 $M_\infty = 7.73$ $Re/FT = 2.21 \times 10^6$ $\alpha = 70°$

$\dot{q}_{FR_{R=1'}} = 7.12$



X INSERTS 1-5 AT $x/c = .17$

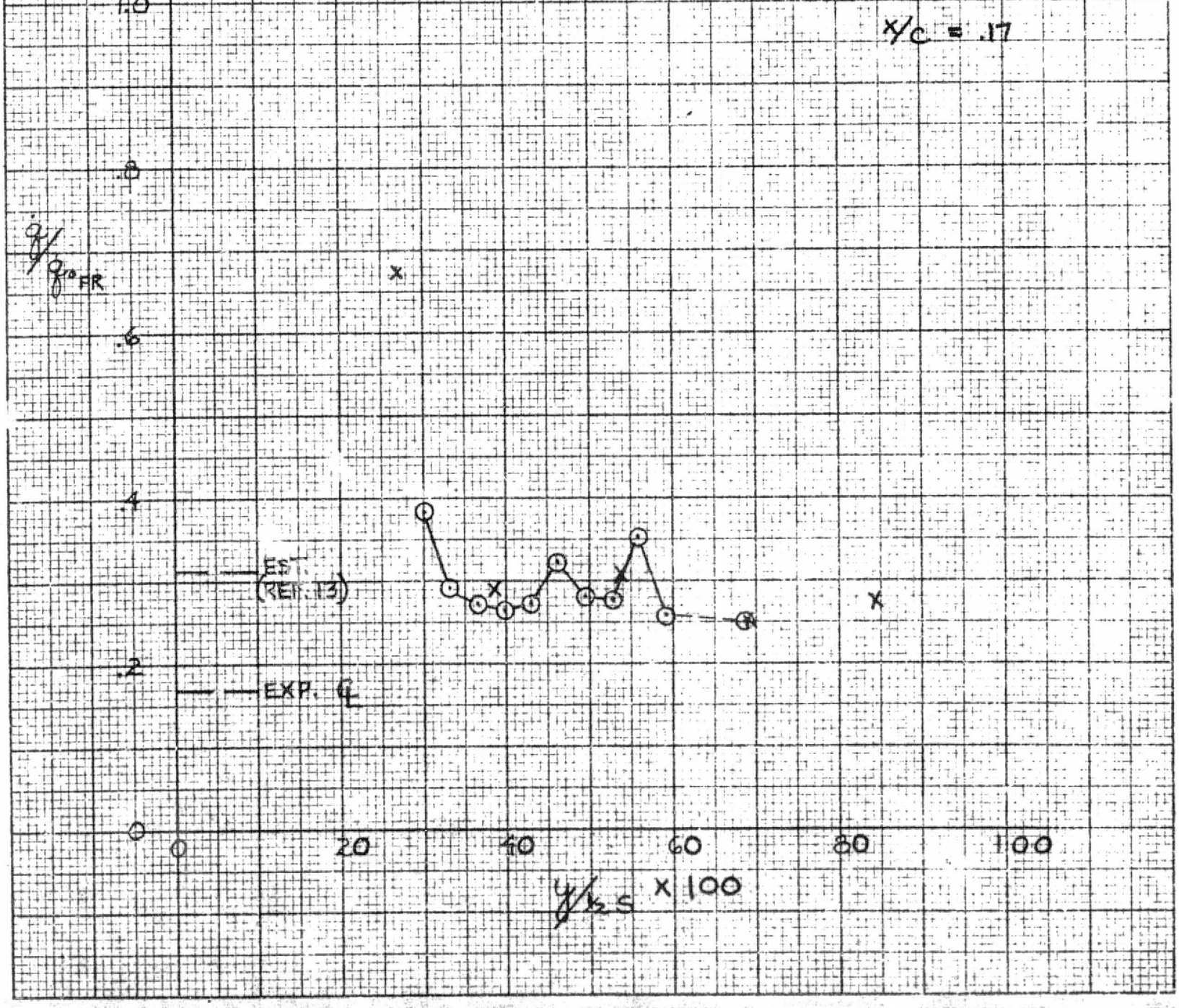


FIGURE 17a

FULL SCALE NORMALIZED CHORDWISE HEATING DISTRIBUTION

NASA/MSC SPACE SHUTTLE

1/80 SCALE

STA ____

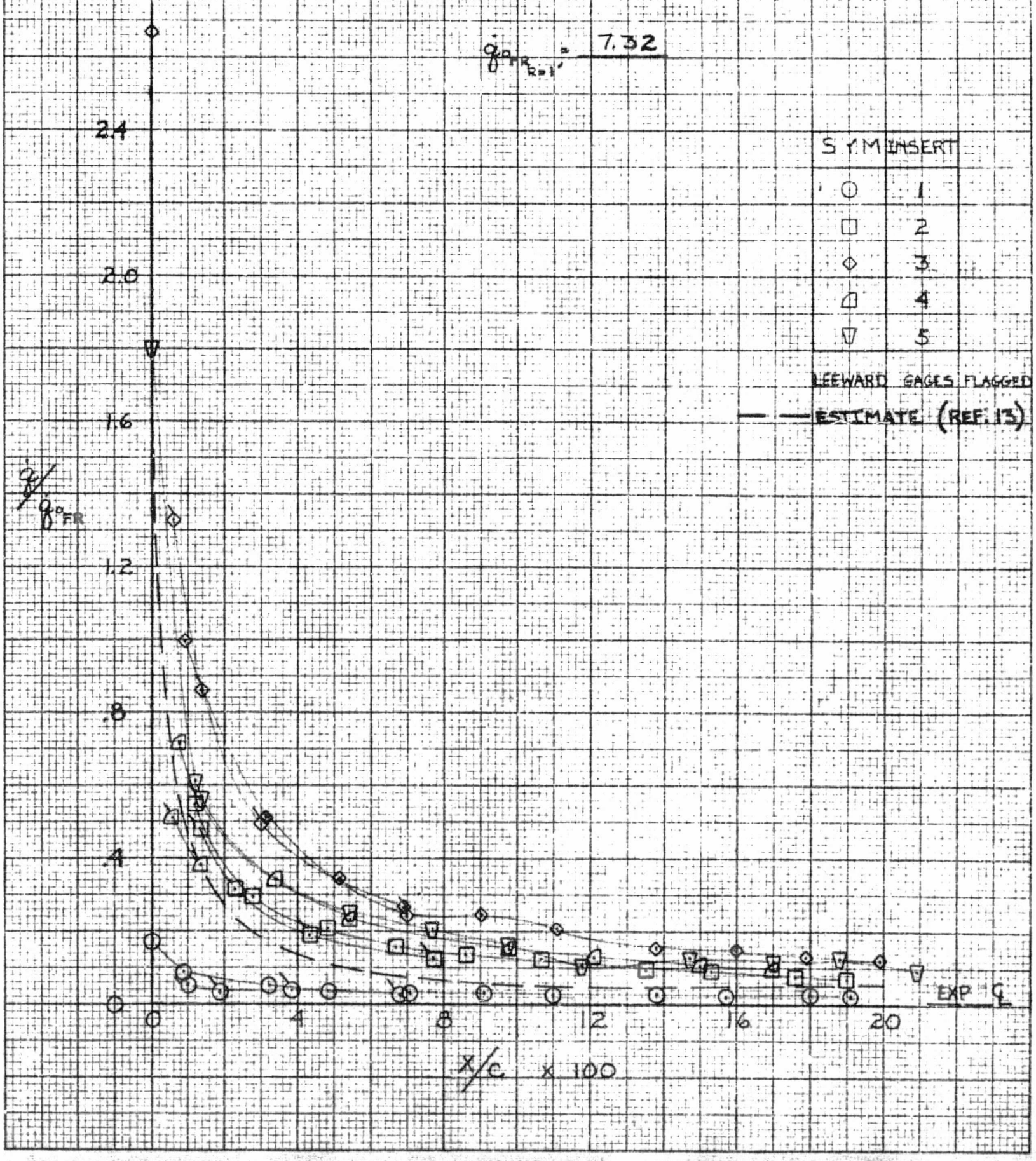
RUN 1 M_∞ = 16.5 $Re/_{FT}$ = 9.73×10^4 α = 0°

$\dot{q}_{R=1'}$ = 7.32

SYM	INSERT
○	1
□	2
◇	3
◁	4
▽	5

LEEWARD GAGES FLAGGED

— — ESTIMATE (REF. 13)



KEUFFEL & ESSER CO

FIGURE 17 b

FULL SCALE NORMALIZED SPANWISE HEATING DISIRIBUTION

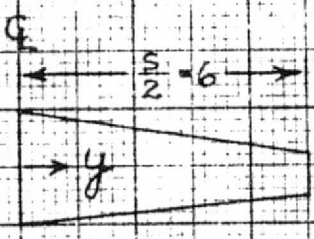
WINDWARD SIDE $X/C = .17$

NASA / MSC SPACE SHUTTLE

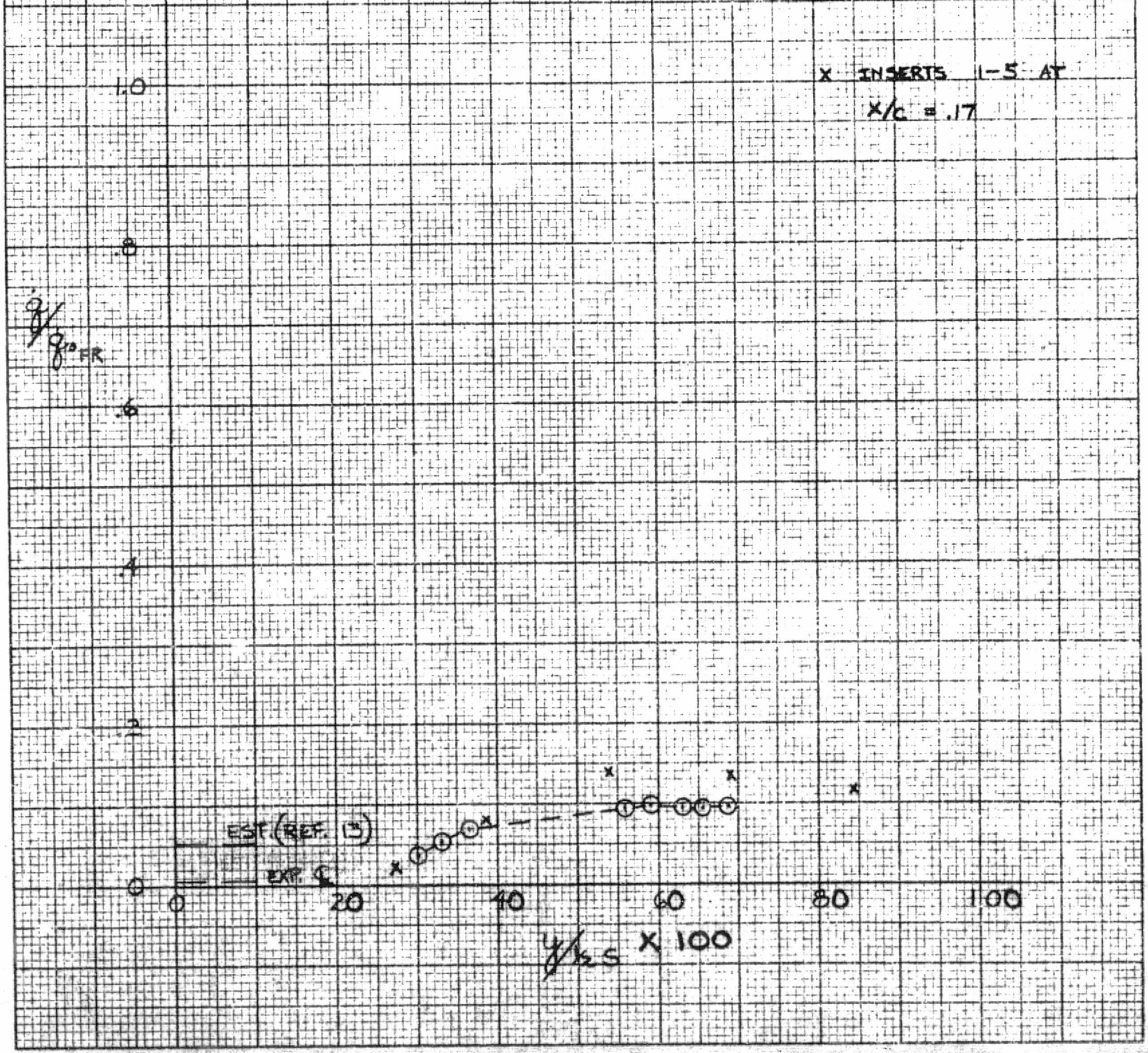
1/80 SCALE

RUN 1 $M_\infty = 16.5$ $Re/FT = 9.73 \times 10^4$ $\alpha = 0°$

$\dot{q}_{\circ FR_{R=1'}} = 7.32$



X INSERTS 1-5 AT $X/C = .17$



7 X 10 INCHES KEUFFEL & ESSER CO. MADE IN U.S.A.

FIGURE 18a

FULL SCALE NORMALIZED CHORDWISE HEATING DISTRIBUTION

NASA/MSC SPACE SHUTTLE

1/80 SCALE

STA ____

RUN 2 M_∞ = 16.2 $Re/_{FT}$ = 9.72×10^5 α = 15°

$\dot{q}_{D_{TR_{R=1}}}$ = 29.2

SYM	INSERT
○	1
□	2
◇	3
◁	4
▽	5

LEEWARD GAGES FLAGGED

— — ESTIMATE (REF. 13)

$\dot{q}/\dot{q}_{D_{TR}}$

2.0
1.6
1.2
.8
.4
0

0 4 8 12 16 20

X/C x 100

EXP. ℄

KEUFFEL & ESSER CO.

FIGURE 18 b

FULL SCALE NORMALIZED SPANWISE HEATING DISTRIBUTION

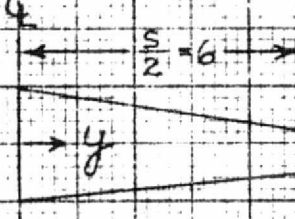
WINDWARD SIDE $X/C = .17$

NASA / MSC SPACE SHUTTLE

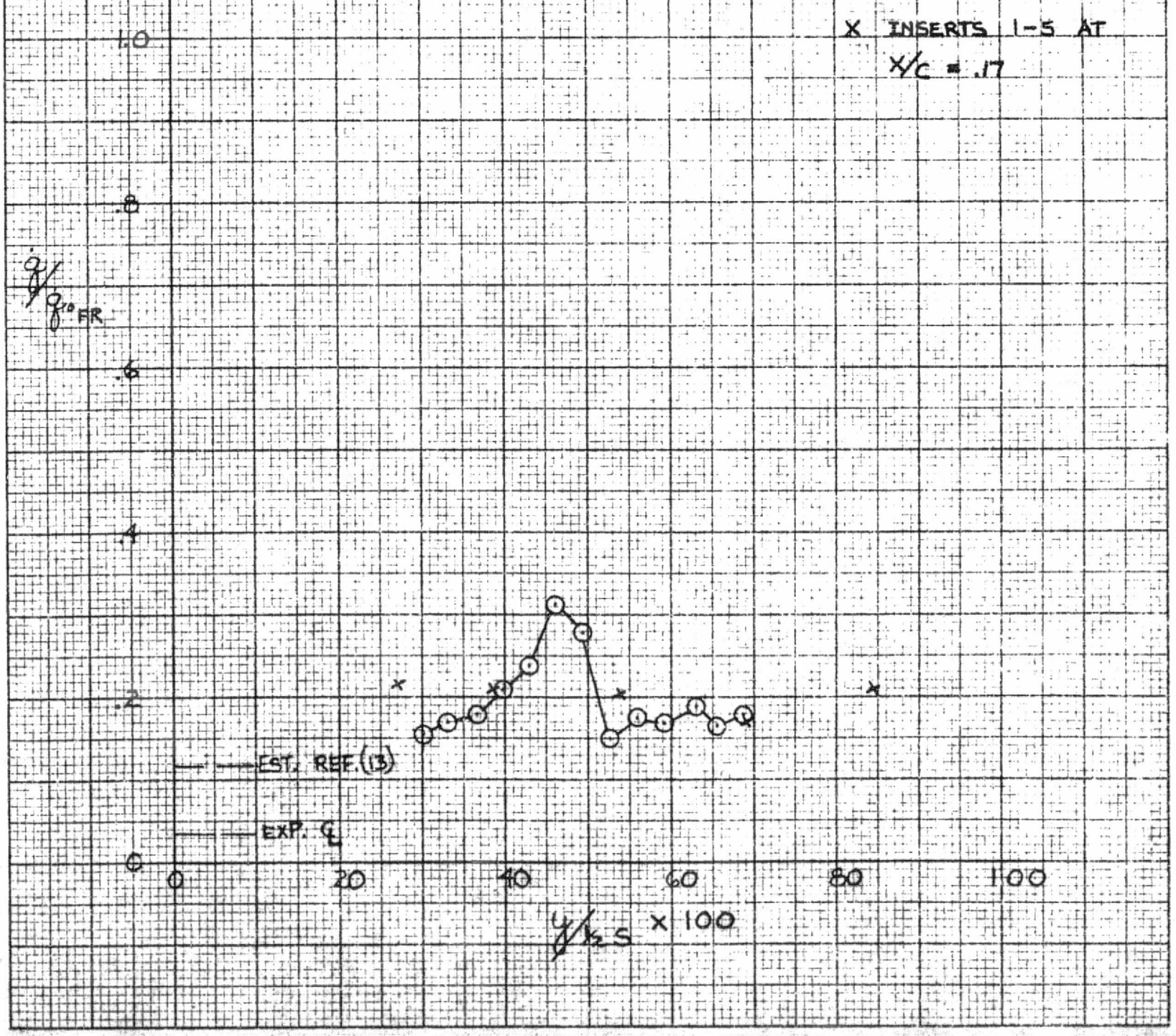
1/80 SCALE

RUN 2 $M_\infty = 16.2$ $Re/FT = 9.72 \times 10^5$ $\alpha = 15°$

$\dot{q}_{0_{FR_{R=1'}}} = 29.2$



X INSERTS 1-5 AT $X/C = .17$



7 X 10 INCHES MADE IN U.S.A.
KEUFFEL & ESSER CO.

FIGURE 19a

FULL SCALE NORMALIZED CHORDWISE HEATING DISTRIBUTION

NASA/MSC SPACE SHUTTLE

1/80 SCALE

STA ____

RUN 3 M_∞ = 16.25 $Re/_{FT}$ = 9.60×10^5 α = 30°

$\dot{q}_{PHR_{R=1}}$ = 30.3

SYM	INSERT
○	1
□	2
◇	3
⏢	4
▽	5

LEEWARD GAGES FLAGGED

— — ESTIMATE (REF. 13)

$\dot{q}/\dot{q}_{PFR}$

2.0
1.6
1.2
.8
.4
0

0 4 8 12 16 20

$X/C \times 100$

EXP. C_F

8 1/2 x 11 7 X 10 INCHES
KEUFFEL & ESSER CO

FIGURE 19 b

FULL SCALE NORMALIZED SPANWISE HEATING DISTRIBUTION

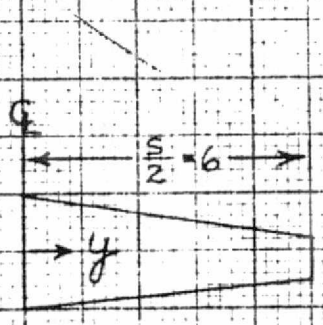
WINDWARD SIDE $X/C = .17$

NASA / MSC SPACE SHUTTLE

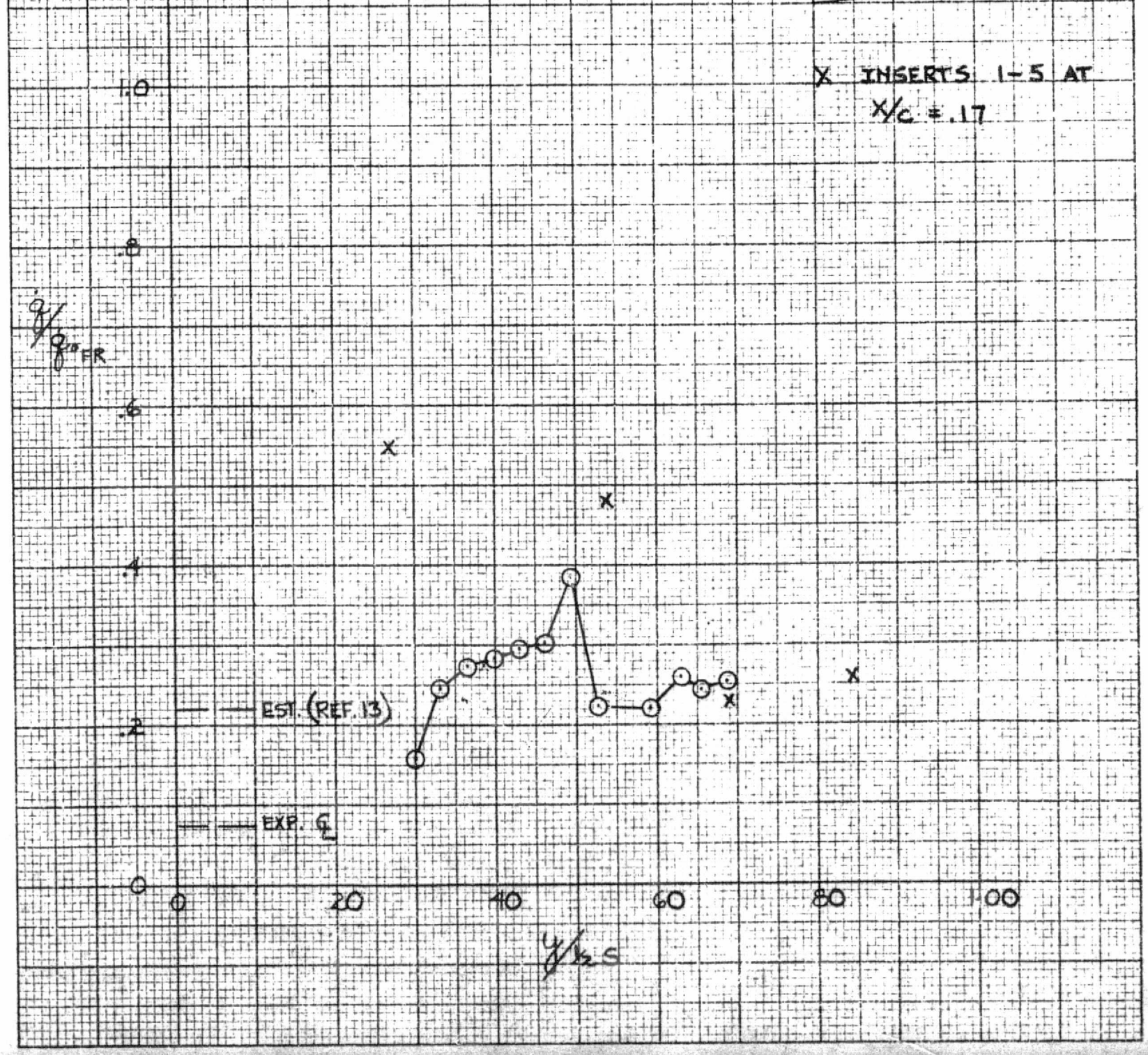
1/80 SCALE

RUN 3 $M_\infty = 16.25$ $Re/FT = 9.60 \times 10^5$ $\alpha = 30°$

$\dot{q}_{\infty_{FR_{R=1'}}} = 30.27$



X INSERTS 1-5 AT $X/C = .17$



7 x 10 INCHES
KEUFFEL & ESSER CO.
MADE IN U.S.A.

FIGURE 20a

FULL SCALE NORMALIZED CHORDWISE HEATING DISTRIBUTION

NASA/MSC SPACE SHUTTLE

1/80 SCALE

STA ____

RUN 7 M_∞ = 16.15 $Re/_{FT}$ = 9.84×10^5 α = 30°

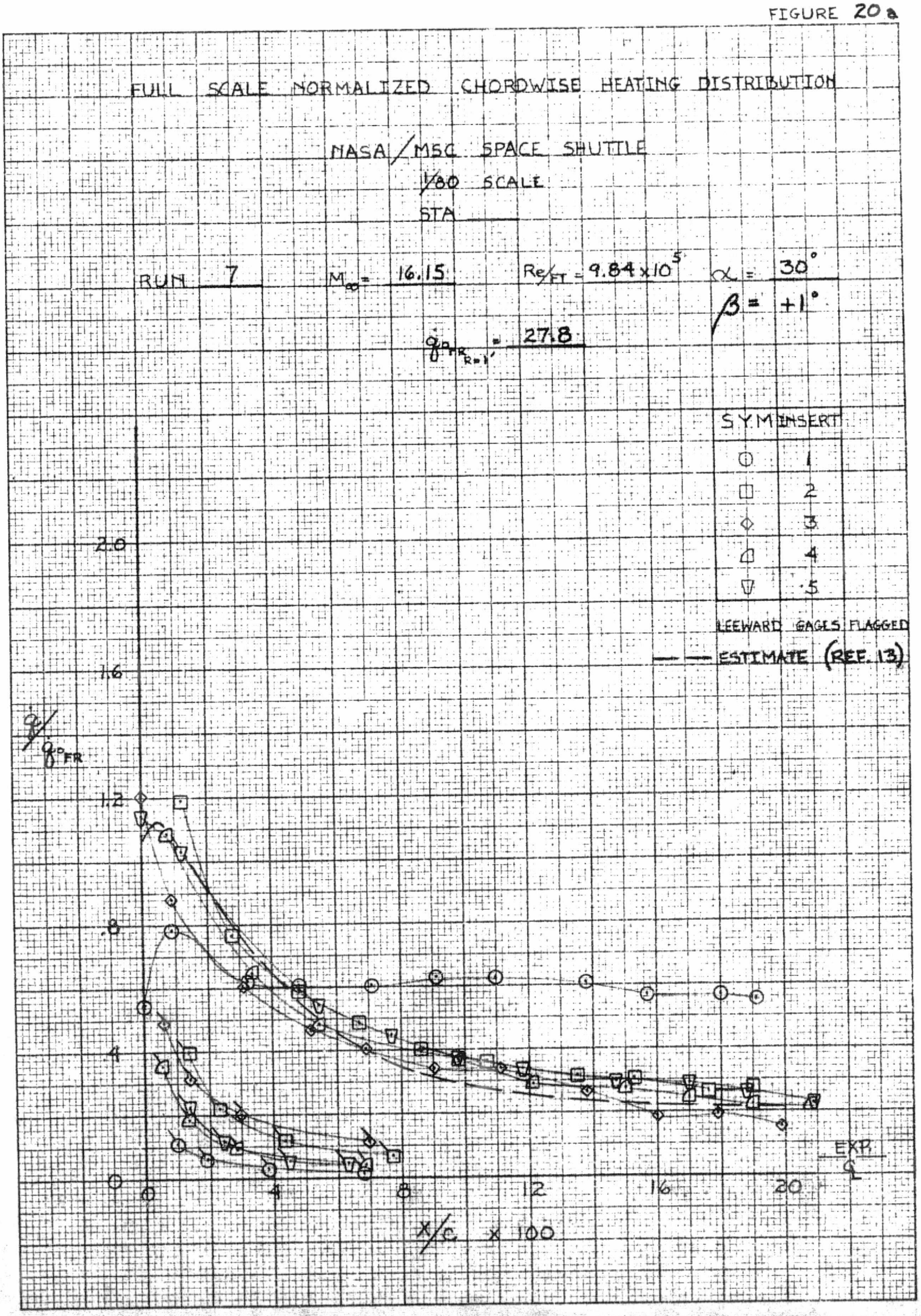
β = +1°

$\dot{q}_{PT_{R=1'}}$ = 27.8

SYM	INSERT
○	1
□	2
◇	3
⏢	4
▽	5

LEEWARD GAGES FLAGGED

— — ESTIMATE (REF. 13)



KEUFFEL & ESSER CO

FIGURE 20b

FULL SCALE NORMALIZED SPANWISE HEATING DISIRIBUTION

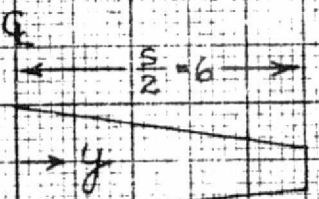
WINDWARD SIDE $X/C = .17$

NASA/MSC SPACE SHUTTLE

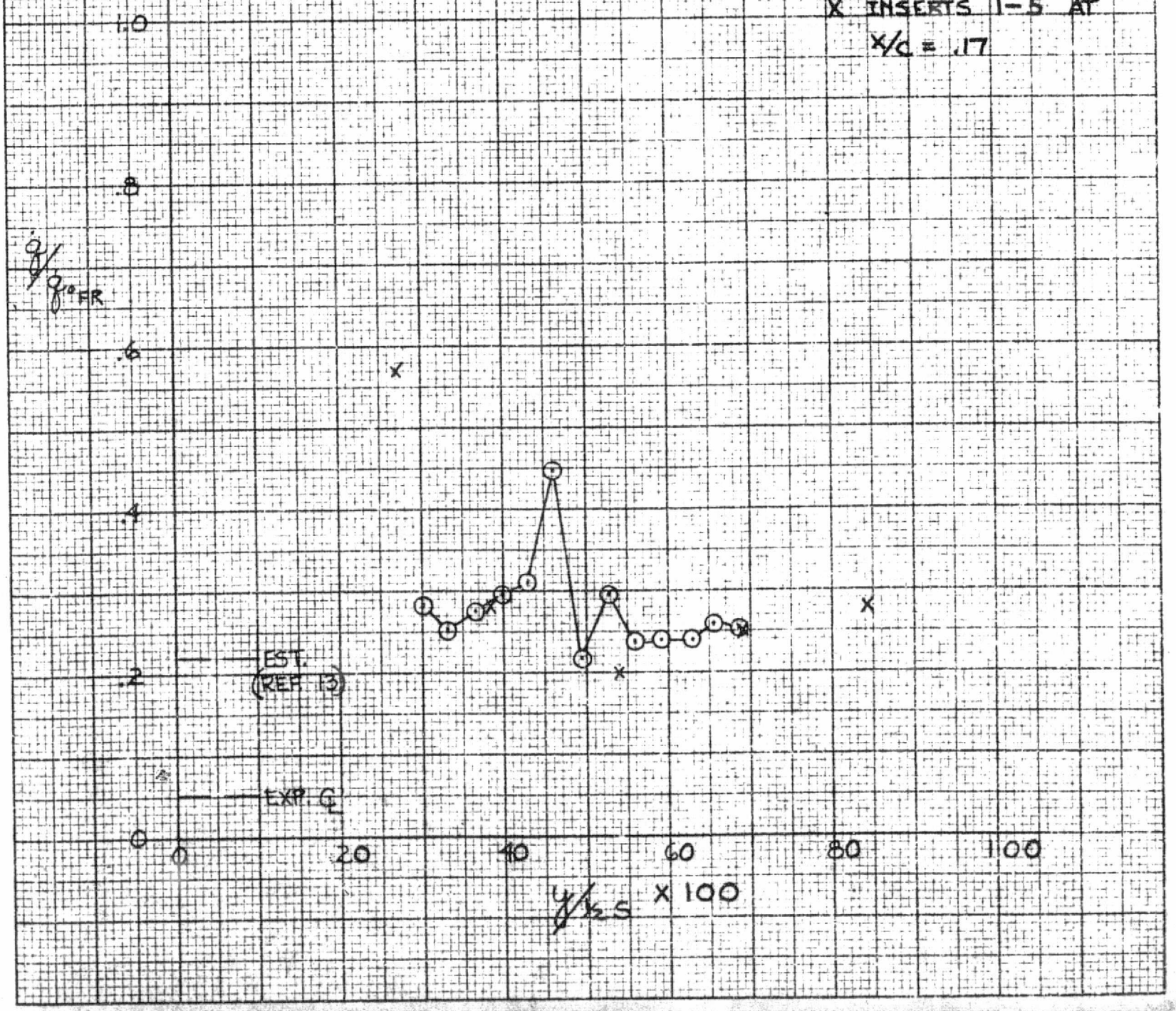
1/80 SCALE

RUN 7 $M_\infty = 16.15$ $Re/FT = 9.84 \times 10^5$ $\alpha = 30°$ $\beta = +1°$

$\dot{q}_{0_{FR_{R=1'}}} = 27.8$



X INSERTS 1-5 AT $X/C = .17$



7 X 10 INCHES MADE IN U.S.A.
KEUFFEL & ESSER CO.

FIGURE 21a

FULL SCALE NORMALIZED CHORDWISE HEATING DISTRIBUTION

NASA/MSC SPACE SHUTTLE

1/80 SCALE

STA ____

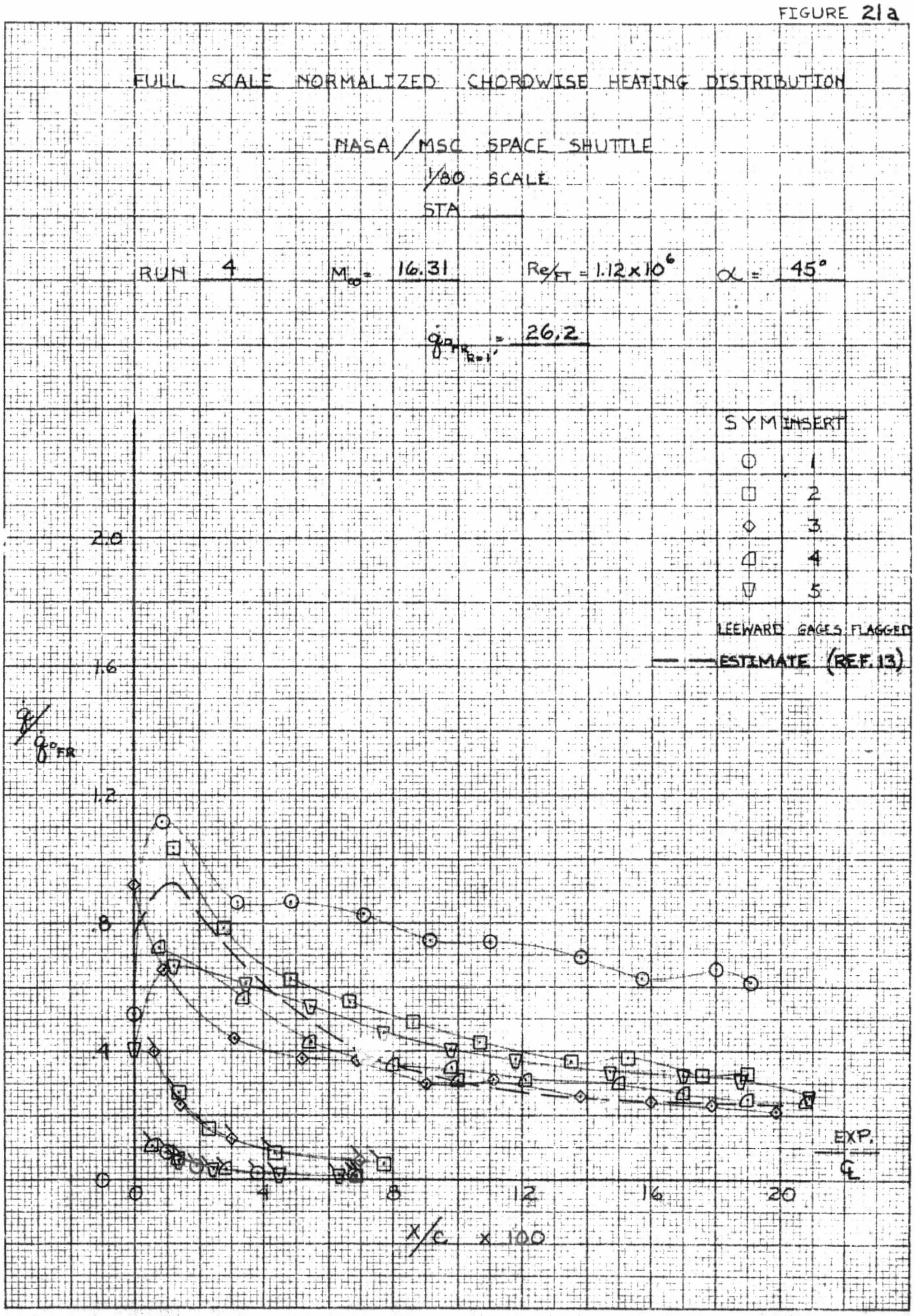
RUN 4 M_∞ = 16.31 $Re/FT = 1.12 \times 10^6$ α = 45°

$\dot{q}_{PFR_{R=1}}$ = 26.2

SYM	INSERT
○	1
□	2
◇	3
◁	4
▽	5

LEEWARD GAGES FLAGGED

— — ESTIMATE (REF. 13)



KEUFFEL & ESSER CO

FIGURE 21 b

FULL SCALE NORMALIZED SPANWISE HEATING DISTRIBUTION

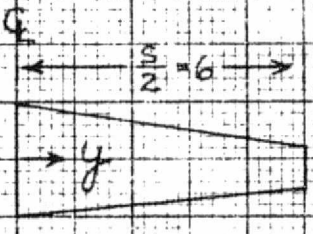
WINDWARD SIDE $X/C = .17$

NASA/MSC SPACE SHUTTLE

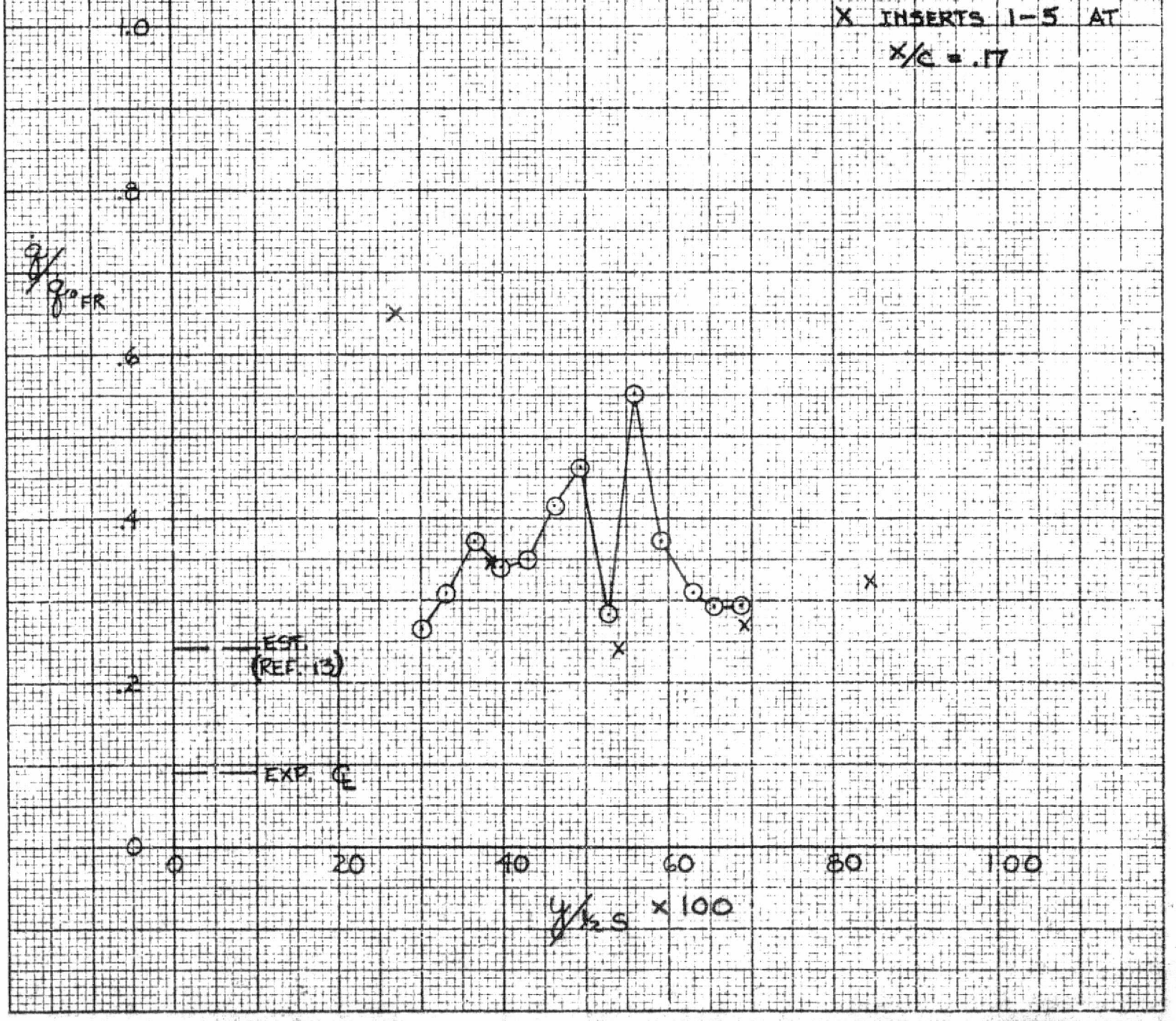
1/80 SCALE

RUN 4 $M_\infty = 16.31$ $Re/FT = 1.12 \times 10^6$ $\alpha = 45°$

$\dot{q}_{\infty_{FR}} = 26.2$ $_{R=1'}$



X INSERTS 1-5 AT $X/C = .17$



KEUFFEL & ESSER CO.

FIGURE 22a

FULL SCALE NORMALIZED CHORDWISE HEATING DISTRIBUTION

NASA/MSC SPACE SHUTTLE

1/80 SCALE

STA ____

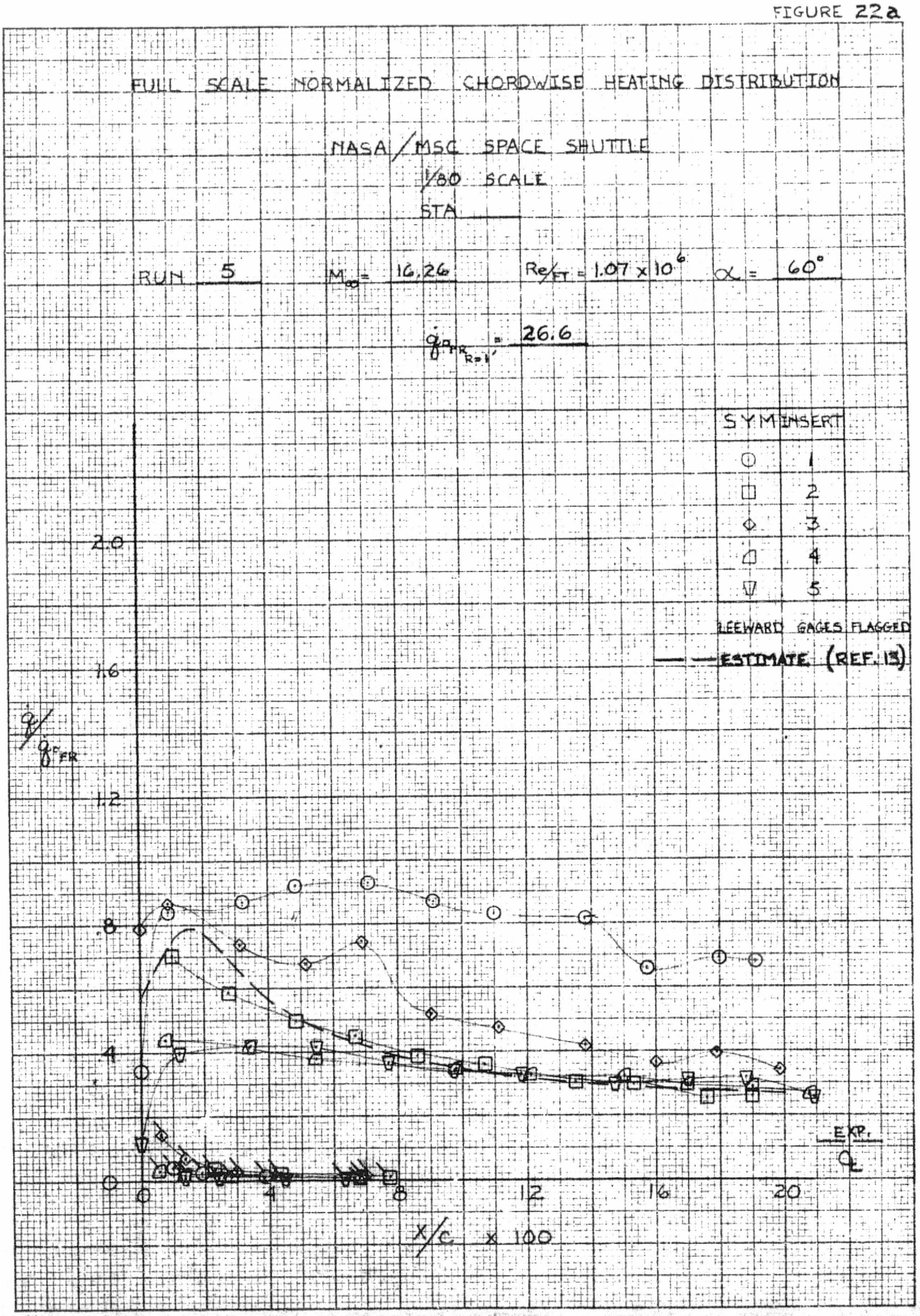
RUN 5 M_∞ = 16.26 $Re/_{FT} = 1.07 \times 10^6$ α = 60°

$\dot{q}_{R=1'}$ = 26.6

SYM	INSERT
○	1
□	2
◇	3
◁	4
▽	5

LEEWARD GAGES FLAGGED

—— ESTIMATE (REF. 13)



KEUFFEL & ESSER CO

FIGURE 22 b

FULL SCALE NORMALIZED SPANWISE HEATING DISTRIBUTION

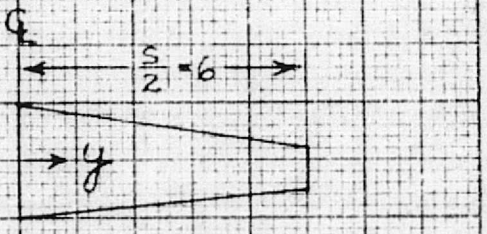
WINDWARD SIDE $X/C = .17$

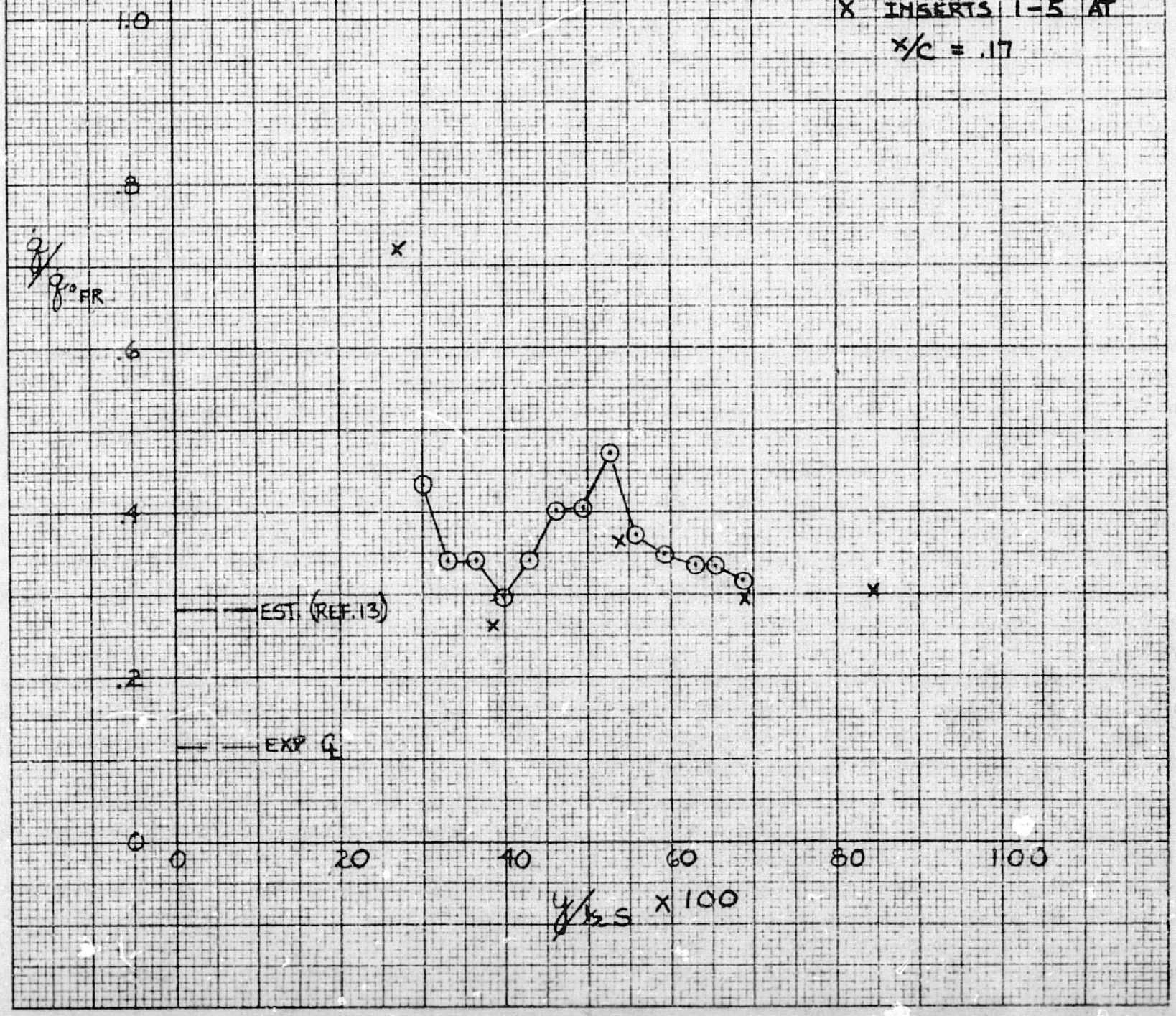
NASA / MSC SPACE SHUTTLE

1/80 SCALE

RUN 5 $M_\infty = 16.26$ $Re/FT = 1.07 \times 10^6$ $\alpha = 60°$

$\dot{q}_{\infty_{FR}} = 26.6$ $_{R=1'}$





KE 7 X 10 INCHES KEUFFEL & ESSER CO. MADE IN U.S.A.

FIGURE 23a

FULL SCALE NORMALIZED CHORDWISE HEATING DISTRIBUTION

NASA/MSC SPACE SHUTTLE

1/80 SCALE

STA ____

RUN 8 M_∞ = 16.17 $Re/_{FT}$ = 9.49×10^5 α = 60°

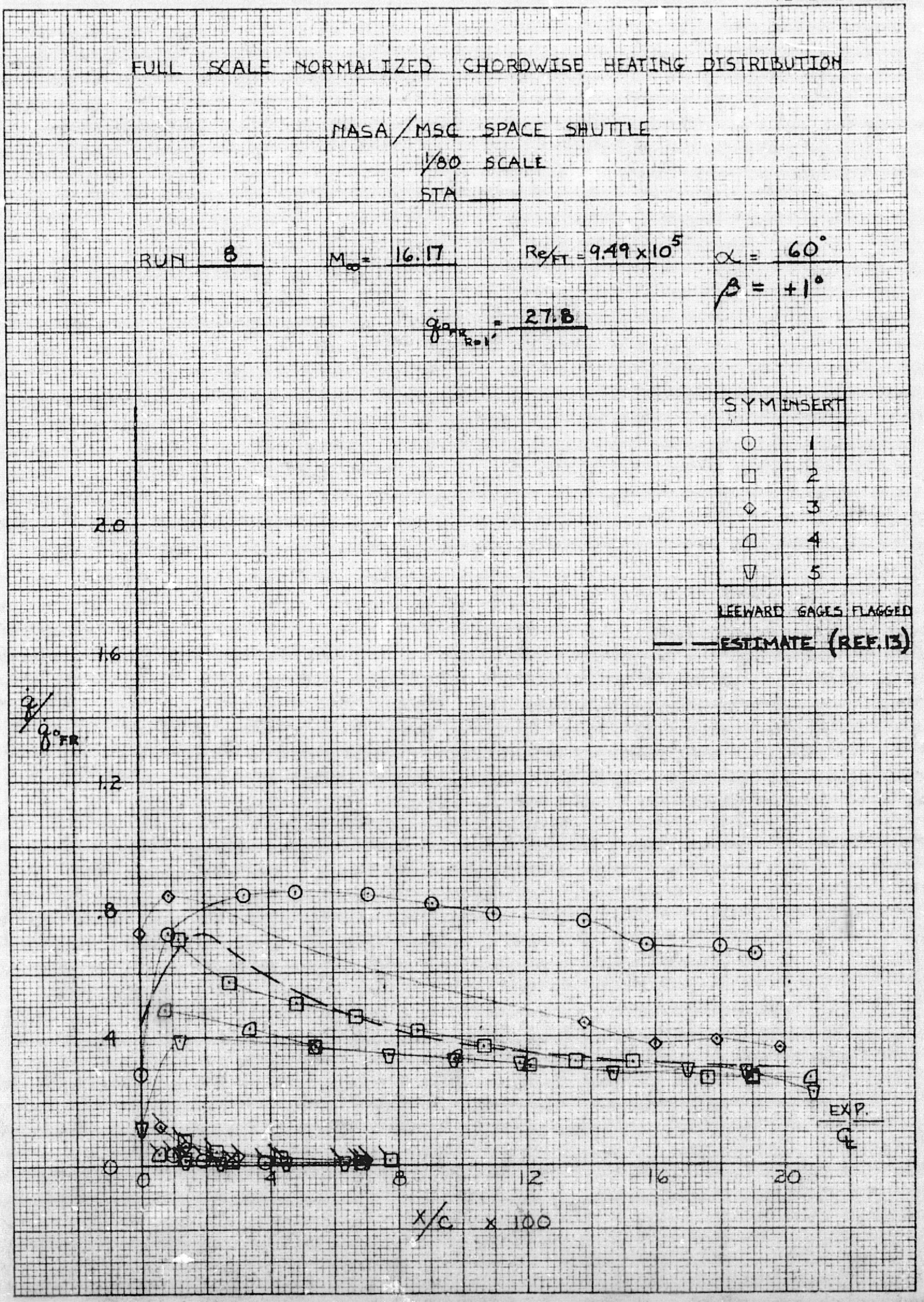
β = +1°

q_{REF} = 27.8

SYM	INSERT
○	1
□	2
◇	3
◁	4
▽	5

LEEWARD GAGES FLAGGED

— — ESTIMATE (REF. 13)



7 X 10 INCHES MADE IN U.S.A.
KEUFFEL & ESSER CO.

FIGURE 23b

FULL SCALE NORMALIZED SPANWISE HEATING DISTRIBUTION

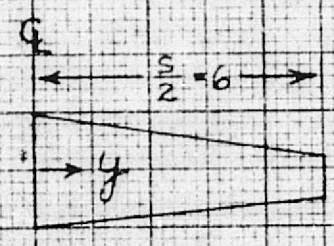
WINDWARD SIDE $x/c = .17$

NASA / MSC SPACE SHUTTLE

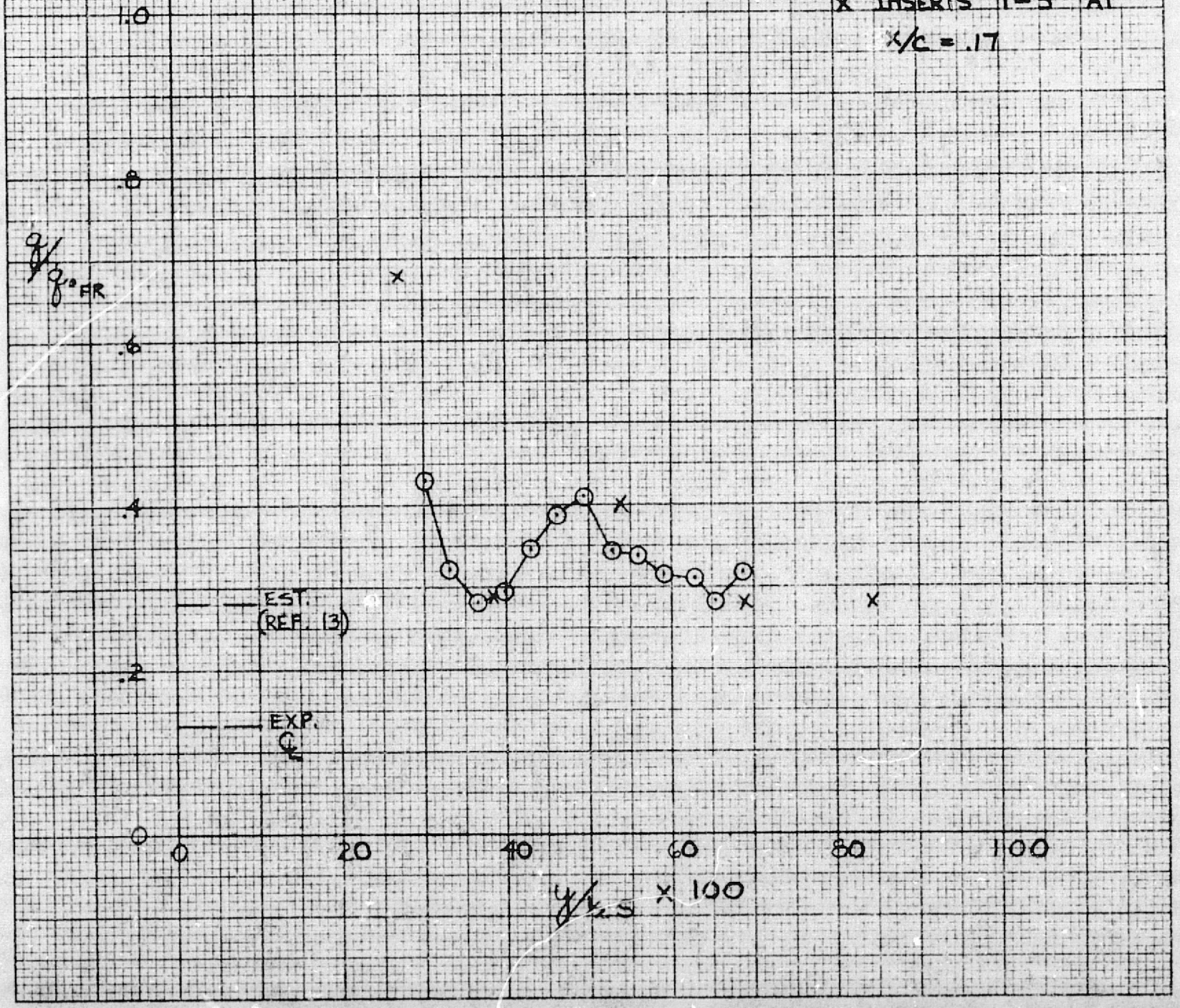
1/80 SCALE

RUN 8 $M_\infty = 16.17$ $Re/FT = 9.49 \times 10^5$ $\alpha = 60^\circ$ $\beta = +1^\circ$

$\dot{q}_{\dot{q}_{FR_{R=1'}}} = 27.8$



X INSERTS 1-5 AT $x/c = .17$



7 X 10 INCHES MADE IN U.S.A. KEUFFEL & ESSER CO.

FIGURE 24a

FULL SCALE NORMALIZED CHORDWISE HEATING DISTRIBUTION

NASA/MSC SPACE SHUTTLE

1/80 SCALE

STA ____

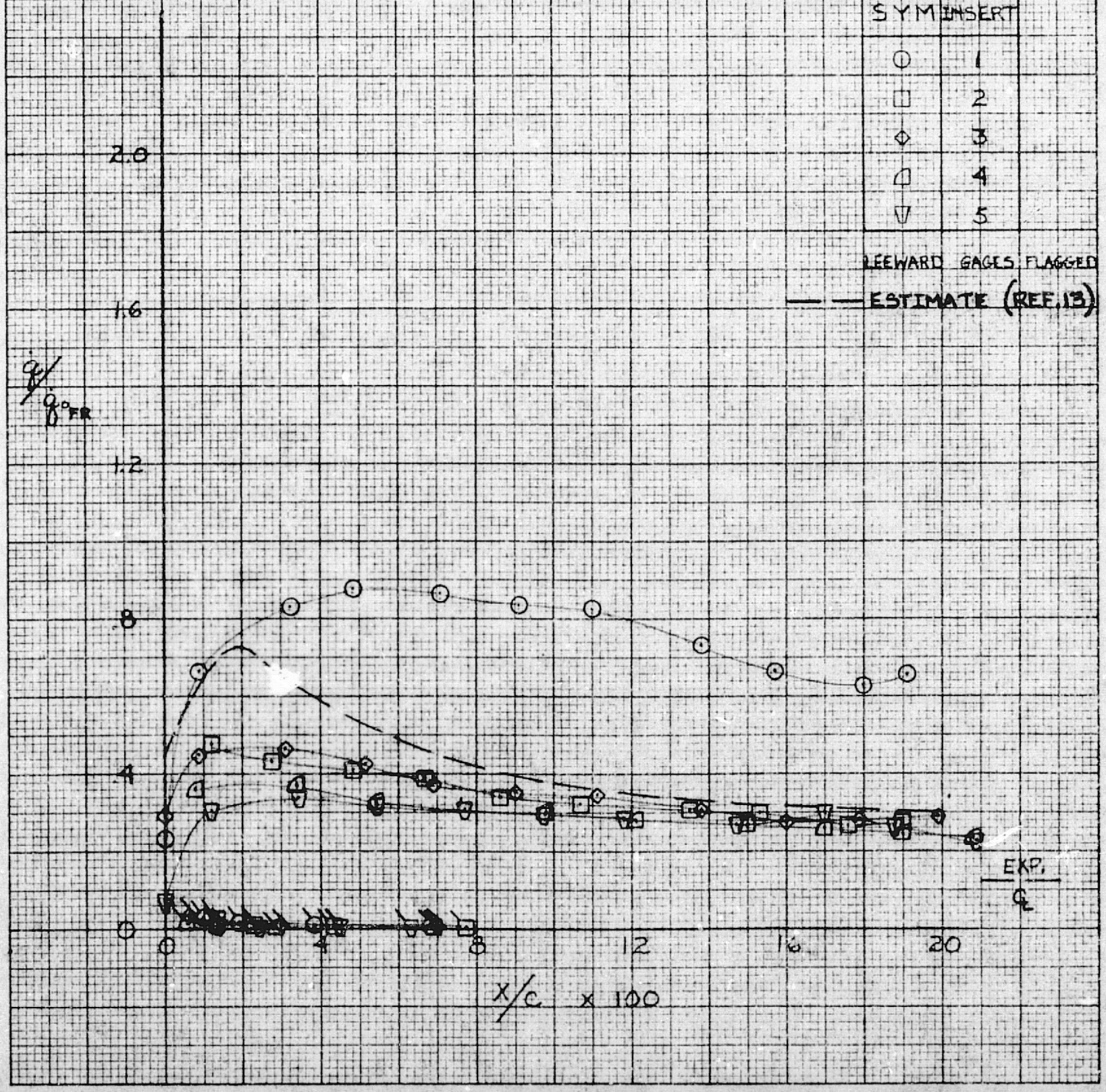
RUN 6 M_∞ = 16.15 $Re/_{FT}$ = 9.50×10^5 α = 70°

$\dot{q}_{0_{FR_{R=1'}}}$ = 28.2

SYM	INSERT
○	1
□	2
◇	3
◁	4
▽	5

LEEWARD GAGES FLAGGED

— — ESTIMATE (REF. 13)



7 X 10 INCHES MADE IN U.S.A.
KEUFFEL & ESSER CO.

FIGURE 24 b

FULL SCALE NORMALIZED SPANWISE HEATING DISTRIBUTION

WINDWARD SIDE $X/C = .17$

NASA / MSC SPACE SHUTTLE

1/80 SCALE

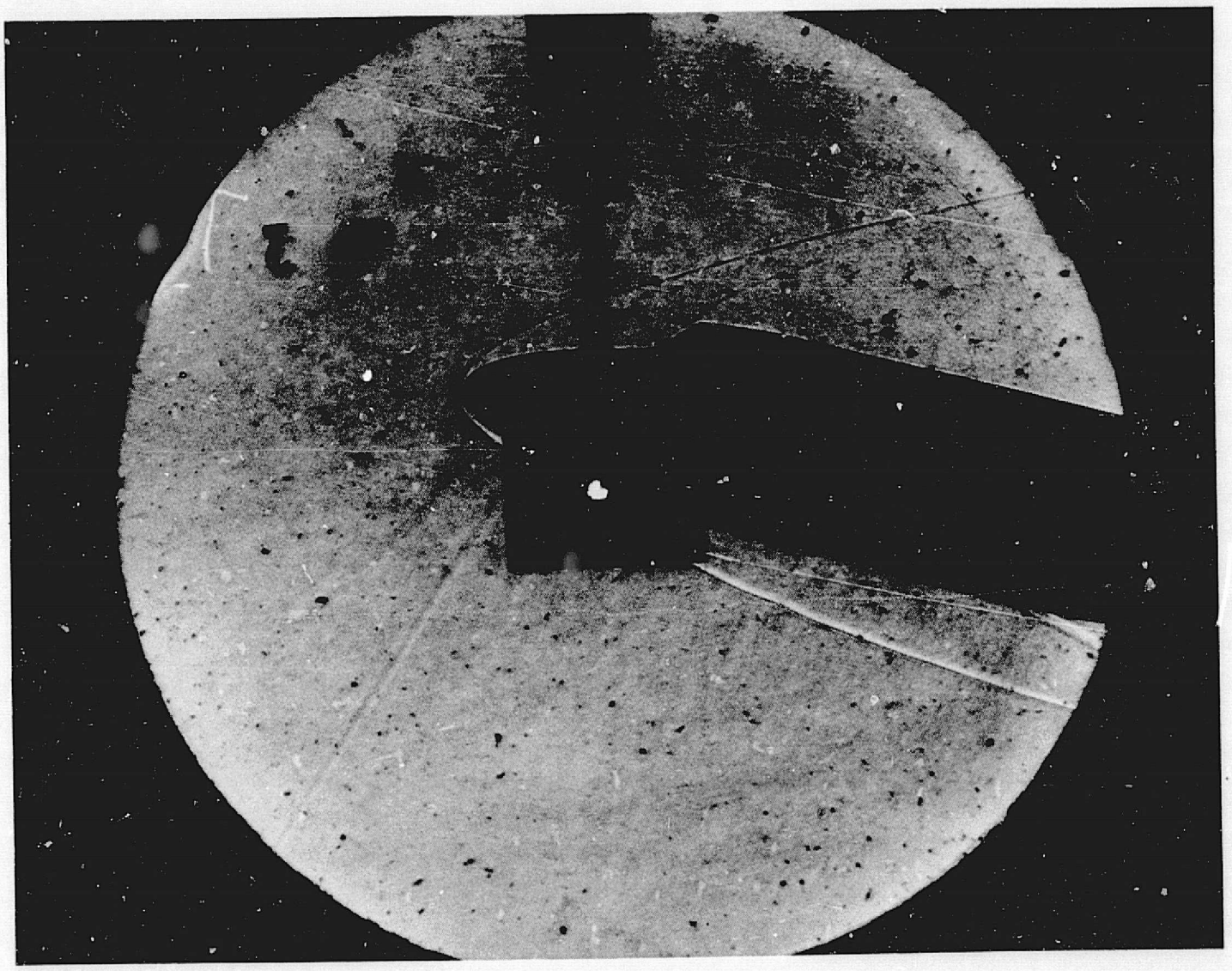
RUN 6 $M_\infty = 16.15$ $Re/FT = 9.50 \times 10^5$ $\alpha = 70^\circ$

$\dot{q}_{\theta_{FR}} = 282$



X INSERTS 1-5 AT $X/C = .17$

7 X 10 INCHES MADE IN U.S.A.
KEUFFEL & ESSER CO.

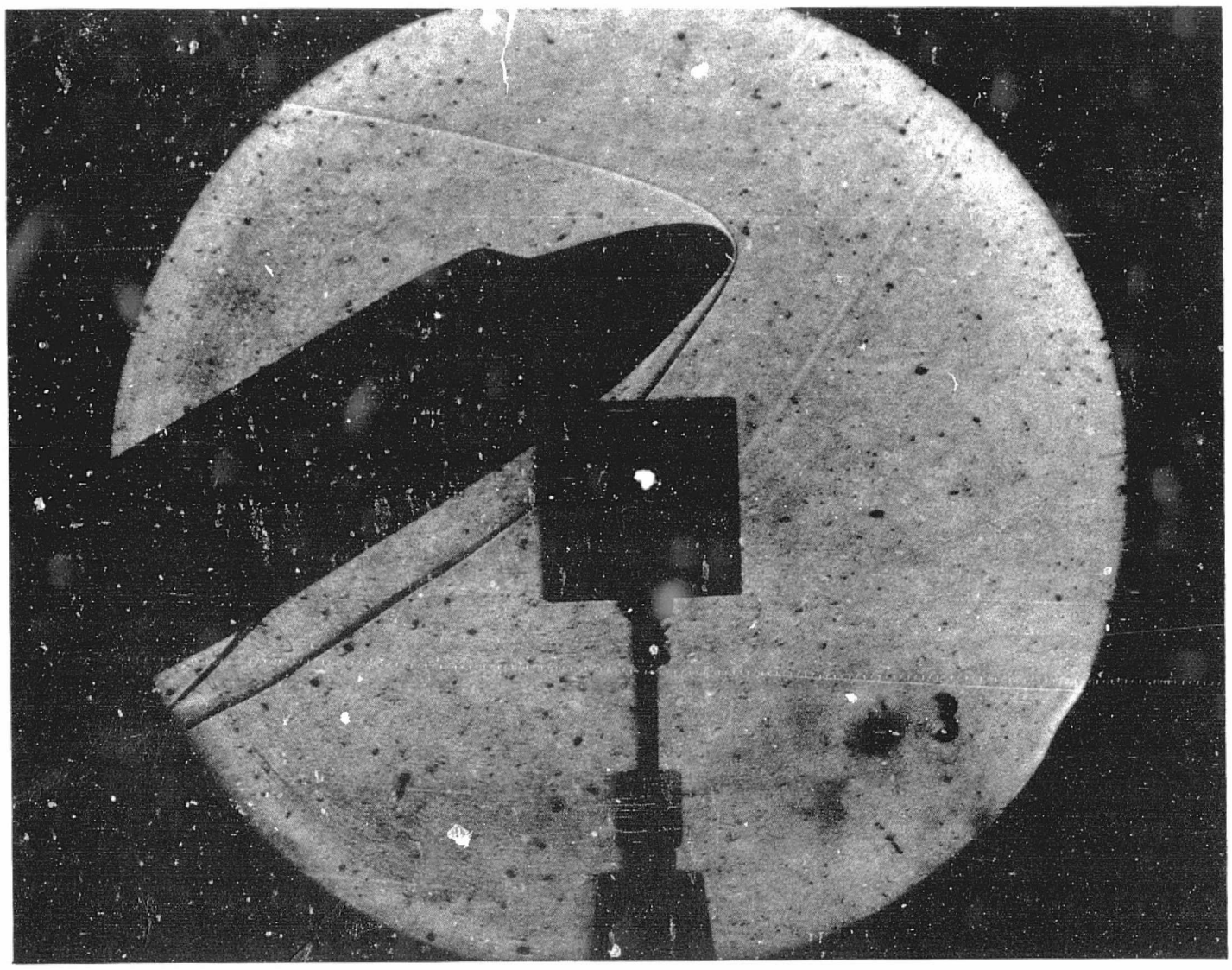


RUN NO. 2 $M_\infty = 16.2$

$\alpha = 15$ $R_E/FT = 0.97 \times 10^6$

$\beta = 0$

Figure 25a SCHLIEREN PHOTOGRAPH OF 1/80 SCALE NASA 12.5K STRAIGHT WING ORBITER

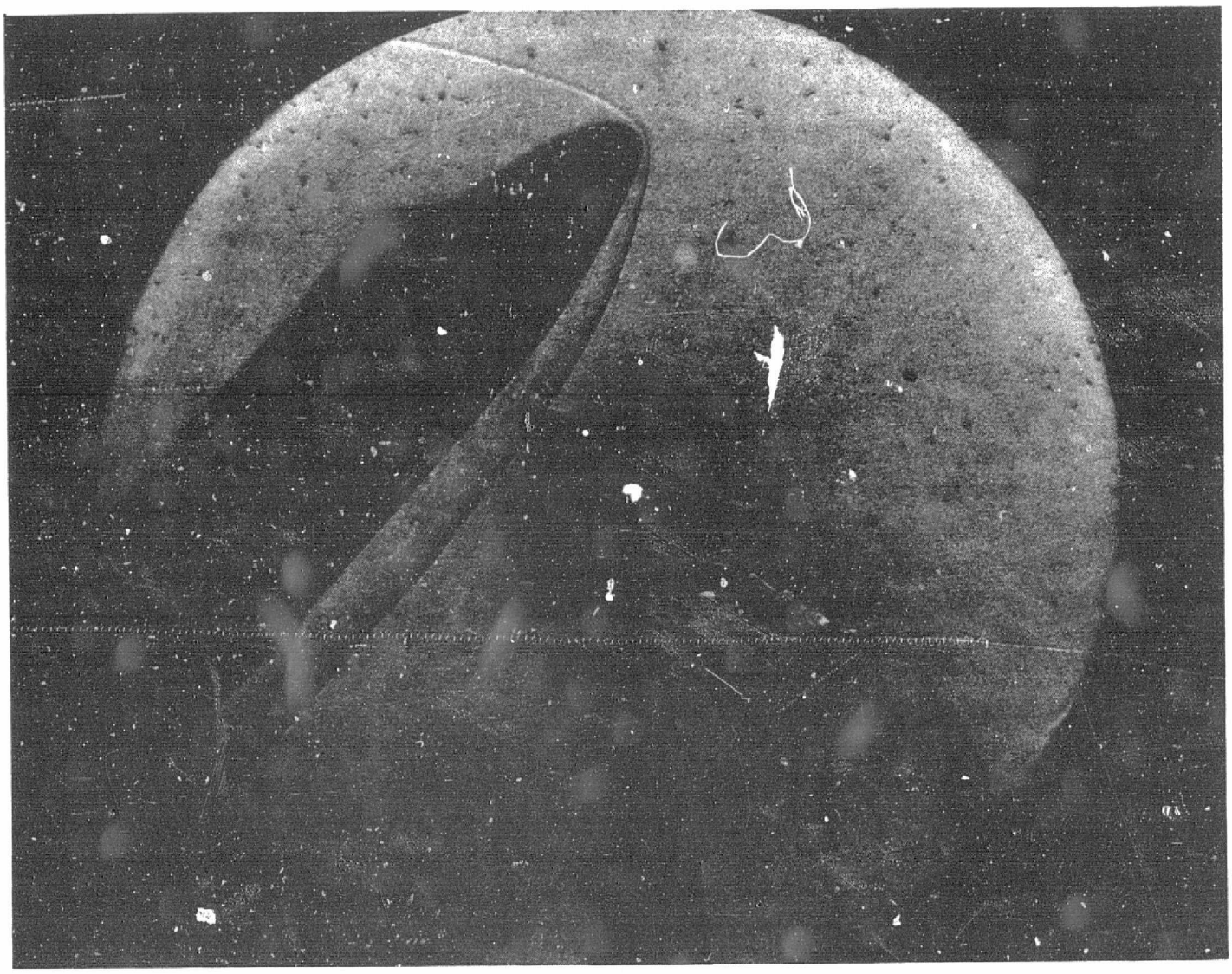


RUN NO. 3 M_∞ = 16.2

α = 30 $R_E/FT = 0.96 \times 10^5$

β = 0

Figure 25b SCHLIEREN PHOTOGRAPH OF 1/80 SCALE NASA 12.5K STRAIGHT WING ORBITER

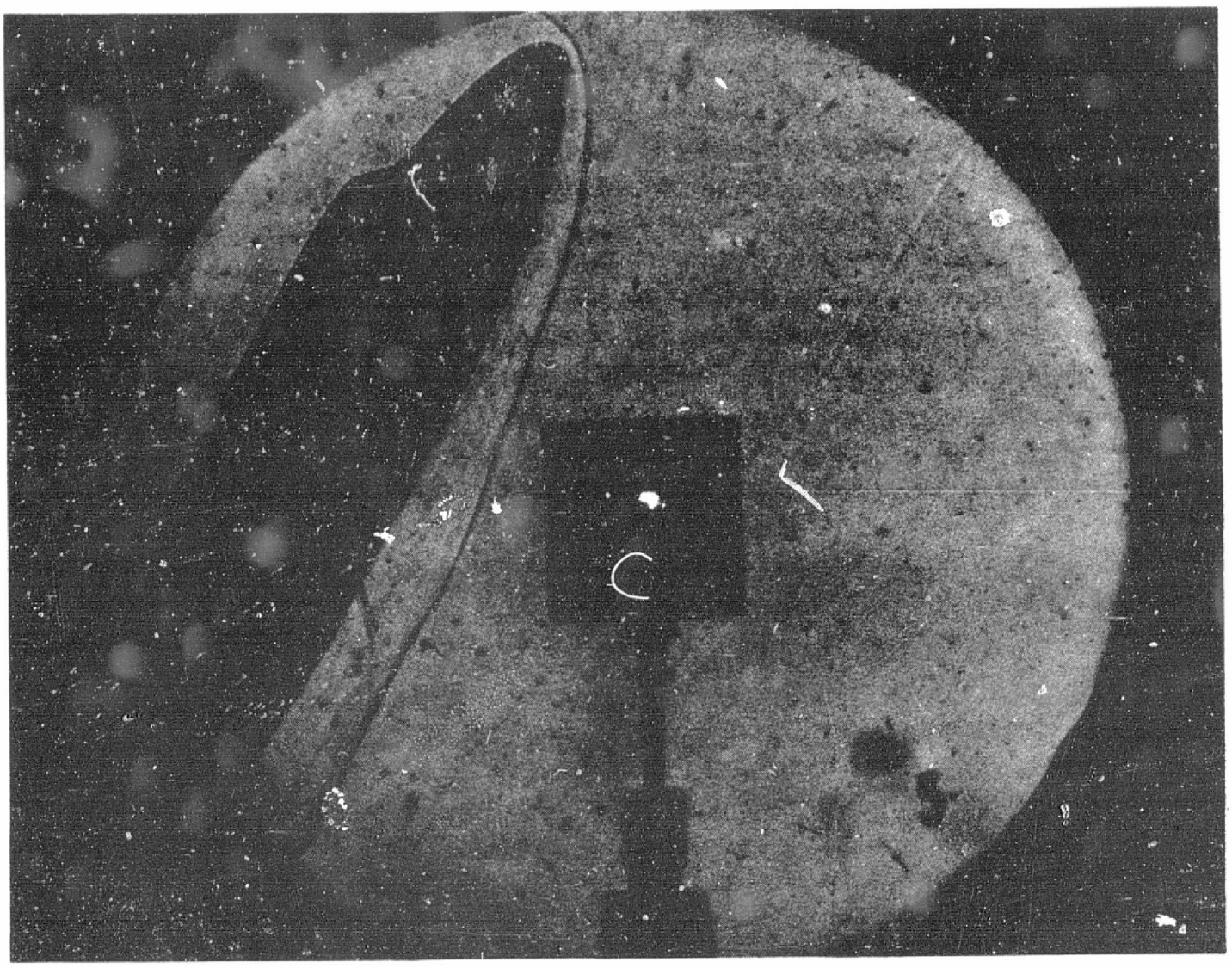


RUN NO. 4 $M_\infty = 16.3$

$\alpha = 45$ $R_E/FT = 1.1 \times 10^6$

$\beta = 0$

Figure 25c SCHLIEREN PHOTOGRAPH OF 1/80 SCALE NASA 12.5K STRAIGHT WING ORBITER

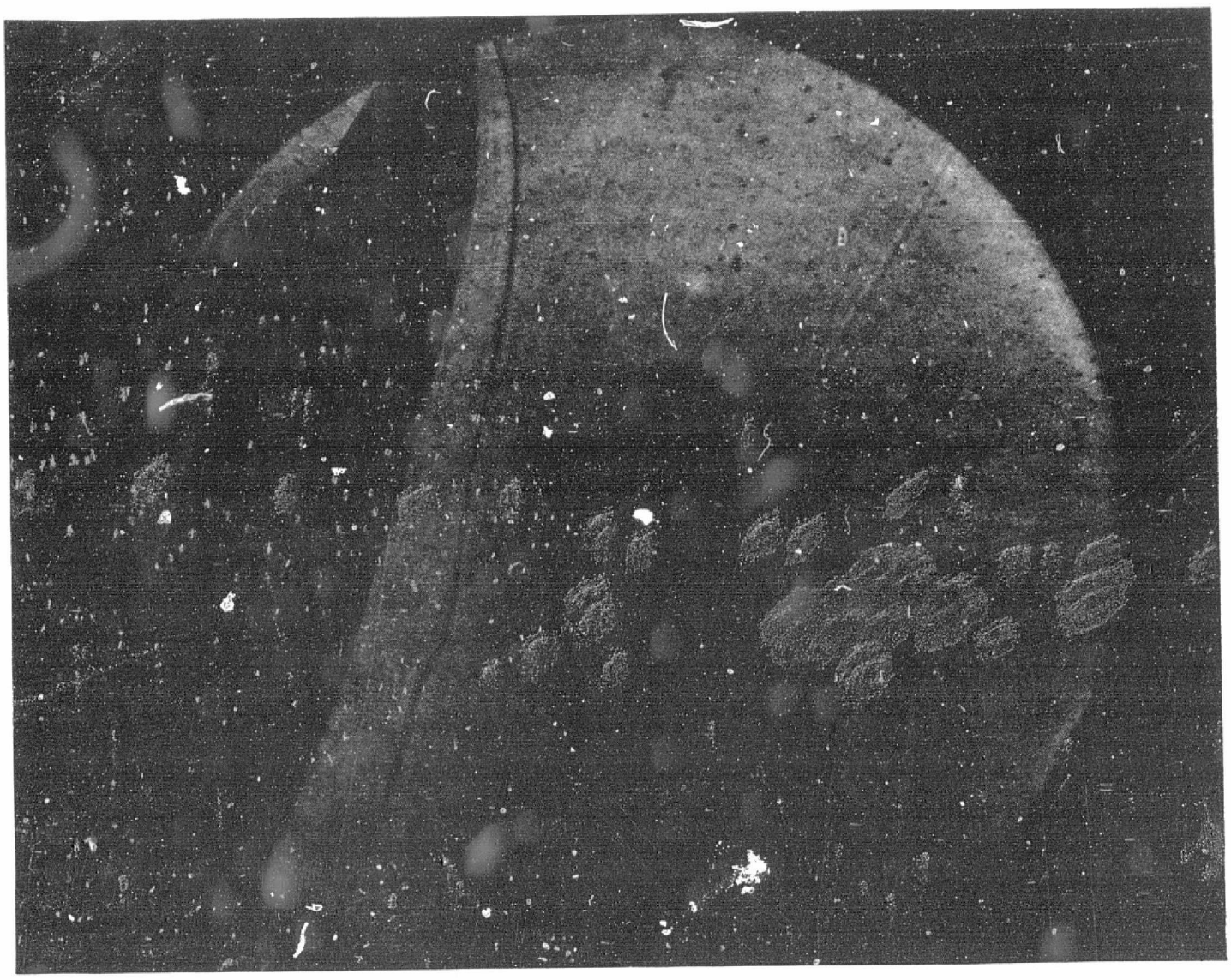


RUN NO. 5 M_∞ = 16.3

α = 60 R_E/FT = 1.1 x 10^6

β = 0

Figure 25d SCHLIEREN PHOTOGRAPH OF 1/80 SCALE NASA 12.5K STRAIGHT WING ORBITER

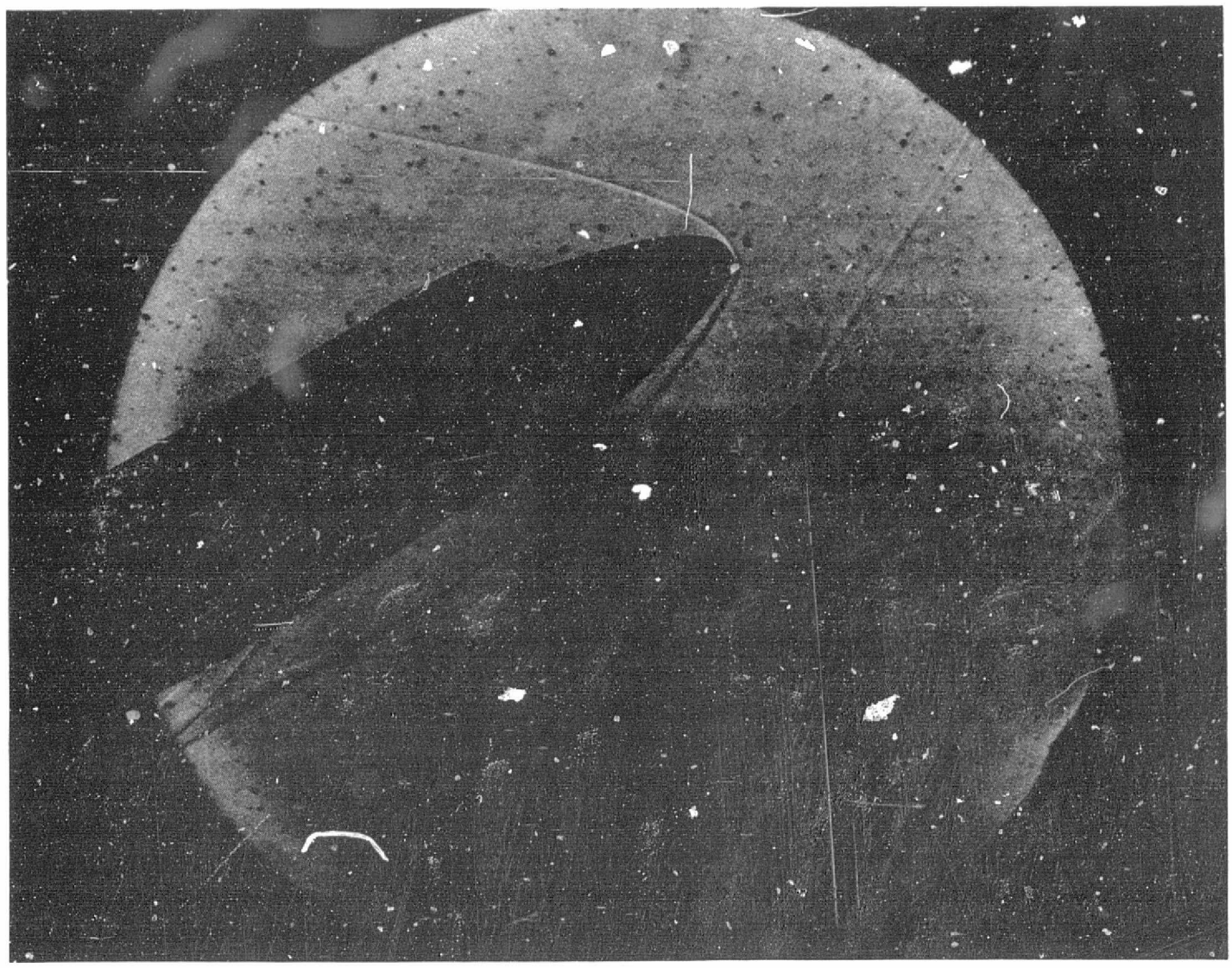


RUN NO. 6 M_∞ = 16.2

α = 70 $R_E/FT = 0.95 \times 10^6$

β = 0

Figure 25e SCHLIEREN PHOTOGRAPH OF 1/80 SCALE NASA 12.5K STRAIGHT WING ORBITER

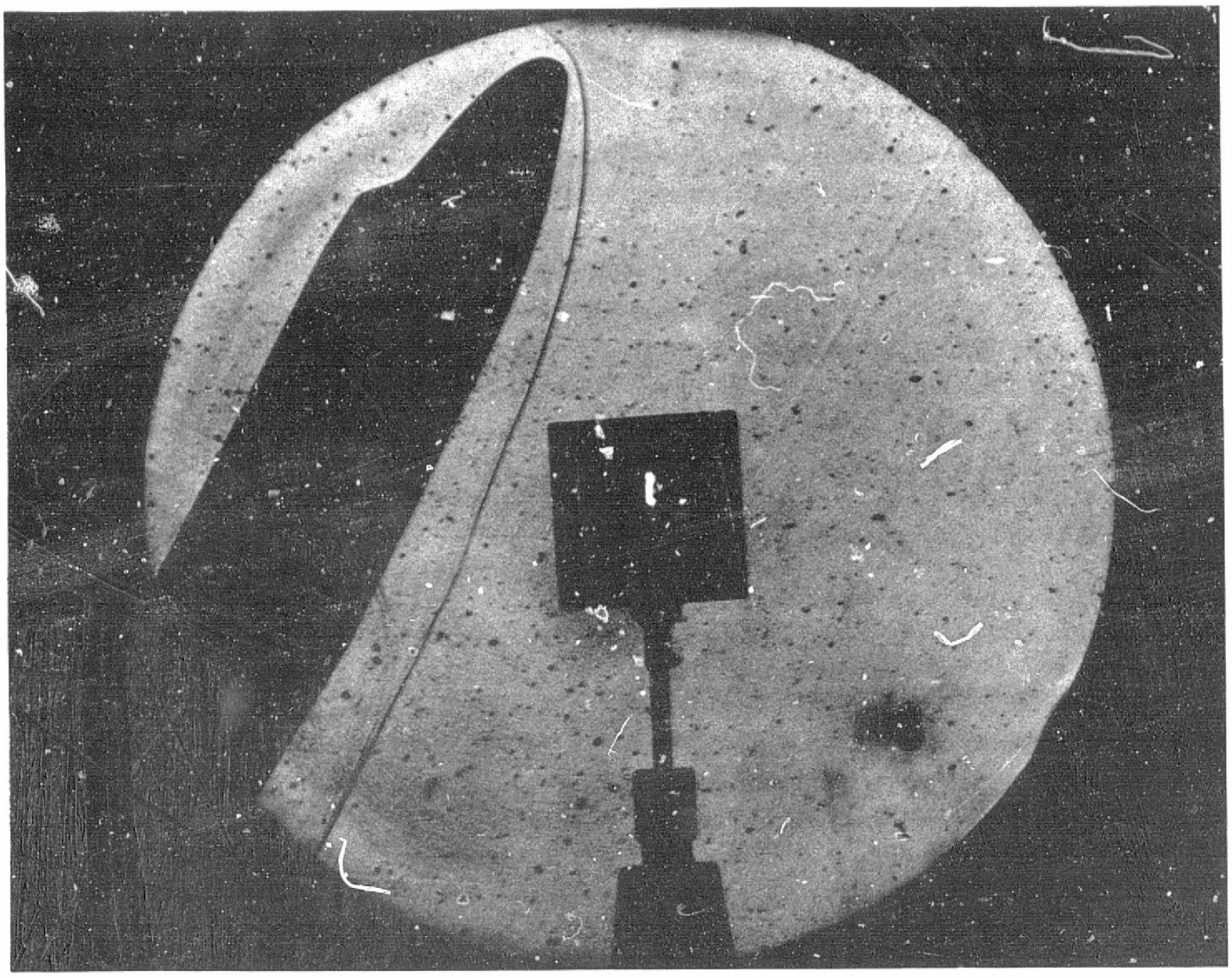


RUN NO. 7 M_∞ = 16.2

α = 30 $R_E/FT = 0.98 \times 10^6$

β = +1

Figure 25f SCHLIEREN PHOTOGRAPH OF 1/80 SCALE NASA 12.5K STRAIGHT WING ORBITER

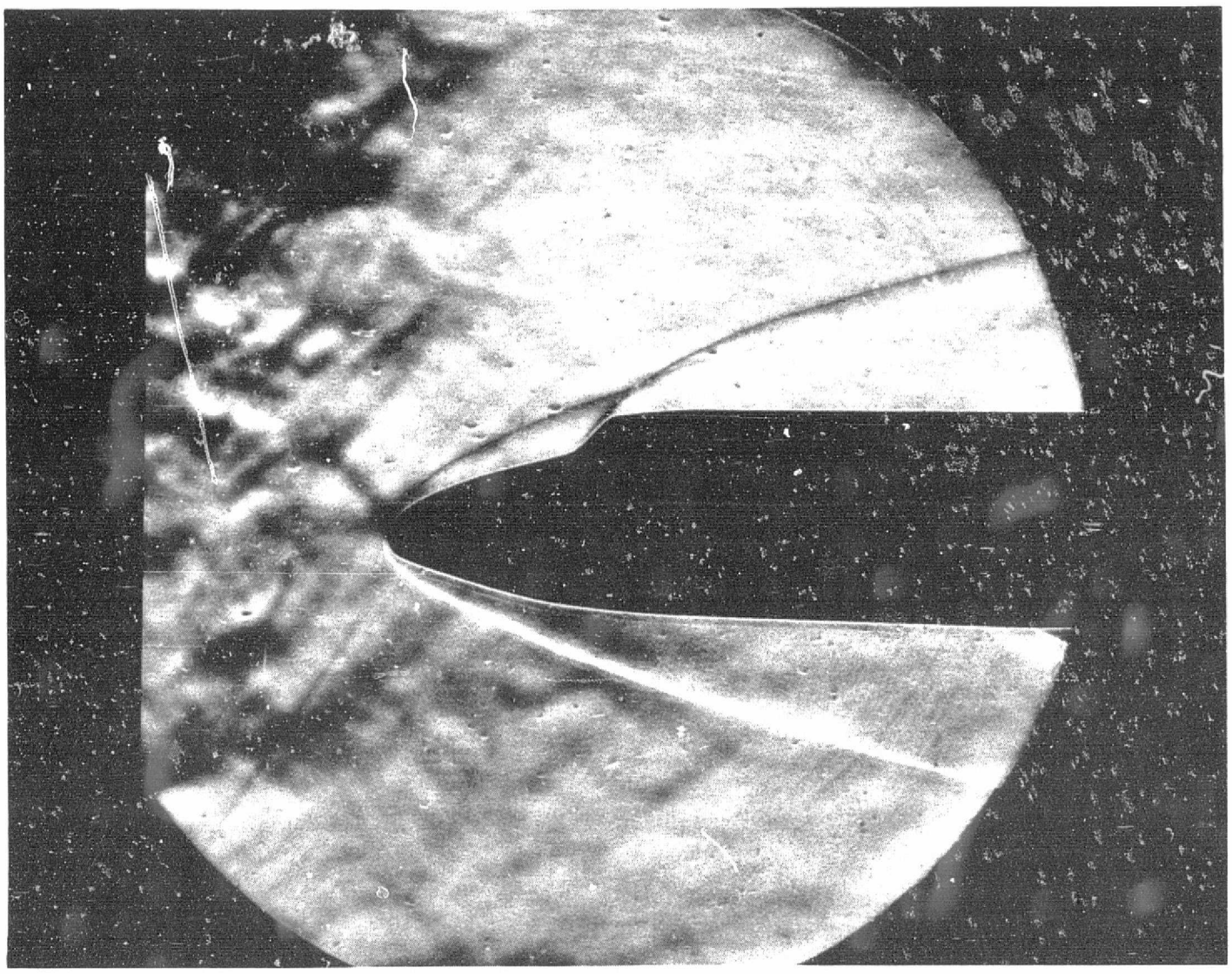


RUN NO. 8 M_∞ = 16.2

α = 60 $R_E/FT = 0.95 \times 10^6$

β = +1

Figure 25g SCHLIEREN PHOTOGRAPH OF 1/80 SCALE NASA 12.5K STRAIGHT WING ORBITER

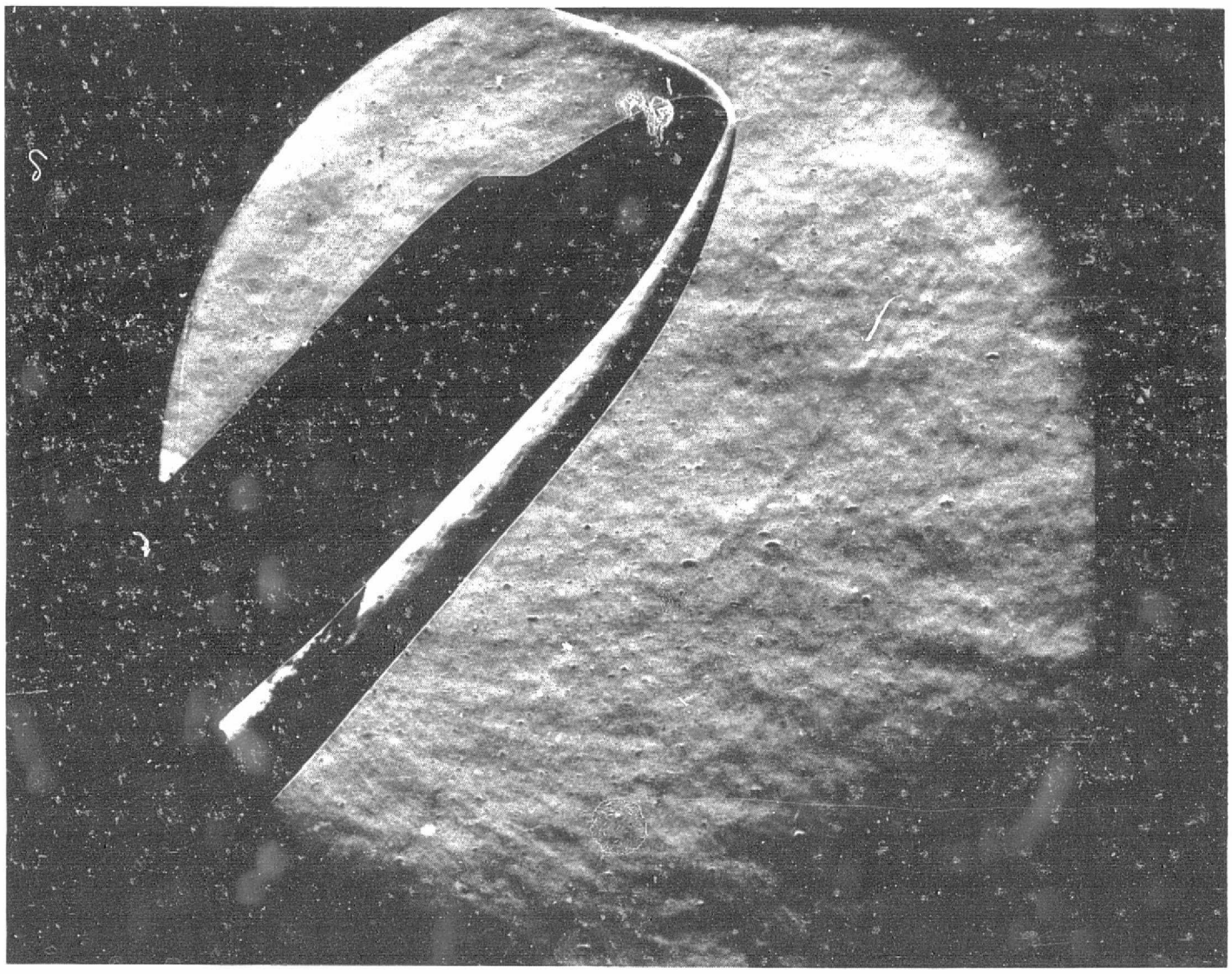


RUN NO. 9 $M_\infty \approx 7.6$

$\alpha = 0$ $R_E/FT \approx 0.37 \times 10^6$

$\beta = 0$

Figure 25h SCHLIEREN PHOTOGRAPH OF 1/80 SCALE NASA 12.5K STRAIGHT WING ORBITER

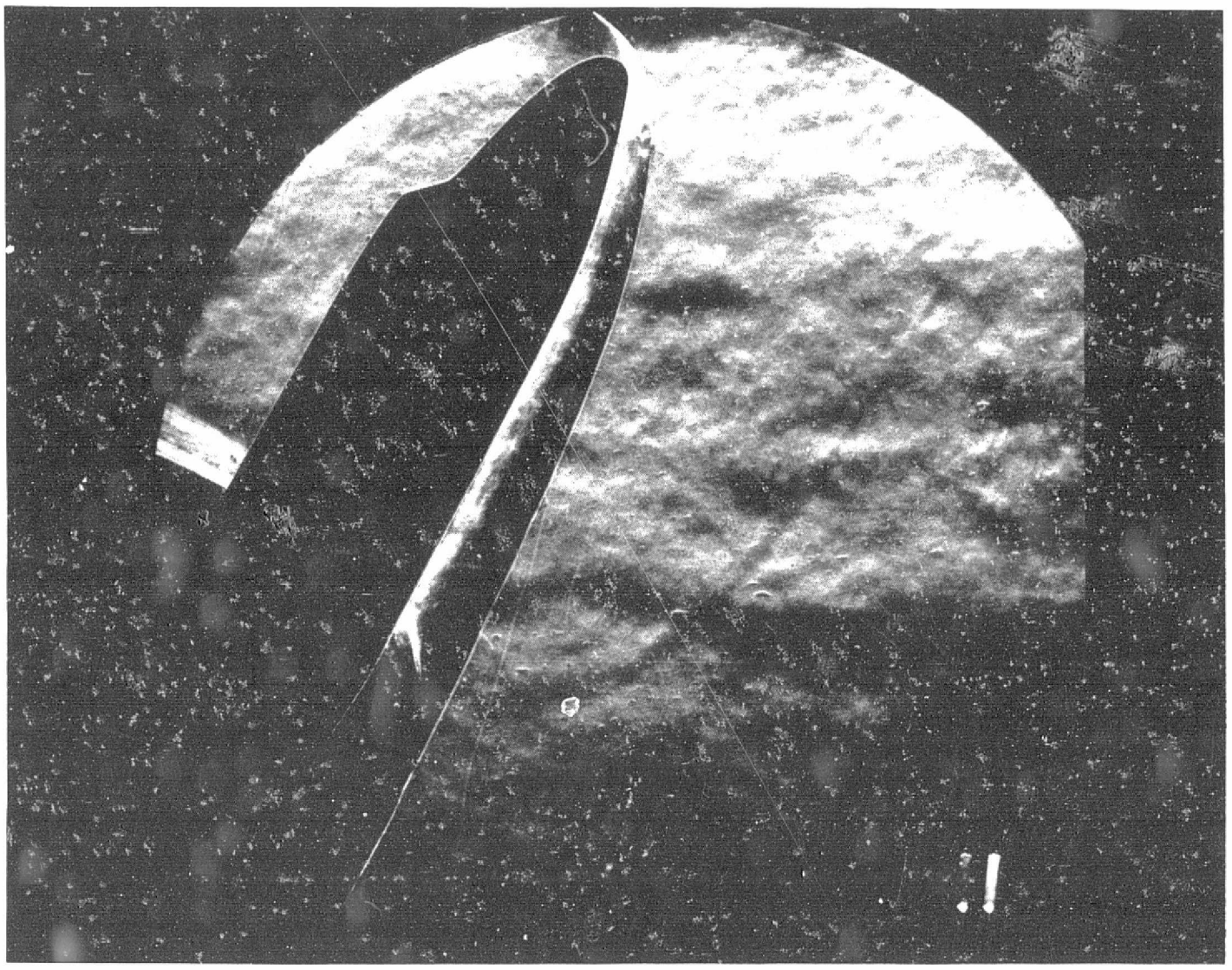


RUN NO. 10 $M_\infty = 7.7$

$\alpha = 45$ $R_E/FT = 2.1 \times 10^6$

$\beta = 0$

Figure 25i SCHLIEREN PHOTOGRAPH OF 1/80 SCALE NASA 12.5K STRAIGHT WING ORBITER

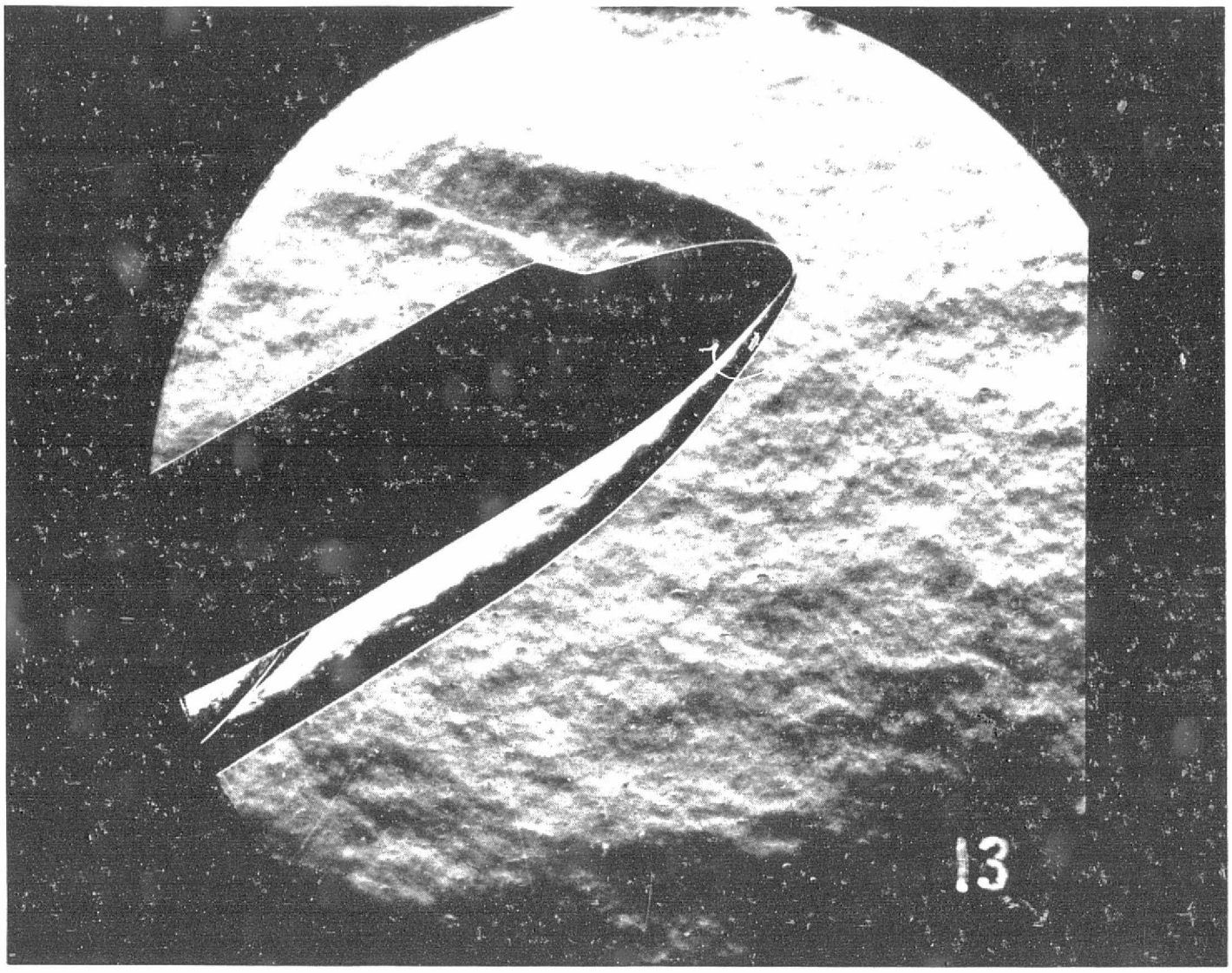


RUN NO. 11 $M_\infty = 7.8$

$\alpha = 60$ $R_E/FT = 2.6 \times 10^6$

$\beta = 0$

Figure 25j SCHLIEREN PHOTOGRAPH OF 1/80 SCALE NASA 12.5K STRAIGHT WING ORBITER

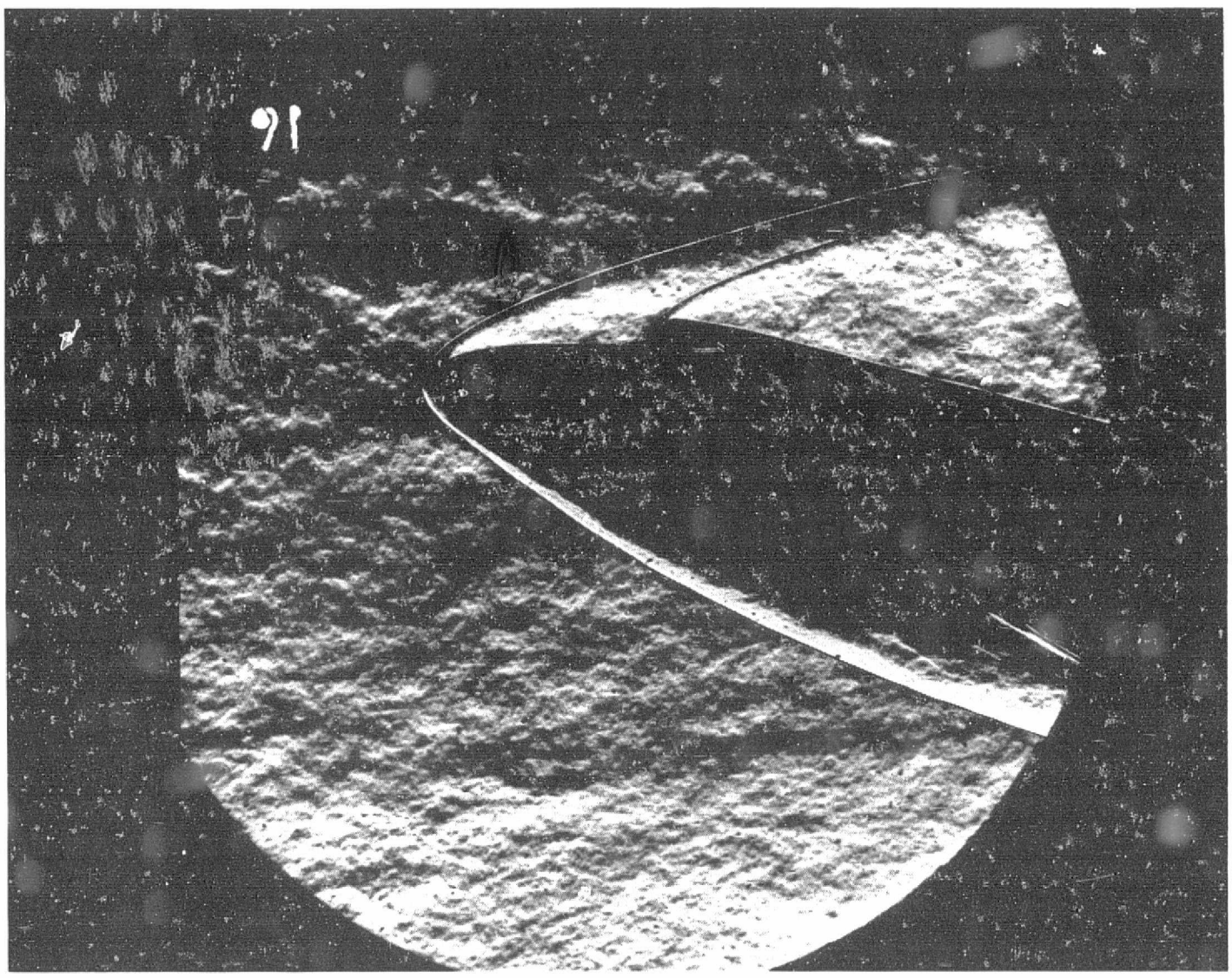


RUN NO. 13 $M_\infty = 7.8$

$\alpha = 30$ $R_E/FT = 4.5 \times 10^6$

$\beta = 0$

Figure 25k SCHLIEREN PHOTOGRAPH OF 1/80 SCALE NASA 12.5K STRAIGHT WING ORBITER



RUN NO. 16 M_∞ = 8.0

α = 15 R_E/FT = 10.8×10^6

β = 0

Figure 25l SCHLIEREN PHOTOGRAPH OF 1/80 SCALE NASA 12.5K STRAIGHT WING ORBITER

FIGURE 26

LEADING EDGE HEATING VERSUS ANGLE OF ATTACK

INSERT 1

SYM	M
□	8
○	16

FLAG $\beta = +1°$

DOUBLE FLAG $\beta = +3°$

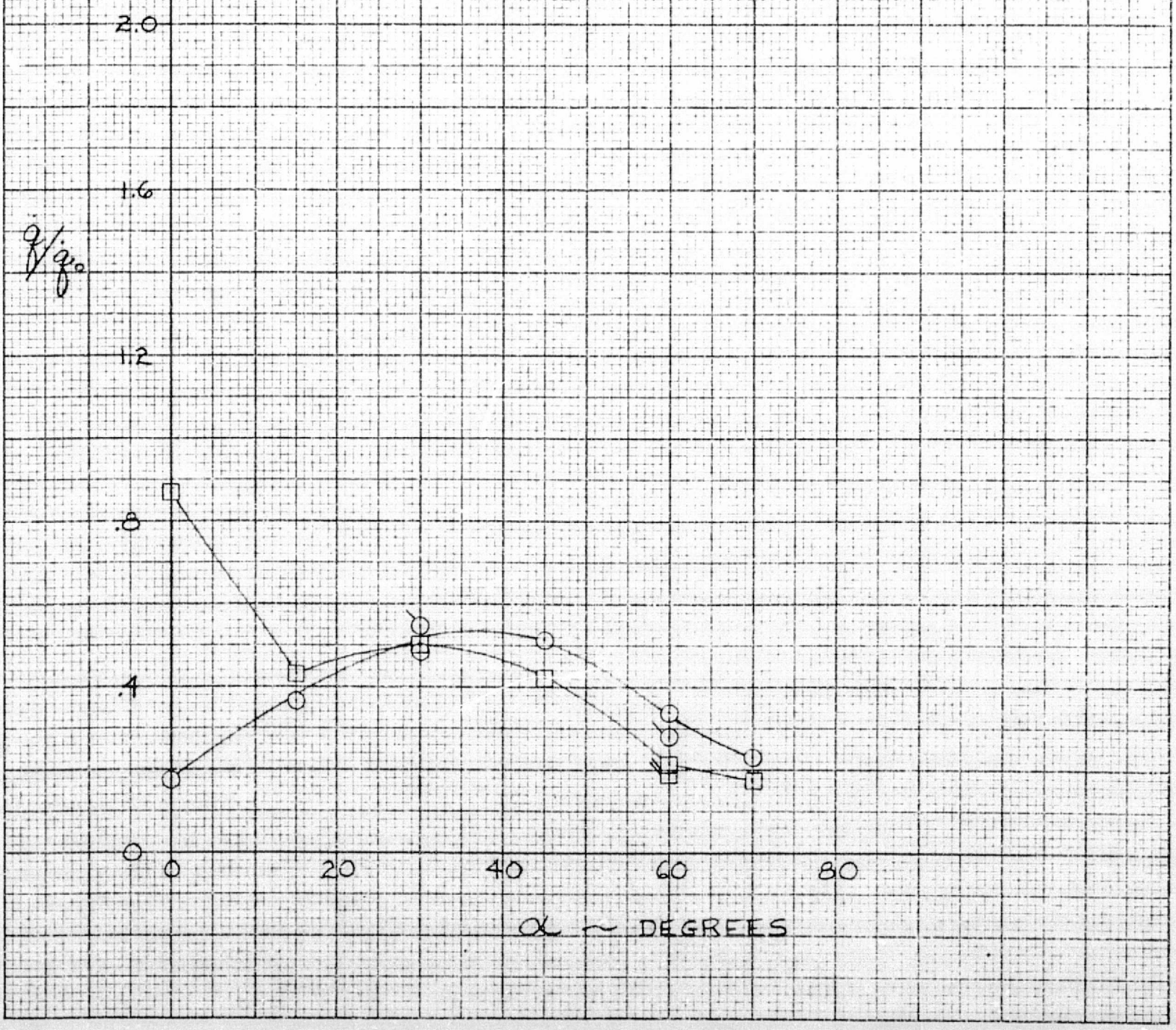


FIGURE 27

17 % CHORD HEATING VERSUS ANGLE OF ATTACK

INSERT 1

SYM	M
□	8
○	16

FLAG $\beta = +1°$

DOUBLE FLAG $\beta = +3°$

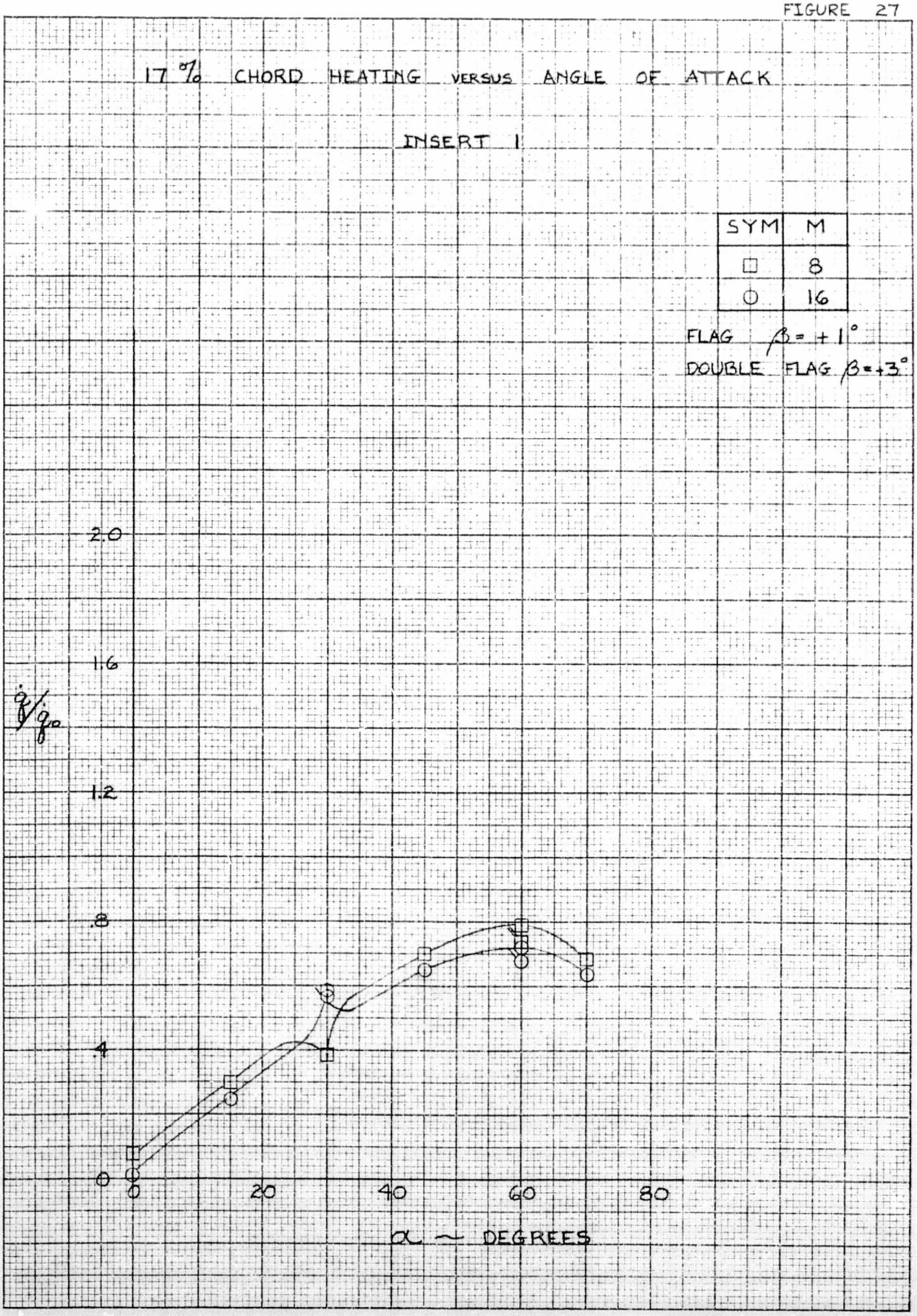
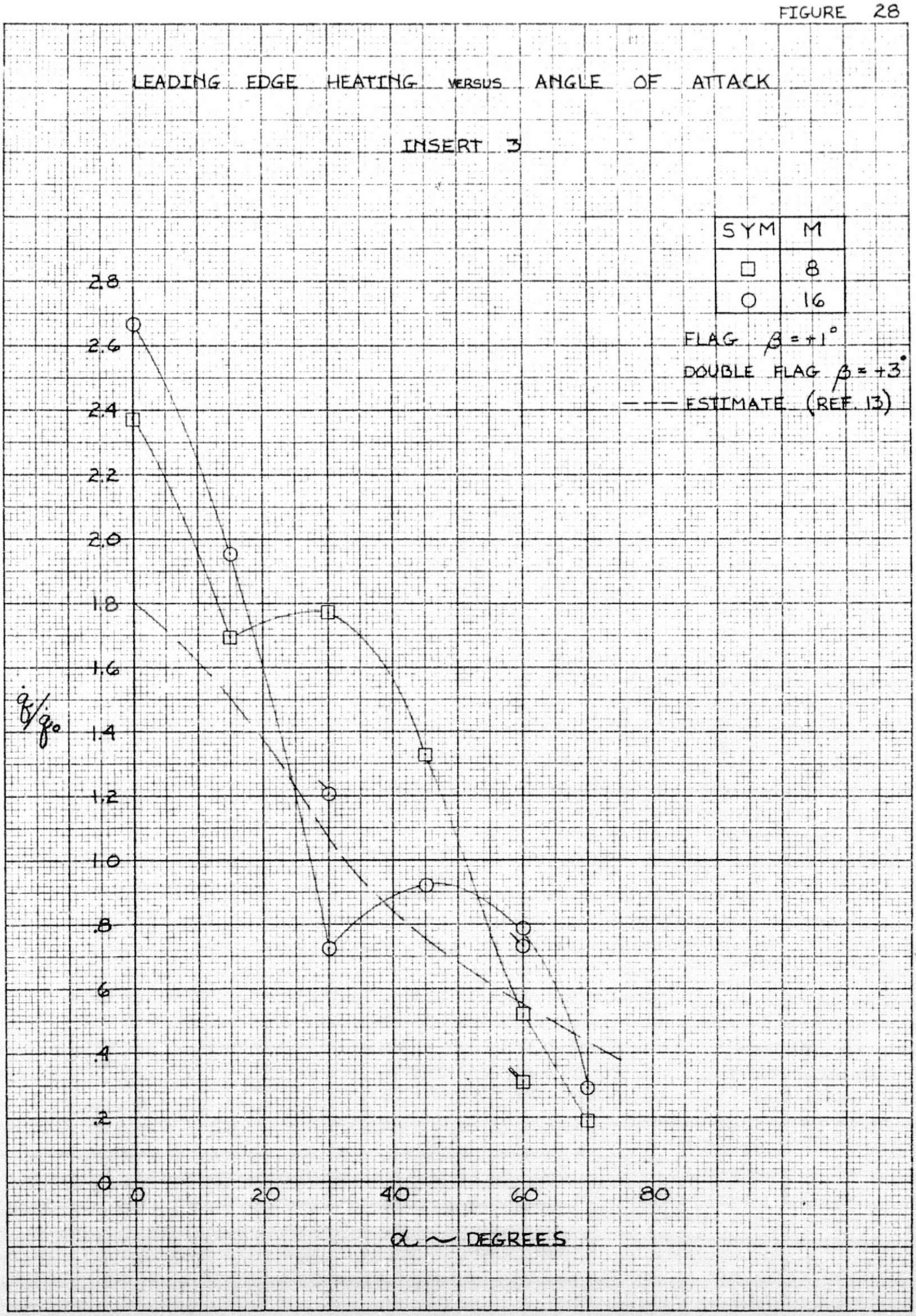


FIGURE 28

LEADING EDGE HEATING VERSUS ANGLE OF ATTACK

INSERT 3



KEUFFEL & ESSER CO. MADE IN U.S.A.

FIGURE 29

17 % CHORD HEATING VERSUS ANGLE OF ATTACK

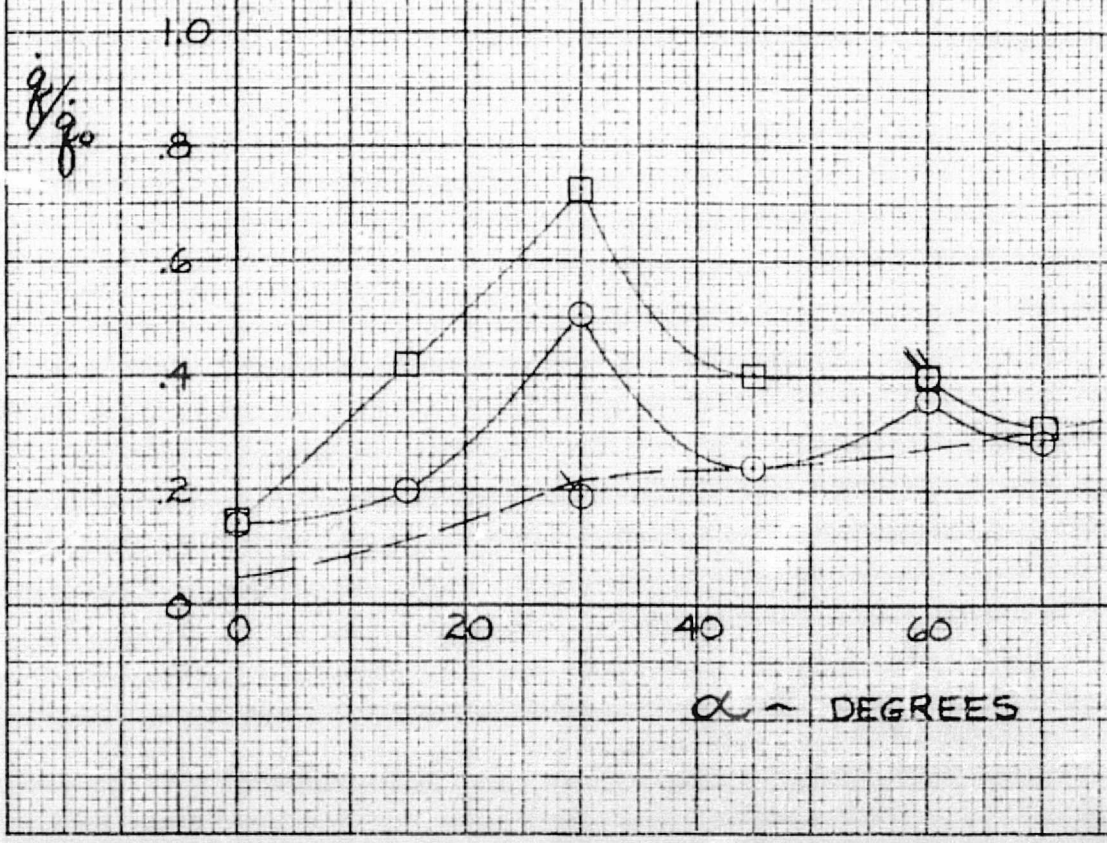
INSERT 3

SYM	M
□	8
○	16

FLAG $\beta = +1°$

DOUBLE FLAG $\beta = +3°$

— — — ESTIMATE (REF. 13)



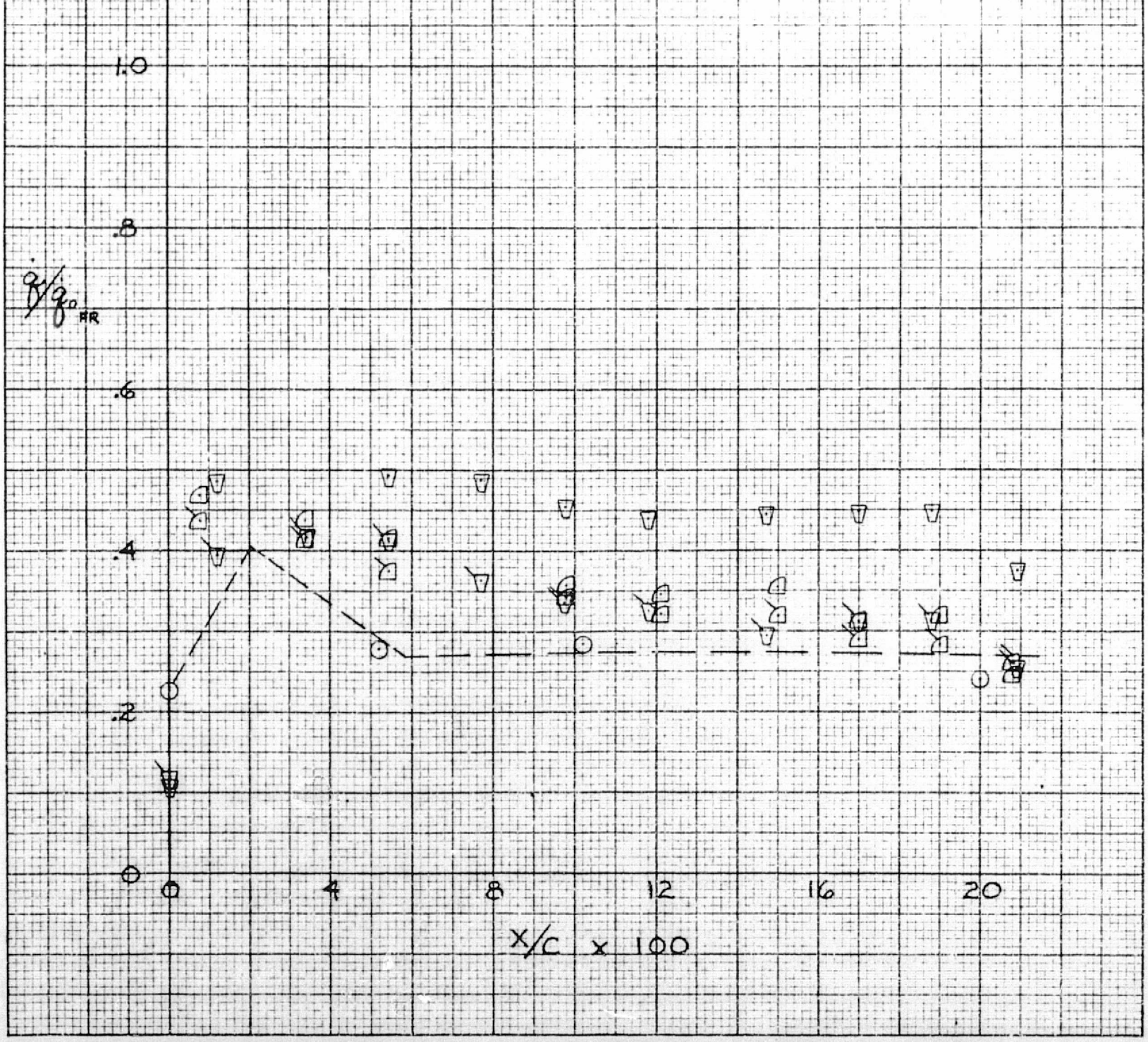
KEUFFEL & ESSER CO

FIGURE 30

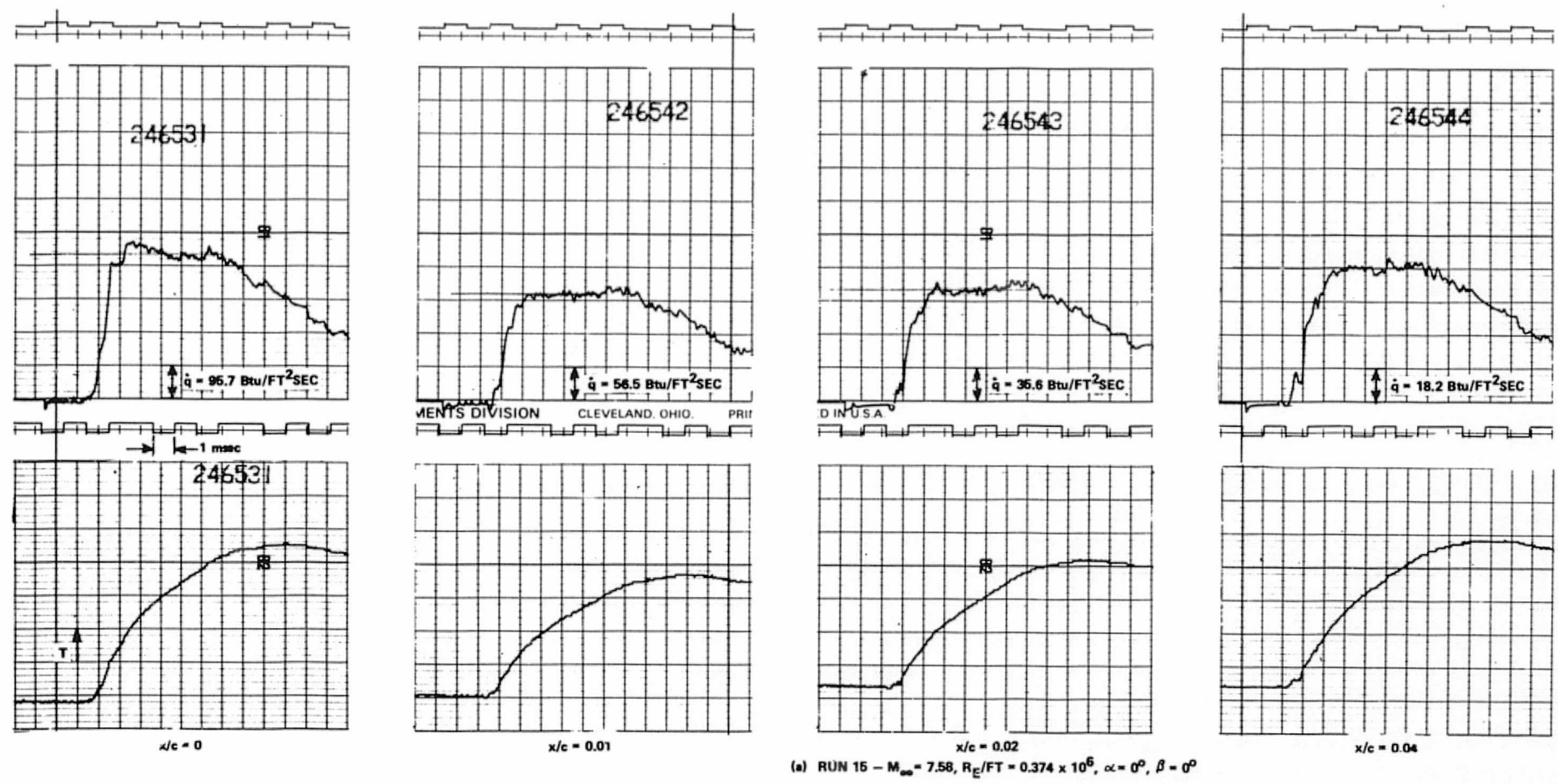
FULL SCALE NORMALIZED CHORDWISE HEATING DISTRIBUTION IN NONPERTURBED REGION OF WING

$\alpha = 60°$

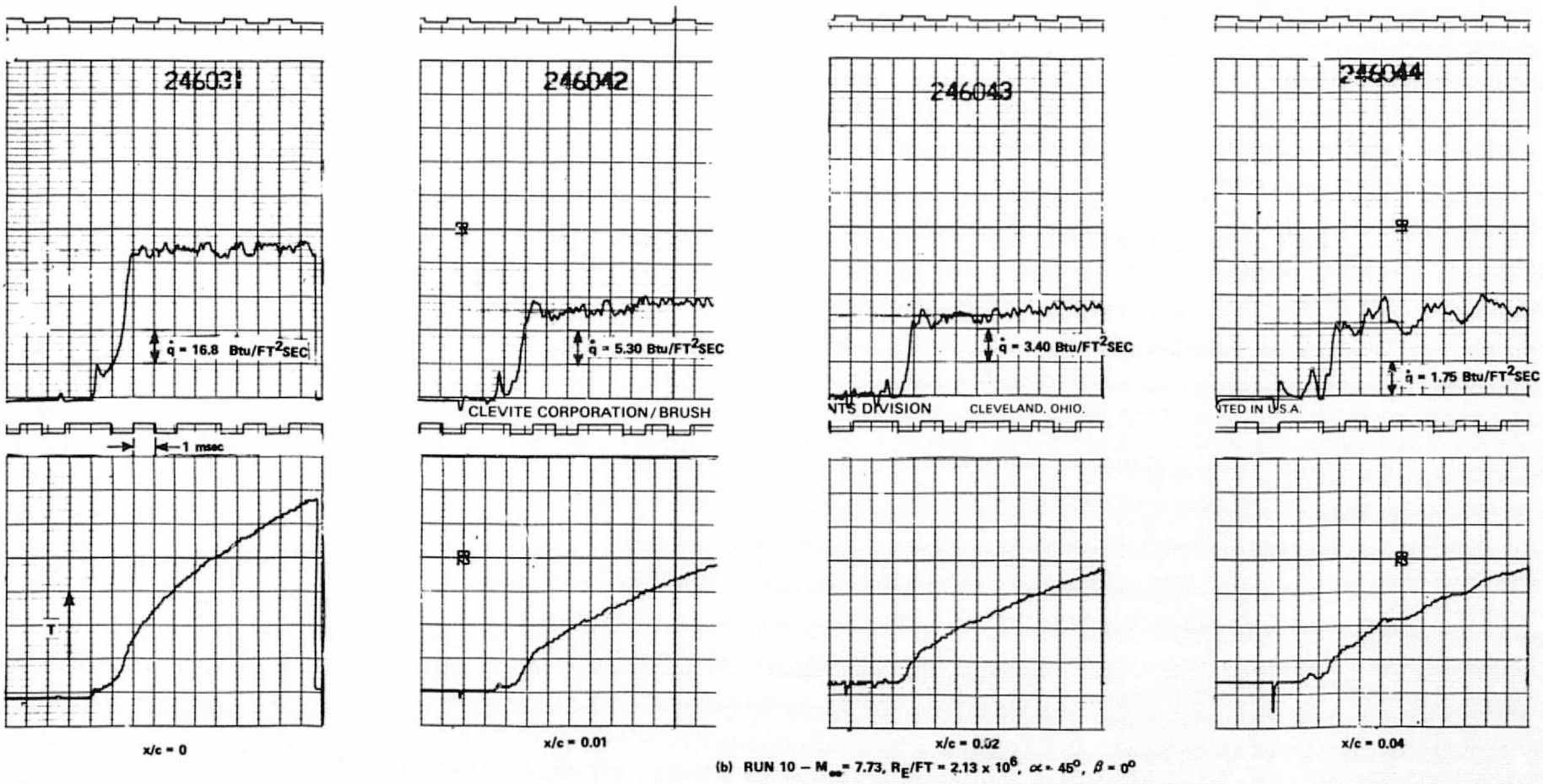
$Re_L \times 10^{-6}$	SYM	M	% EXPOSED SPAN	REF.
2.57	□	7.75	60	CAL
↓	▽	↓	80	↓
1.07	◺	16.26	60	↓
↓	▽	↓	80	↓
1.0	○	7.4	70	14
	- - -			15



KEUFFEL & ESSER CO

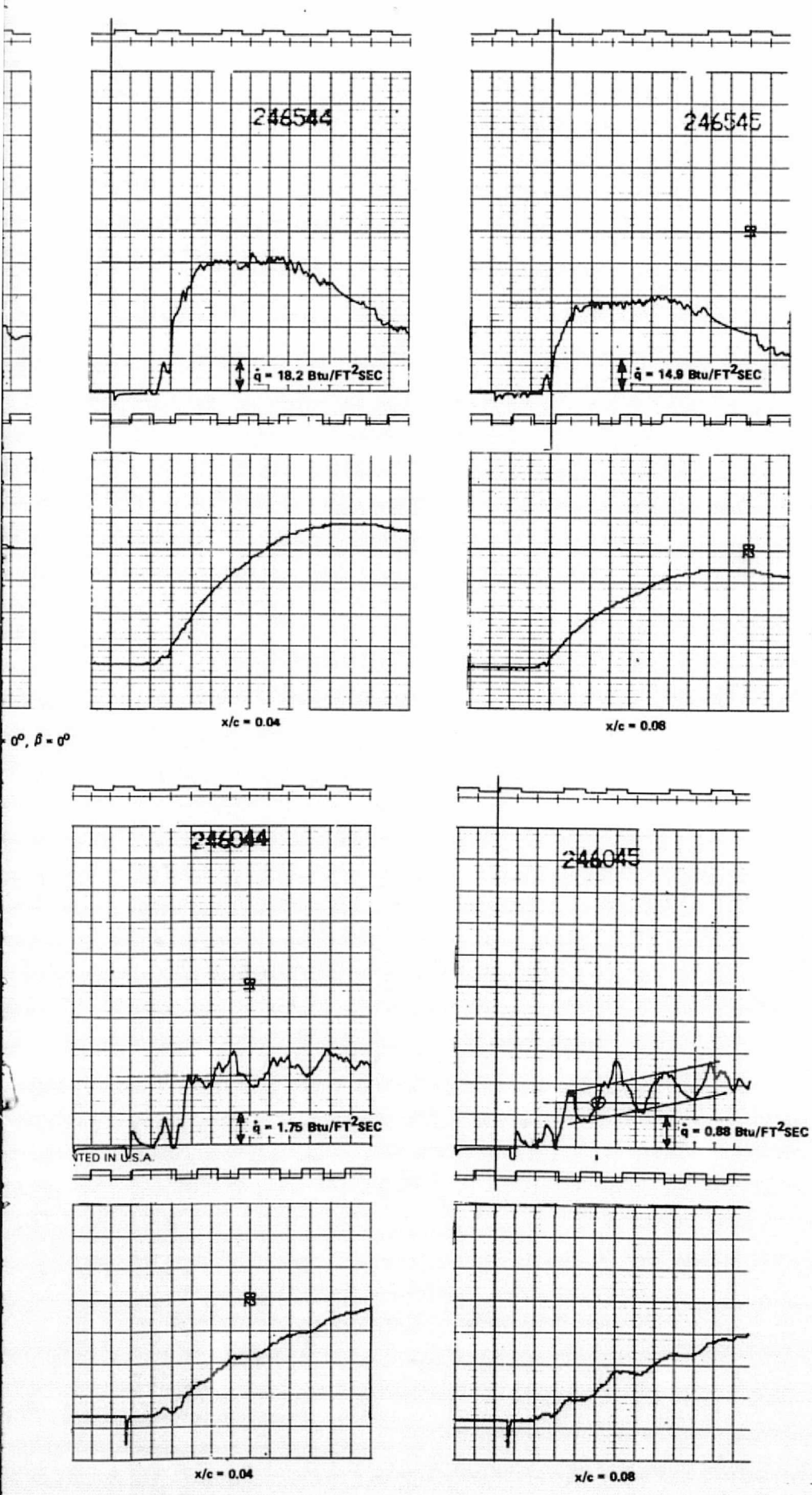


(a) RUN 15 – M_∞ = 7.58, R_E/FT = 0.374 x 10^6, α = 0°, β = 0°



(b) RUN 10 – M_∞ = 7.73, R_E/FT = 2.13 x 10^6, α = 45°, β = 0°

FOLDOUT FRAME 1



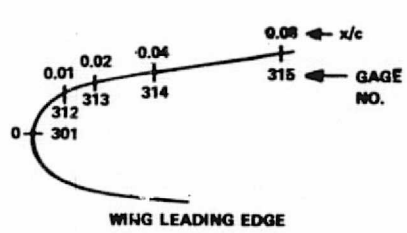


Figure 31 TEMPERATURE AND HEAT TRANSFER RATE TRACES FROM INSERT NO. 3

FOLDOUT FRAME 2